THE MESSENGER

EL MENSAJERO

No. 32 – June 1983

Comets – Distant and Nearby

R. M. West, ESO

Comet P/Halley Observed at ESO

With the recovery of Comet Halley on October 16, 1982, the interest in comets has received a new impetus. Everybody knows this famous comet and when the predicted orbit for its current return was published in 1977, several astronomers started a systematic search to recover the object.

Apart from the honour of being the first to see P/Halley (P/ is used for *periodic* comets with periods of less than 200 years), there was also a very practical aspect. No less than four spacecraft are planned to intercept Comet Halley in 1986, and it was of obvious necessity to learn, as early as possible, the exact orbit of the comet upon its return.

Following the recovery 5 m Palomar observations, teams of astronomers at the Kitt Peak 4 m and the Canada-France-Hawaii 3.5 m telescopes were immediately successful in detecting P/Halley. At ESO, the first (unsuccessful) attempts were already made in 1980, with the ESO 3.6 m telescope on photographic plates and with the Danish 1.5 m telescope by means of the electronographic McMullan camera. These attempts were heroic but since at that time, as we know now, the comet's magnitude was certainly much fainter than 25, they were doomed from the beginning.

With the installation of a CCD camera at the Danish 1.5 m telescope, it became possible, during the past year, to observe extremely faint objects. It was, however, still somewhat doubtful whether it would be possible to observe P/Halley which according to the American and French observations would have a magnitude of approximately 24.5. The main problem was that extremely accurate tracking of the comet would be necessary to keep the few photons received from it falling on the same pixels of the CCD camera throughout the exposure. Since it was impossible to "see" the comet, *blind tracking* was necessary, that is letting the telescope follow the predicted motion of the comet, but without any possibility of checking that it actually does so.

Through a combination of very good seeing, exceedingly accurate tracking and admittedly a bit of good luck, Holger Pedersen was finally able to obtain the first ESO picture of Comet Halley on 10 December 1982. Near the centre of a 45-minute exposure through a broad-band filter (3700–7800 Å) there was a very weak spot which could barely be seen on the

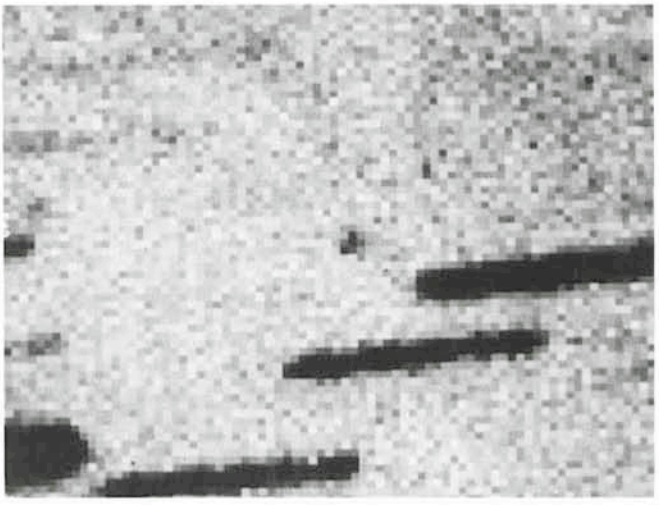

Fig. 1: *P/Halley as seen on 45-min broad-band (3700–7800 Å) frame, obtained with a CCD on the Danish 1.5 m telescope, January 14, 1983. 1 pixel = 0.47 arcseconds.*

Prof. Otto Heckmann, 1901–1983

It is with deep regret that we have to announce the death of Professor Otto Heckmann on 14 May 1983. Professor Heckmann was Director General of ESO from 1962 to 1969. An obituary will follow in the next issue of the *Messenger*.

cleaned and field-corrected picture. He brought the frame to ESO, Garching, where we were able to measure the exact position of the "spot", and we were happy to learn that, since the measured position coincided exactly with that predicted from the orbital motion, it was indeed P/Halley which could be seen in the frame.

H. Pedersen was again successful on 14 January 1983 when he obtained the picture shown here. Now there was no doubt about the reality of the object and, again, the position was correct. Indeed, the residuals from the expected motion are less than 1 arcsecond, and the ESO observations were a good contribution to the exact determination of the orbit and were therefore of some help to the planned spacecraft experiments.

Is Halley Active?

On the first picture the measured magnitude was 24.5 ± 0.3. It is indeed impressive that such a faint object can now be observed with a 1.5 m telescope! However, the measured magnitude on the January 14 picture was 23.5 ± 0.2, or 1 magnitude brighter! Even with the expected uncertainties it thus appears that P/Halley underwent a definite brightening during a few weeks. This could be due to the onset of nuclear activity, that is vaporization of the ices in the comet nucleus or, perhaps, rotation of the nucleus.

Nobody knows for sure what the nucleus of the comet looks like, and the ESO observations cannot alone give any answer to that. Still, with the addition of further observations at other telescopes, it may perhaps become possible to learn at which distance the activity of the nucleus first sets in and also whether the tiny object (estimated at 6 km diameter by the French group) rotates, or not.

H. Pedersen and I expect to carry through a long series of observations of P/Halley during its next opposition in early 1984. We hope, by obtaining several frames every night during a period of two weeks, to learn whether regular light variations are present and to measure the rotation period, if possible.

International Halley Watch

In order to coordinate observations of Comet Halley, the International Halley Watch has been set up. This group of astronomers will take care of the planning of observations and the subsequent archiving of all data obtained during this Comet Halley apparition, so that future generations of astronomers can better profit from all the efforts. Anybody interested in performing observations of P/Halley should therefore contact one of the lead centers. He will then receive further information.

Please write to: Dr. Ray L. Newburn – IHW Lead Center, Western Hemisphere, Jet Propulsion Laboratory, 4800 Oak Grove Drive, Pasadena, CA 91103, USA; or Prof. J. Rahe – IHW Lead Center, Eastern Hemisphere, Astronomical Institute, Sternwartstraße 7, D-8600 Bamberg, FRG.

Comet 1983 d Passes the Earth

When Comet Halley was first observed at ESO, it was still at a distance of 10.5 AU or roughly 1,600 million km, or beyond the orbit of Saturn.

At the opposite range of distances, a newly discovered comet, IRAS-ARAKI-ALCOCK (1983d), passed only 4.5 million km from the earth on 11 May 1983. The European Southern Observatory was also involved in observations of this object, but in a somewhat unusual way.

When the IRAS satellite detected an infrared source in the sky towards the end of April 1983, it was not immediately known what kind of object it was. However, two amateur astronomers independently discovered 1983d, and by connecting the positions given by IRAS, Araki (Japan), and Alcock (UK), Dr. Brian Marsden of the IAU Central Telegram Bureau was able to calculate a preliminary orbit. It immediately became clear that 1983d would pass very close to the earth and that the object could become of exceptional interest. A telegram went out from the Bureau stressing the paramount importance of obtaining accurate positions in order to improve the precision of the orbit, so that observations could be made with large radio and optical telescopes at the closest passage.

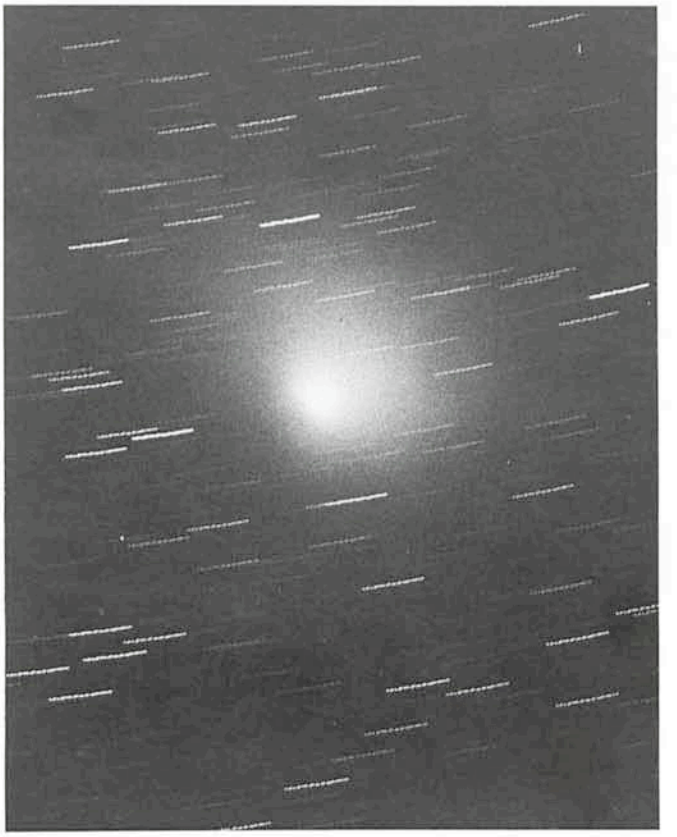

Fig. 2: *Comet IRAS-ARAKI-ALCOCK (1983d) observed by Mr. P. Stättmayer at Herrsching near Munich, on May 9.8 1983; exposure time 12 minutes on 103-aE emulsion.*

Upon reading the telegram in the ESO library at Garching, I wondered whether it would be possible in some way to obtain observations from Munich. Not being at La Silla, I felt that it would be useful to see whether any means were available, near the ESO headquarters, of obtaining these crucial positional measurements. I therefore contacted Mr. Peter Stättmayer of the Munich Volkssternwarte who runs an amateur observatory in Herrsching near the beautiful Ammersee, just south of Munich, and was happy to learn that he was willing to try to make photographic exposures of the object. Although the weather was not very cooperative, Mr. Stättmayer made a series of short exposures during the night between May 9 and 10, when the comet was moving rapidly across the sky at a distance of only 8 million km. We measured the 35 mm Tri-X frames in the same way as the large ESO Schmidt plates by means of the OPTRONICS measuring machine at ESO, Garching, and although the plate scale was only 3.5 microns per arcsecond (roughly 4 times smaller than that of the ESO Schmidt), it was possible to obtain an accuracy of approximately ± 2 arcsec. The principal error source was the diffuseness of the comet coma. We transmitted the positions to Dr.

Marsden about 12 hours after the observations and were quite happy to learn that they contributed significantly to the improvement of the orbit and thereby directly to the success of e.g. the radar experiments with the Arecibo and Goldstone antennas.

Late in the evening of 11 May, just after the closest approach to the earth, it was again possible to observe through a hole in the clouds over Munich, and this time Dr. Marsden received the positions only 4 hours later. (It should here be noted that this was only possible because there is no speed limit on the German highways!)

The above story is a nice illustration of how amateur astronomers can contribute significantly to our science. Without the dedication of Mr. Stättmayer, it would not have been possible to obtain these crucial observations and thus to help the professional astronomers pointing their telescopes in the correct direction.

Absolute Photometry of HII Regions

J. Caplan and L. Deharveng, Observatoire de Marseille

Today it is possible to observe HII regions not only in the visible part of the spectrum, but also in the radio, millimetre, infrared, and ultraviolet ranges. Combining photometric data from several of these wavelengths helps us to understand the properties of HII regions and of their exciting star clusters. But often, rather surprisingly, the measurements are quite good at these "exotic" wavelengths but only qualitative, or of low accuracy, in the optical region.

A few years ago we decided to try to remedy this lack of accurate absolute surface photometry of emission nebulae by constructing a special photoelectric photometer, which was modified in 1981 by the addition of a scanning Fabry-Perot interferometer. We have since used it at the Observatoire de Haute Provence in France and at the 50 cm and 1.52 m ESO telescopes at La Silla.

Choosing the Instrument

A grating instrument was immediately rejected. This kind of device is good for measuring accurate relative intensities of lines, but it uses an entrance *slit,* which has an inconvenient shape for comparison with radio maps and with photographs; also, total flux measurements are difficult. We chose photoelectric photometry with interference filters (and, later, a Fabry-Perot) because it is sensitive, accurate, can be put on an absolute scale using standard stars, and works with a circular diaphragm of much larger area than a slit. This makes it fairly easy to calibrate photographs, and we can generally arrange to have a diaphragm comparable in diameter to the beam of a radio telescope so as to facilitate radio/optical comparisons.

Nebular photometry requires accurate knowledge of the transmission curves of the filters used. Unfortunately, interference filters are often rather non-uniform in their transmission characteristics, especially near the edges. Therefore we place our filters in a collimated beam, near the image of the entrance pupil, rather than near the focal plane of the telescope as we do for less critical applications. Furthermore, we calibrate our filters *in situ:* we leave them in our instrument and illuminate the entrance aperture with light from a monochromator. Exactly the same part of each filter is used during calibration and during the observations, thanks to a mask placed at the image of the entrance pupil and adjusted at the telescope.

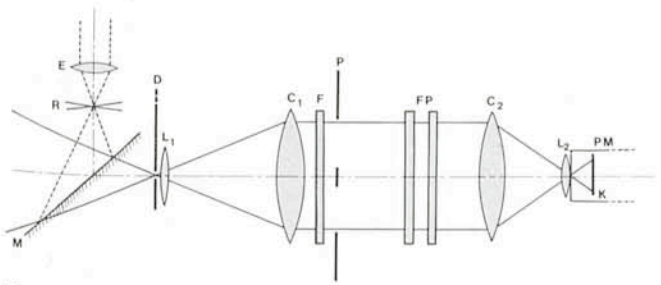

Fig. 1: *Basic optical design of the spectrophotometer, showing principal components. E: eyepiece; R: reticle; M: mirror; D: diaphragm; L_1: field lens; C_1: collimating lens; F: filter; P: mask (image of telescope entrance pupil); FP: scanning Fabry-Perot; C_2: imaging lens; L_2: Fabry lens; PM: RCA C31034 photomultiplier; K: cathode.*

Another requirement is high-accuracy pointing. Unlike stellar photometry, in general not *all* of the light from our emission region falls within the diaphragm. Thus interpretation of the observations requires accurate knowledge of the diaphragm's position. There is not always a star visible at the desired coordinates, so offset pointing is necessary. At the ESO 50 cm telescope, pointing of the telescope itself is sufficiently good for us to offset from a nearby star, but such accuracy is unusual. Hence our spectrophotometer has an x-y offset system which uses micrometer screws to shift the position of the guiding reticle and the eyepiece with respect to the diaphragm. This system was particularly useful at the ESO 1.5 m telescope. At the beginning of our observing run, we measured the relative positions of several stars and (by least-squares) derived the plate scale and a rotation parameter. We were then able to do offset pointing to better than a second of arc.

Photometric methods. So far we have described the basic properties of our instrument – as shown in Fig. 1 – except for the Fabry-Perot. Before proceeding further, it is useful to consider how we would use the photometer if we did not have the FP.

First, we must calibrate the photometer-telescope combination, using observations of standard stars through continuum filters for which the transmission curves have been accurately measured. This gives us an *effective collecting area,* which includes the effects of telescope size, reflectivities, photomultiplier quantum efficiency, etc. (but *not* the filter transmission). Now we can observe an H II region using a narrow-band (10 or 15 Å) filter centered on an emission line. Dividing the emission-line signal (in photons per second) by the transmission of this filter and by the effective collecting area gives us the line flux of the region. (Of course, we must correct for atmospheric extinction.)

The main problem is that, even with such filters, there is often a fair amount of continuum radiation which gets through

The article by D. Enard and G. Lund about "Multiple-Object Fiber Spectroscopy" will be published in the next issue of the *Messenger* (September 1983) and not in the present one as was announced in the *Messenger* No. 31.

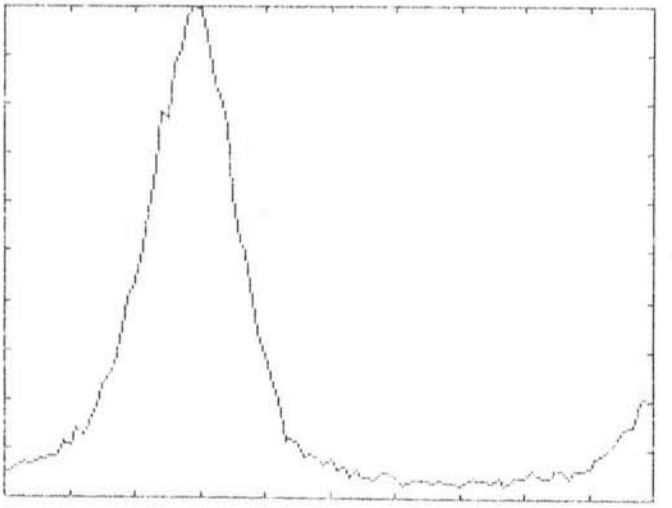

Fig. 2: *An Hα scan of the H II region N 79 in the LMC, obtained at La Silla (ESO 50 cm telescope, integration time 200 s).*

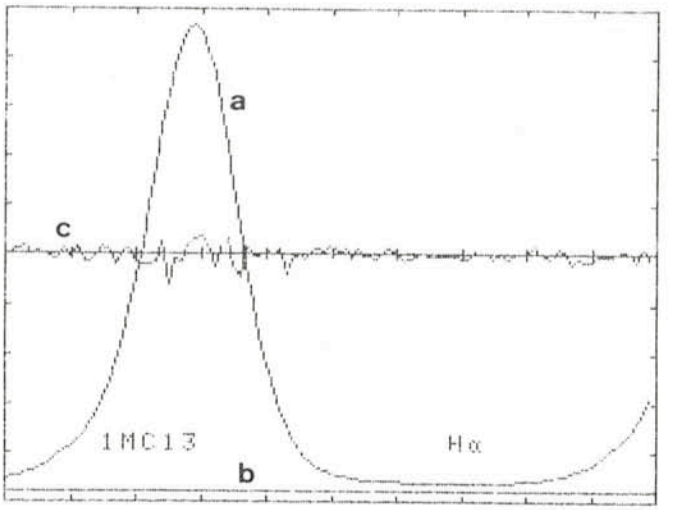

Fig. 3: *Least-squares fit to the scan of Fig. 2. The analytic function (a) representing the convolution of the instrumental profile with a Gaussian, plus a constant (b), is shown on the same scale as in Fig. 2. The residuals (c) are shown also.*

(particularly from OB stars embedded in the nebulosity). To correct for this, we must also measure the continuum radiation adjacent to the line. This is a rather delicate measurement, and a potential source of error.

The Fabry-Perot. The originality of our method comes from the use of a scanning Fabry-Perot interferometer in the photometer itself, so that we have, in the same instrument, rapid filter changes, choice of diaphragm, etc., plus the spectral scanning qualities of a spectrometer. A few years ago it would have been necessary to use compressed gas to scan the interferometer, but we use the extremely stable servo-controlled piezoelectric system developed by Hicks et al. (1974, *J. Phys. E. Sci. Instrum.* **7,** 27) at Imperial College in London.

Fig. 2 shows a sample scan obtained with one of the FPs we have used at La Silla. The total scan corresponds to 5.2 Å, which is somewhat greater than the free spectral range (distance between overlapping orders) of 4.4 Å. Profiles such as this allow us to study the Doppler broadening in H II regions, to detect line splitting, etc. From the photometric point of view, one advantage of observing the profile of each line is that we can detect unwanted night-sky emissions. But the principal advantage is that it simplifies the problem of correcting for the underlying continuum. Fig. 3 shows a least-squares fit, to the scan of Fig. 2, of the FP instrumental profile convolved with a gaussian, plus a constant representing the sum of the dark-count signal and the continuum. (This constant is slightly less than the minimum signal because the FP transmission is never quite zero.) This method is quicker than using a separate continuum filter. It is also more reliable, as it does not depend critically on the transmission curves of the filters. And it is a lot more satisfying to really see the continuum!

To find the absolute intensity in a line, we proceed as outlined above, measuring standard stars through wide-band continuum filters and the H II region through narrow-band line filters (but we do not need to measure the underlying continuum). For each filter *we scan the FP.* The stellar continuum measurements give us an effective collecting area which now includes the FP transmission averaged over one free spectral range. Reduction of the emission line scans gives us the line signal averaged over one free spectral range and corrected for the continuum. We simply divide this line signal by the effective collecting area and by the filter transmission to get the absolute flux for each line.

Instrument Control and Data Acquisition

The entire instrument is controlled by a Hewlett-Packard desktop computer which has a parallel I/O interface. A simplified block diagram is given in Fig. 4. A typical observation of an H II region might proceed as follows. The filter wheel rotates to the position of the Hβ filter. A preselected number (typically six) of 100-point FP scans (each lasting 17 seconds) are performed, and the scans are summed in the computer. The filter wheel then moves to the next requested filter, Hα, where the process is repeated (typically two scans). If these are the only two filters requested, the computer beeps, and we can display the observations on the screen. We can then ask for the observations to continue, or tell the computer to stop. The accumulated scans can be stored on data cassettes. The same microcomputer is used for our data reduction.

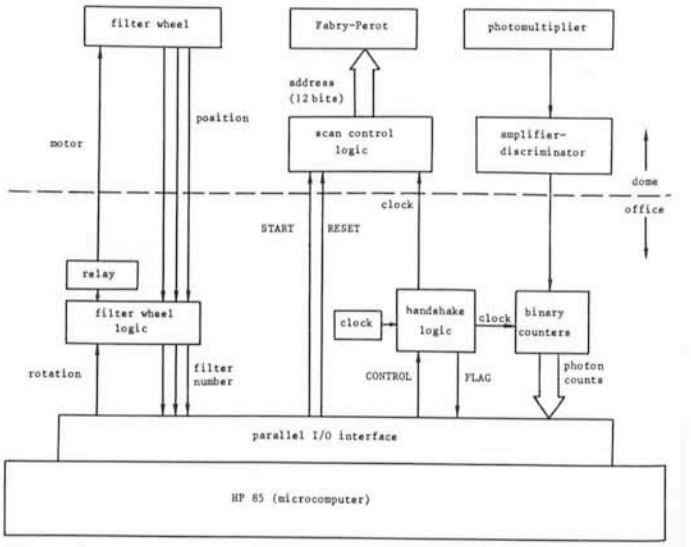

Fig. 4: *Block diagram of the microcomputer control and acquisition system.*

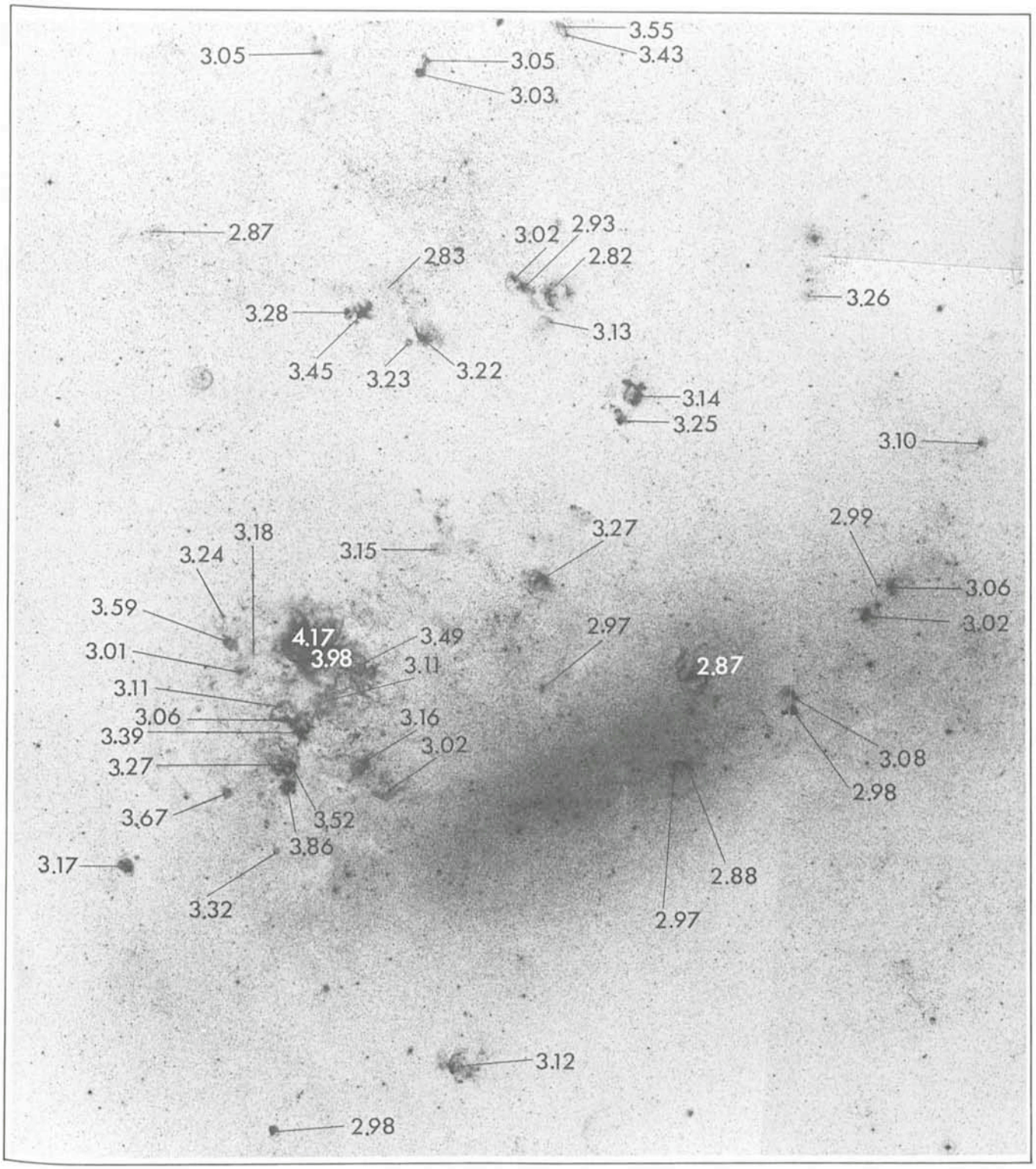

Fig. 5: *Hα/Hβ ratios for H II regions in the LMC, shown on a red ESO Schmidt plate.*

Example: Reddening and Extinction in the Large Magellanic Cloud

Extinction is an important parameter, especially for the interpretation of far UV observations. For example, a colour excess E(B-V) of 0.5 mag in the LMC corresponds to an "absorption" $A_{1600\ Å}$ of about 5 mag. Extinction corrections are thus crucial for determining the intrinsic properties of star clusters.

The extinction in the LMC is generally estimated from stellar photometry. But the far UV observations of Page and Carruthers (1981, *Astrophysical Journal* **248,** 906) show that around 70 % of the detected UV sources are associated with Hα emission (originating in giant H II regions ionized by these hot star clusters). Because of the nebulosity, stellar photometry in the H II regions, even when it exists, is of low reliability. Consequently the extinction is unknown for the majority of the LMC H II regions and associated exciting star clusters.

Extinction in H II regions can be estimated by comparison of the absolute Hα or Hβ fluxes with the radio continuum fluxes (of course, the optical and radio determinations must refer to the same points in the sky and must have comparable angular resolutions). Or we can measure the Balmer decrement – in particular the Hα/Hβ ratio – which provides the total extinction via the reddening law. If the extinction occurs well outside the emission region, and is uniform over the solid angle observed, these two methods are equivalent and give the same results for, say, A_v. In practice this does not always work. For example, Israel and Kennicutt (1980, *Astrophysical Letters* **21,** 1) show that A_v estimated from a comparison of the optical and radio fluxes of giant extragalactic H II regions is almost always greater than that derived from the Balmer decrement. These questions are discussed by Lequeux et al. (1981, *Astronomy and Astrophysics,* **103,** 305). Quite aside from any possible deviations from the standard reddening law, differences between the two determinations are expected if the external extinction is not uniform and/or if the dust is located within the H II region. Further effects arise because of scattering of the nebular light. Thus, comparison of these two determinations of A_v can give information on the characteristics and location of the dust.

Observations and first results. We observed about 50 of the optically brightest H II regions of the LMC with the ESO 50 cm telescope in December 1981. The circular diaphragm had a diameter of 4.9 arcmin, which allows comparison with the 6 cm continuum observations of McGee et al. (1972, *Australian Journal of Physics* **25,** 581) which were made with a 4 arcmin Gaussian beam. In addition, some regions were observed at several positions, with higher resolution. This was the case for N 159, which is formed of several small components and is situated near a region of active star formation.

Both atmospheric extinction and absolute instrumental calibration were determined primarily with the standard star χ Eri (Tüg, 1980, *Astron. Astrophys. Suppl.* **39,** 67). From each observation we have obtained the absolute Hα and Hβ fluxes and thence the Hα/Hβ ratio. Results obtained from repeated measurements, some with different filters and on different nights, indicate errors of a few per cent in the ratio.

Note that FPs are generally coated for a rather narrow range of wavelengths, and therefore cannot be used for *both* Hα and Hβ. Prof. E. Pelletier, of the Ecole Nationale Supérieure de Physique in Marseille, kindly supplied us with the special broadband dielectric coatings which were used for these observations.

Fig. 5 indicates the ratios measured in the LMC. Extinction in the Cloud is generally low. It is very low (or zero) for the regions located along the bar (N 23, N 103, N 105, N 113, N 119, and N 120). It is also low for all the large ring-shaped H II regions such as N 154, N 120, N 11, N 51 D, and N 206. The highest extinction (Hα/Hβ > 4, corresponding to E(B-V) > 0.3 mag), is measured in the 30 Doradus Nebula, and it remains high in the nearby H II regions N 157 B and MC 69. A relatively high extinction is also found in the direction of N 160 and especially of N 159 (Hα/Hβ ~ 3.9, corresponding to E(B-V) ~ 0.28 mag), H II regions situated at the edge of the LMC's largest H I molecular complex, an area of active star formation (as shown by the presence of OH and H_2O masers and of the only compact IR source yet observed in the LMC). The regions N 48, N 79, N 81, N 83, N 59, and N 164 also exhibit a relatively high extinction for LMC H II regions.

These ratios are generally consistent with those obtained for a few objects by Peimbert and Torres-Peimbert (1974, *Astrophysical Journal* **193,** 327) and Dufour (1975, *Astrophysical Journal* **195,** 315), with slit spectrographs. Comparison of the absolute fluxes with the radio measurements is underway. The results will be submitted to *Astronomy and Astrophysics.*

Concluding Remarks

Our spectrophotometer may soon become obsolete. A new generation of Fabry-Perot instruments, including the English TAURUS (see Atherton et al., 1982, *The Messenger* **28,** 9) as well as CIGALE, which we have developed at the Observatoire de Marseille, uses two-dimensional photon-counting detectors. The result is a wavelength scan for *each pixel.* So far, the emphasis with such instruments has been on kinematic work, but thanks to recent progress in detectors, there is no reason why they cannot be used for accurate two-dimensional photometry.

CN Orionis, Cooperative Observations for 24 Hours per Day Monitoring

R. Schoembs, Universitäts-Sternwarte, Munich

Introduction

When modern technologies open the possibility of astronomical measurements in wavelength regions from γ rays to the ultraviolet and from the infrared to the radio band, the visual range shrinks to a very small interval in the flux diagrams. However, the time of use of the necessarily complex and expensive instruments is very limited. Observing runs of an hour or so are of little use for the investigation of astronomical events like stellar outbursts which evolve with timescales of days. So even optical telescopes with apertures below 1 m still have a relevance for long-time observational programmes.

An interesting group of objects which is known to show variations in the time scale mentioned is the class of cataclysmic variables (CV). The general model for all members consists of a Roche lobe filling secondary (near the main sequence) which transfers matter via the Lagrangian point L_1 to the highly evolved primary, a white dwarf or neutron star. Due to its angular momentum the mass stream does not impact but rather surrounds the small primary, building a more or less circular accretion disk. A hot bright spot is produced where the initial stream collides with the already circulating material of the disk. By angular momentum exchange part of the disk material finally reaches the primary.

The increasing amount of information from all kind of observations has made clear that the class of CVs comprises many kinds of interesting objects like X-ray sources, oblique magnetic rotators with synchronized rotation or with rotation with

critical periods of up to 10s and systems emitting highly polarized radiation from strong magnetic fields of 10^7 G. Prominent properties of CVs are eruptions with a large range of amplitudes. The more violent events, nova eruptions (> 10 mag) are caused by thermonuclear runaways on the primary. This explanation is quite secure although the nova explosion of a system is so rare that until now it was observed only once for an individual object. The dwarf novae brighten up by a factor of 10 or 100 for a few days only, but every 10 to 1,000 days. In spite of the more detailed observations, there is no generally accepted explanation for their eruption.

Dwarf Nova Eruption and Theory

At present two models are under discussion, challenging observational and theoretical attempts in order to find the decisive result or argumentation. Certainly, the increased radiation of a dwarf nova eruption originates in the accretion disk. But no agreement has been achieved about the initializing mechanism. One hypothesis (Osaki, 1974) assumes that after an interval of quiescence during which the accretion disk accumulates the incoming material, an instability causes a sudden increase of the viscosity, yielding rapid outward transport of angular momentum and hence inflow of matter. Consequently, gravitational energy is released heating up the disk. The problem is that the physics of the viscosity and its variations are not well understood. The theoretical work of Meyer and Meyer-Hofmeister, 1981, is a step towards a better understanding. Currently there are still doubts whether this model can fully explain the observations.

The alternative hypothesis is based on theoretical work by Bath (1973) who found repeating instabilities in the secondary which cause an increase in the mass transfer rate. The disk is assumed to be stationary, i.e. the same amount of matter which enters into the disk leaves it through a transition layer onto the white dwarf. Since the disk luminosity is determined by the gravitational energy released from the throughput of material, a sufficiently increased mass transfer rate in a stationary disk would be seen as an outburst.

Observable Properties and Observing Programme

As mentioned before, the impact of the mass stream onto the disk's edge causes a bright spot, which is a relevant radiation source in many systems. Its manifestation in the lightcurve is a criterium for mass exchange and hence classification of the star as CV. Since the density in the stream and/or the outer disk fluctuates, corresponding variations in brightness are observed. In those cases where the orbital inclination is large ($i \gtrsim 50°$), the bright spot is obscured behind the disk for ½ of the orbital period, causing a hump-shaped lightcurve. Thus the hump intensity, flickering, phase and shape can be taken as indicators for the mass stream, its transfer rate, homogeneity, trajectory and cross section. All of these characteristics can be analysed in the case of CVs with $i > 75°$, since they show a hump and eclipses of primary, disk and bright spot. But until now only few such objects are known and they do not show outbursts very frequently. Non-eclipsing CVs with humps in their lightcurves are less appropriate, though still valuable for an investigation of the mass stream in the sense that some effect must be observed in the hump shape, intensity, or phase when the stream increases by an order of magnitude, as is assumed in Bath's model for the dwarf nova eruption.

Previous photometric observations of the hump during rise and maximum of an outburst did not indicate large variations of its amplitude. However, the results obtained during the bright phase are quite inaccurate since the relative hump amplitude decreases to a few per cent. If Bath's model applies, variations in the bright spot are expected before the disk brightens and at that time they should be easily detectable.

Dwarf nova eruptions are not exactly predictable, so that their observation generally is initiated by messages from the amateur astronomer associations. Thus the transition phase from quiescence to an eruption is scarcely covered by observations. Another complicating fact for the observations is that the increased mass transfer might last for a short time interval only. Such a mass pulse will endure at least for the hydrodynamical timescale of the secondary of the order of hours, equivalent to the orbital period. This guarantees that the flashing of the bright spot is principally observable and cannot be missed while being obscured by the disk.

The necessary observational programme is clear: Start a 24^h per day photometry of a dwarf nova in quiescence and continue until an eruption takes place (i.e. eventually for a whole eruption cycle). The selected object should at least show a hump in its lightcurve, the eruption cycle should be as short as possible and the object should be bright, since only small telescopes would be available for an observing run of approximately the outburst cycle. 24^h per day observations involve at least three observatories during summertime when the weather is good. More difficulties than usual arise in such programmes: The coordination of observing time at several observatories, the weather at different sites and the activity of the object.

The First Campaign

Joint observations for 16 nights could be organized at Cape Observatory, ESO and Hobart Observatory for December 1981. Dr. B. Warner kindly took care of the observations at Cape. Dr. B. Stolz from Sternwarte München travelled to Hobart Observatory and the author went to La Silla. The final selection of the object was facilitated by the help of the Royal Astronomical Society of New Zealand, which sent information about what was going on with the candidates befor our observing run. The favourite candidates were CN Ori and VW Hyi. CN Ori has a very short eruption cycle of 14 days, shows humps, but the orbital period was not exactly known at that time, its sky position was good, except that the full moon would come very close to it and it would be at the brightness limit during quiescence for the 50 cm ESO telescope. VW Hyi, the brightest southern dwarf nova, shows a hump and its sky position was optimal, far from the moon. But its outburst cycle is 30^d. The final choice depended entirely on their activity just before the start of the observations. Unfortunately, none of the eclipsing systems could be selected. A few days before the run, messages from F. Bateson, New Zealand, and Dr. B. Warner, South Africa, arrived, telling "VW Hyi in outburst!". Thus there was no chance to observe another eruption within the 16 days of our run. Unfortunately, CN Ori had also brightened, but there was still a possibility of another eruption. Hence CN Ori was selected, and this turned out to be right as can be seen from Fig. 1. Now the 50 cm ESO telescope had to be powered up by an image tube eyepiece, which had been taken along from Munich. This proved to be essential, since the minimum of CN Ori (fainter than 15.5 between the humps) happened to coincide with the date of full moon at a distance of around 20°. "Fortunately", the brightest nights before and during full moon have been the only cloudy ones and lost. During the night after full moon, with a seeing of 5–7" it was difficult but possible to centre the object. The important phase, 2 days before outburst until maximum light, was covered as shown in Fig. 1. It demonstrates clearly that there is no large variation in the hump amplitude, shape or phase just before the eruption. This rules

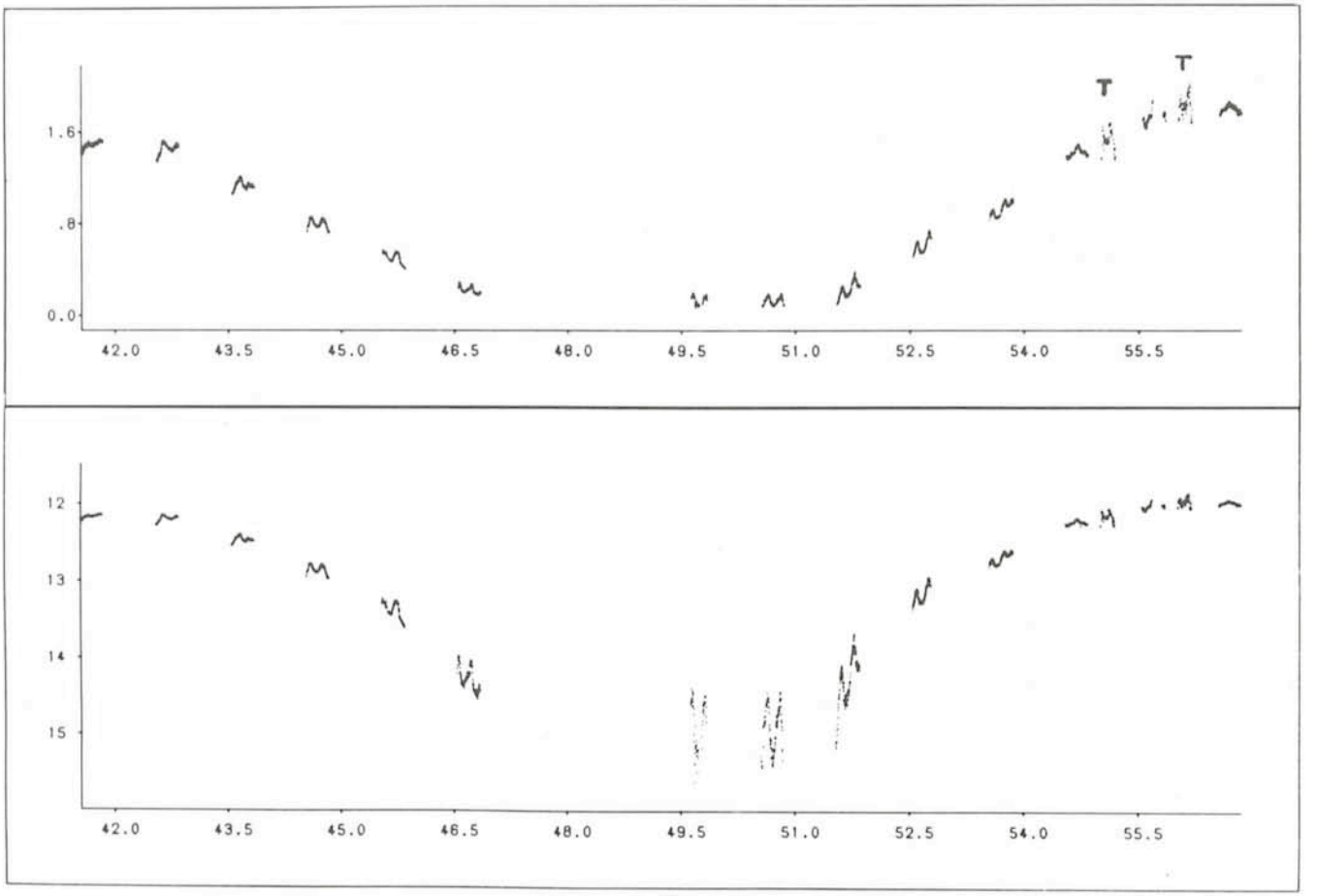

Fig. 1: *Lightcurves of CN Ori in white light (blue sensitive cathode S11) obtained during 1981, December 3 to 18 at La Silla and Hobart Observatory (denoted by T). Upper panel: Intensity ratio to a nearby comparison star. Lower panel: Magnitudes (λ_{eff} = 4000 Å). Time: HJD-2444900.*

out a relevant longer lasting increase in the mass transfer rate (Schoembs, 1982). A short mass burst could have been missed during the daily breaks. It is likely, however, that the eruption started with a symmetric brightening of the disk while the mass stream remained unchanged, i.e. the Osaki model can be applied. At the two other observatories, observations were almost completely frustrated by the weather conditions. Two nights of photometry were obtained at Hobart and only a few hours at Cape. The Hobart data (Fig. 1, runs marked by T) showed stronger variations than those of the ESO nights. Unfortunately, the intermediate La Silla observation, which also displays increased variations, is of low quality itself (break is due to passing clouds). On the other hand, a lightcurve obtained by Warner (1982) during another eruption in 1972 Feb. 17 shows a similar behaviour. So at that moment it was not possible to draw any other conclusion from the increased variability than that it is very important to observe this phase again. The increased light variations in the 3 consecutive runs near maximum around JD 2444955-56 may indicate irregularities in the mass transfer rate. But this must be interpreted in terms of feedback of the increased disk radiation to the secondary and not in the context of an initial instability as the reason for the eruption. Such feedback effects may also be important in the case of the so-called superoutbursts (SO). The cycle of SOs is larger and more regular than that of the normal short outbursts (NO), showing that an additional clock is effective. This clock could be the timescale of the secondary, which allows a reaction to the feedback, only after the corresponding interval of the order of 100 days (Vogt, 1983).

The fact that SOs were observed for the short-period systems only, may be understood in this context: The masses of the primaries do not depend strongly on the orbital period. Generally one may also assume that the disk luminosity in outbursts does not strongly depend on the period. Thus the

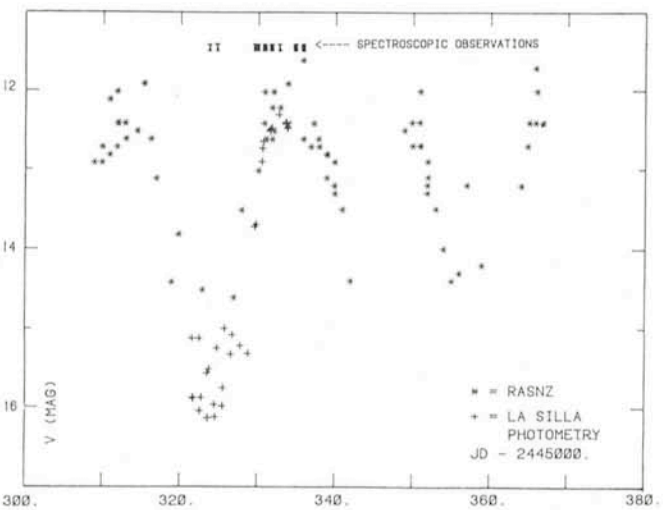

Fig. 2: *Visual magnitudes (*) of CN Ori as observed by the Royal Astronomical Society of New Zealand and magnitudes in white light (+) obtained at La Silla (S11 cathode) during 1982, November until 1983, February.*

secondaries in the smaller short-period systems are more affected by the outburst radiation. TU Men shows SOs although it has an unusual large orbital period but its outburst amplitude is also exceptionally large. Hence it is probable that both outburst models have their physical counterpart.

A periodogram analysis of the whole set of data for CN Ori revealed two similar photometric periods of $0^d.163$ and $0^d.159$. The longer one with approximately twice the amplitude of the shorter one. Double periods have been observed in the case of a few other CVs as well, e.g. V603 Aql.

The Second Campaign

The breaks in the photometric sequence, the detection of 2 photometric periods, and the increased variation at light maximum motivated another attempt for continuous observations in late 1982 from an increased number of sites including spectroscopy. The following observatories and observers participated in that programme:

Country	Observatory	Observation	Observer
Australia	Mount Stromlo	S	Barwig
	Siding Spring	P	Barwig
Brazil	São Paulo	P	Jablonski Steiner
Chile	La Silla	P/S	Seitter, Schoembs
India	Kavalur	P	Ravendran, Ashok
Israel	Mitzpe Ramon	P	la Dous, Schmid
Mexico	San Pedro Martir	P	Haefner
New Zealand	Auckland	P	Marino
South Africa	Cape	P	Warner
Spain	Calar Alto	P	Hartmann, Metz
Tasmania	Hobart	P	Waterworth

S = Spectroscopy: P = Photometry

Observations and Preliminary Results

This time CN Ori was at minimum and stayed so for a long time. 120 hours of almost uninterrupted photometry during quiescence were obtained. Later on, the weather caused several breaks. In total, observations from 28 days partly in UBVRI and/or white light and 75 spectra were collected. The photometric data have not all arrived in Munich, but reduction has been started. Final results cannot be given yet. Fig. 2 shows the visual brightness of CN Ori as obtained by the Royal Astronomical Society of New Zealand (*) and mean values obtained from observations in white light at La Silla (+). The large scatter is due to the unresolved hump in the lightcurve. Times of spectroscopic observations at La Silla are also indicated. The daily mean of the spectra taken at La Silla are shown in Fig. 3. They mainly could be obtained because of the kind cooperation of Prof. W. Seitter. A smooth continuum has been subtracted to demonstrate the variation of the lines. The first two spectra obtained during quiescence exhibit H_α and H_β in emission. Starting with the very beginning of the eruption, the spectra display broad absorption lines of Hydrogen and HeI which prevail throughout the whole bright stage. At maximum brightness the lines are strongest. The 6th spectrum is a single one, badly calibrated due to clouds; the line intensity is

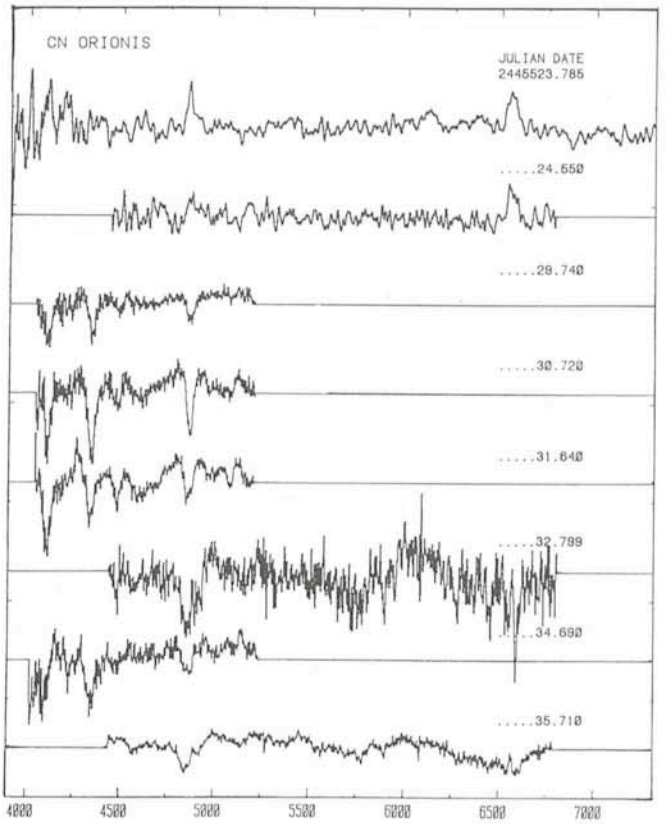

Fig. 3: *Nightly mean spectra of CN Ori obtained at La Silla during 1982, December 20 until 1983, January 1.*

exaggerated. Some spectra show emission wings of extreme width, occasionally symmetric or only on the red or blue side. In the later spectra narrow emission peaks within the broad absorption profiles of H_β and more clearly H_α can be seen. The absorption lines become weaker in the last two nights. There are indications of filling in by broad emissions. During the last night, variable cirri and moon light caused incomplete sky elimination. Hopefully the 37 spectra from La Silla together with additional 38 obtained at Mount Stromlo will allow to determine the orbital period from radial velocities and to distinguish which one of the two photometric periods is the orbital one.

Short-period Oscillations of CN Ori

The photometric data with high time resolution of the first campaign (roughly 100,000 integrations of 2 sec) were analysed for very short periodic light oscillations, which are frequently observed in cataclysmic variables. If strictly periodic, they are explained by the rotation of an oblique magnetic white dwarf. Dwarf novae often show transient oscillations during the declining part of the outburst. The periods vary inversely to the brightness. The relative amplitude of these oscillations is rather small ($< 1\%$) with a period around 30 s. Fig. 4 shows the power spectra of all nights from 1981. Two significant peaks are marked with the corresponding periods. They confirm the inverse correlation with the system brightness. Their relative amplitudes are of the order 10^{-3}. Interpretations of the mechanism are still speculative. Patterson (1981) showed that the observed quasi-periodic oscillations of this kind just exceed the period of critical rotation of the primary. Any relation of the oscillation period with the mass and radius of the primary would be quite important, since it could provide an additional method to determine the still relatively uncertain masses of the primaries in CVs.

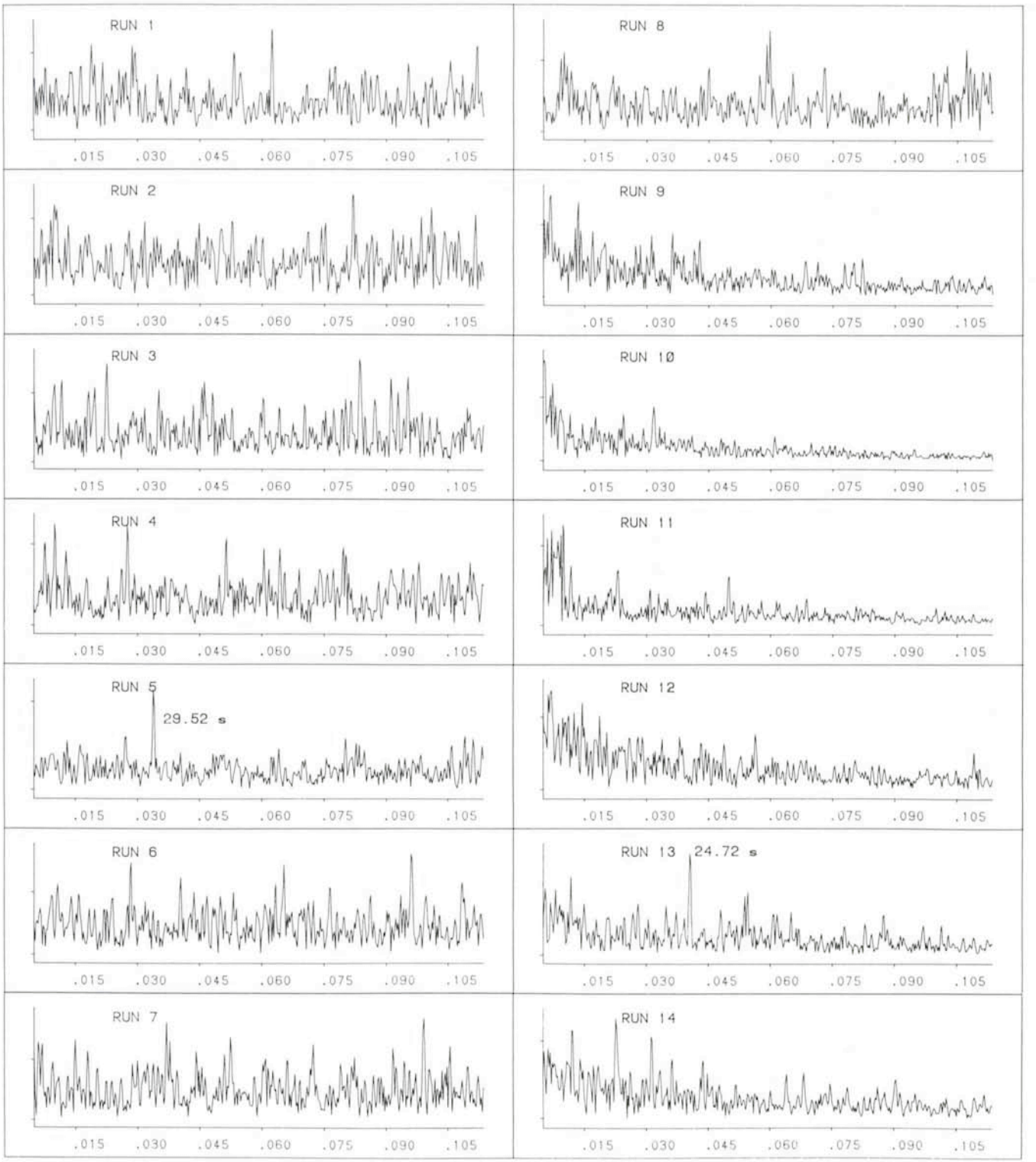

Fig. 4: *Power spectra of the photometric runs obtained at La Silla in 1981, December 3 to 18. Two significant periodic oscillations are indicated in runs 5 and 13. All other peaks remain below the 3σ significance limit.*
Ordinate: Relative Power. Abscissae: Frequency in Hz.

Acknowledgement

The author wishes to thank all participants in both of these campaigns, those who helped to organize, those who provided telescope time, those who observed and assisted in the observations, and those who helped and help to reduce the large amount of data. These campaigns were partly supported by the Deutsche Forschungsgesellschaft, grant Scho 255/2.

References

Bath, G. T.: 1973, *Nature Phys. Sci.* **246,** 84.
Meyer, F., Meyer-Hofmeister, E.: 1981, *Astron. Astrophys.* **104,** L10.
Osaki, Y.: 1974, *PASP* **26,** 429.
Patterson, J.: 1981, *Astrophys. J. Suppl.* **45.** 517.
Schoembs, R.: 1982, *Astron. Astrophys.* **115,** 190.
Vogt, N.: 1983, *Astron. Astrophys.* **118,** 95.
Warner, B.: 1983, MNASSA, preprint.

R136: The Core of the Ionizing Cluster of 30 Doradus

J. Melnick, ESO

Introduction

I first read that R136 contained a supermassive object some time ago in the Sunday edition of the Chilean daily newspaper *El Mercurio,* where it was announced that . . . "European astronomers discover the most massive star in the Universe!". Since *El Mercurio* is almost always wrong I did not take the announcement very seriously until the paper by Feitzinger and co-workers (henceforth the Bochum group) appeared in *Astronomy and Astrophysics* in 1980. More or less simultaneously with the publication of these optical observations, a group of observers from the University of Wisconsin, headed by J. Cassinelli (henceforth the Wisconsin group) reached the same conclusion on the basis of ultraviolet observations obtained with the International Ultraviolet Explorer (IUE).

After these papers where published, and since I have been interested in R136 for a long time, I started to consider the matter (a little) more seriously. I knew that R136 was in the centre of the 30 Doradus nebula but I had never heard of R136a before. Since, as you may imagine, 30 Doradus plays a crucial role in the whole story, I will give a brief description of this remarkable object.

The 30 Doradus Nebula and R136

The 30 Doradus nebula (thus named because it lies in the Constellation of Doradus) is an outstanding complex of gas, dust and stars in the Large Magellanic Cloud (LMC), the nearest galaxy to our own. Beautiful colour photographs of the LMC and the 30 Doradus region can be found in the December 1982 issue of *The Messenger*. The diameter of 30 Dor is several hundred parsecs and, although emission nebulae as large or larger than 30 Dor exist in other galaxies, none is found in our own. The visual light emitted by the nebula is produced almost entirely by hydrogen recombination lines and in order to maintain this radiation the equivalent of about 100 O4 stars (the hottest stars known have spectral type O3) are required. For comparison, the most massive stellar associations in our Galaxy, like the Carina nebula, for example, contain only a few such stars.

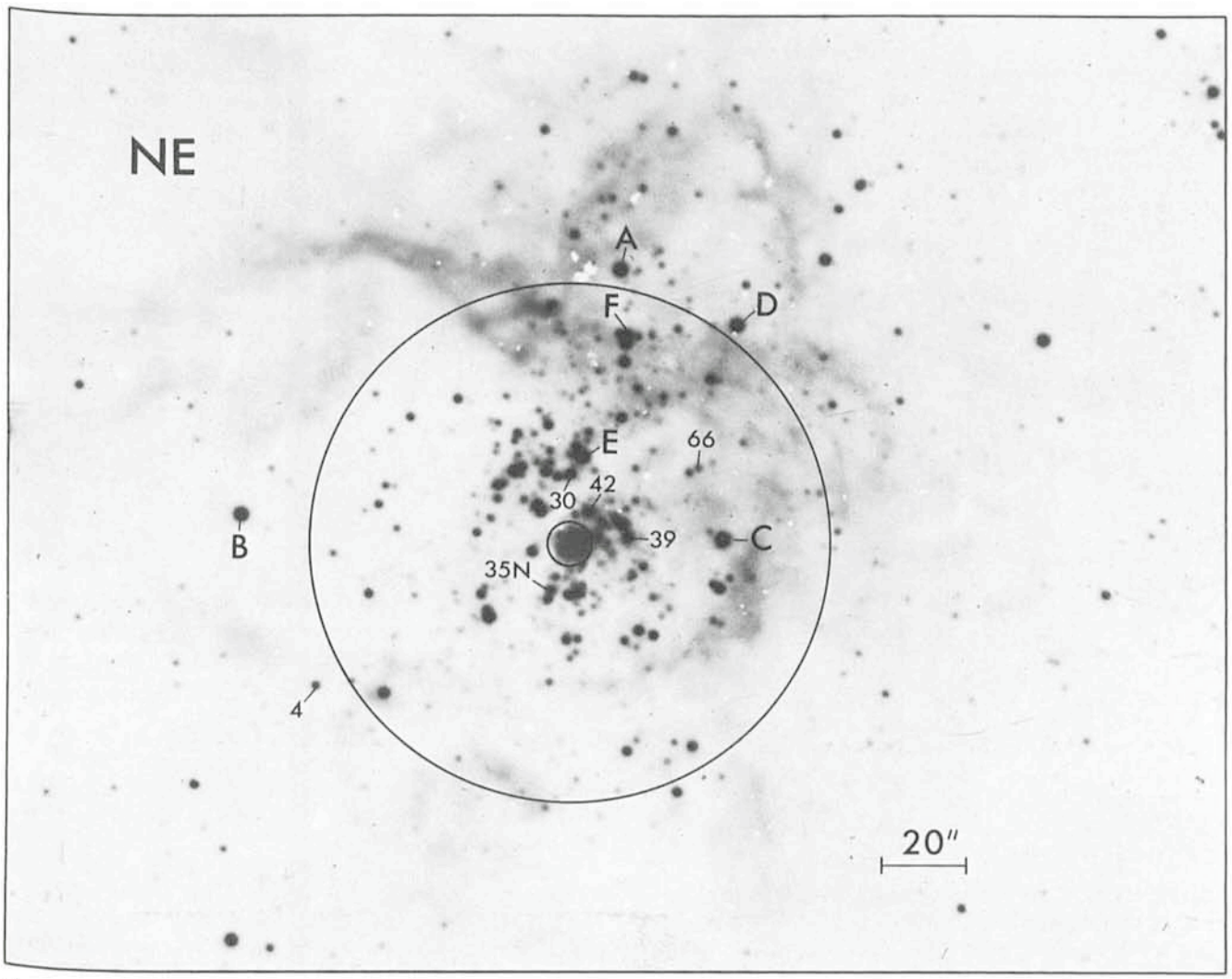

Fig. 1: *Negative enlargement of a 3-minute V exposure of 30 Doradus taken by Preben Grosbøl with the McMullan camera at the Danish 1.5 m telescope at La Silla.*

In Fig. 1 I have reproduced a visual electronograph of 30 Doradus exposed for 3 minutes with the Danish 1.5 m telescope at La Silla. The large circle in the photograph has a radius of one arc minute and marks the region I will refer to as the core of 30 Doradus as this region contains most of the central cluster stars as well as most of the nebular gas and dust. The diffuse object in the centre of the cluster is R136 (the 136th entry in the Radcliffe catalogue of LMC stars compiled in 1960 by Feast, Thackeray and Wesselink). Although R136 appears clearly non-stellar in the figure it looks almost stellar on small scale plates and this justifies its inclusion as an LMC star.

Some 10 years ago Nolan Walborn suggested that R136 was the unresolved core of the central cluster of 30 Doradus. This is why I was surprised when it was announced that R136 was or contained a single supermassive object. Using short-exposure photographs taken with the ESO 3.6 m telescope, the Bochum observers found that R136 contained three bright components (a, b and c), the brightest of which, R136a, is located more or less in the centre of the small circle drawn in Fig. 1. Components b and c lie NW of the centre and give R136 its "comma" shape.

A Supermassive Star

The distance modulus to the LMC is about 18.6 magnitudes. Thus, even if there was no extinction at all, it is clear that the brightest component of R136 must be extremely luminous since it is burned out even in the 3-min exposure reproduced in Fig. 1. In fact, the Bochum and the Wisconsin observers found that in the optical as well as in the ultraviolet the luminosity of R136a corresponds to the equivalent of more than 10 of the most massive O or Wolf-Rayet stars known. Thus, if R136a is a single object it must be extremely massive indeed.

Several other arguments have been presented in favour of the supermassive nature of R136a. I will not discuss these arguments in detail since all make the a-priori assumption that R136a must be a single object and/or that it must provide most of the energy required to ionize the 30 Doradus nebula. The crucial question therefore ist: What is the size of R136a?

Two groups have used the technique of speckle interferometry to determine the size of R136a. (A description of the speckle interferometry technique is given on page 23 of the *Messenger* No. 30, December 1982.) This is a very difficult experiment because, even when using the largest available telescopes, this technique can only be used for bright stars and because the interpretation of speckle observations for complex objects is somewhat subjective and therefore often ambiguous.

Gerd Weigelt from the Physikalisches Institut, University of Erlangen, used the ESO 3.6 m telescope and (in his latest unpublished result) finds that R136a is dominated by 2 stars separated by 0.46 arc-seconds surrounded by about 4 other fainter stars, all superposed on a complex background. On the other hand, J. Meaburn and collaborators from the University of Manchester, using the Anglo-Australian 3.9 m telescope find that R136a is a single object and thence that its size must be smaller than the diffraction limit of the AAT which, at the distance of the LMC, corresponds to about 1,000 AU. Interestingly enough, in a recent preprint, Moffat and Seggewiss have remarked in the astrometric observations made in 1927 from South Africa by Innes (who finds R136a to be a multiple system at the centre of which is a double star) a separation, position angle and magnitude difference almost identical to that found by Weigelt.

Before proceeding with the discussion of R136a I will present my own (previously unpublished) observations of R136 and the 30 Doradus cluster which (I hope) will make the R136a story clear.

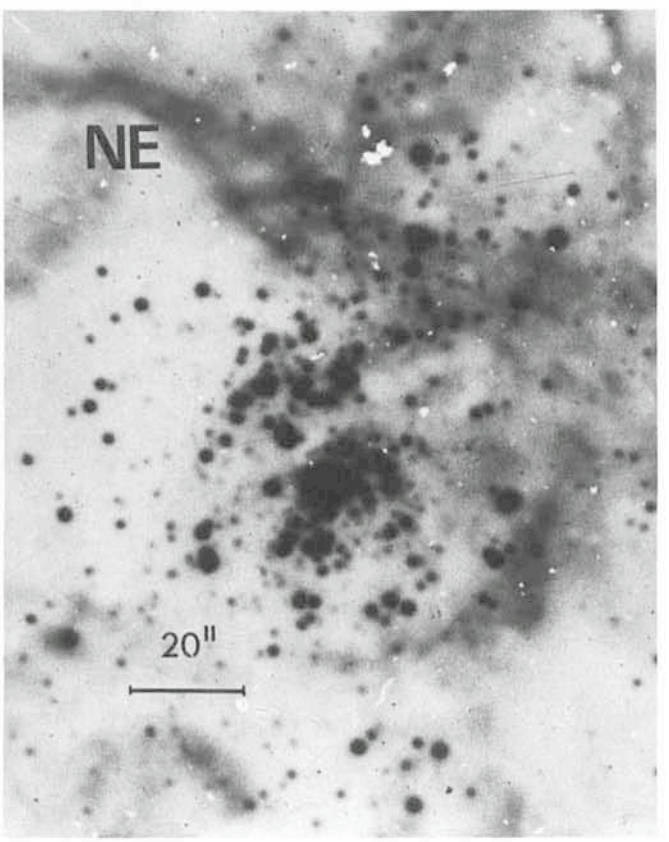

Fig. 2: *Contrast-enhanced version of Fig. 1.*

My Story

One of the principal motivations of the interest in R136 was the need to explain the energy source of the gigantic 30 Doradus nebula. In fact the effective temperature used in the early papers was derived assuming R136 produced most of the ionization of the nebula. Until recently, all that was known about the rest of the cluster was that it contained a large (in fact the largest known) concentration of Wolf-Rayet stars. However, most of these stars are late types (WN6–WN7), too cold to contribute significantly to the ionization of the nebula. Since WR stars are believed to be evolved O stars, it was considered that most of the stars in the cluster were too evolved to produce the large amount of ionizing photons required to account for the observed nebular emission.

In collaboration with Preben Grosbøl, I started a programme to obtain UBV electronographic photometry of a large number of stars in the core of 30 Doradus. Fig. 2 shows a contrast-enhanced print of our 3-min V exposure where the problems of doing photometry in 30 Dor are illustrated; a strong, highly inhomogeneous background and crowding. In fact photoelectric photometry is very difficult even far from the centre of the cluster because of the strong inhomogeneous background while photographic work is impossible because the nebular emission pre-flashes the plates. By comparison, the 40 mm McMullan camera at the Danish telescope combined all the features (good blue response – not available with most CCDs – fine grain, large dynamic range and linearity required for this project (and in fact for any photometry project). A set of programmes was incorporated into the ESO IHAP image processing system to handle this photometry which permitted to obtain reliable results down to about 15.5 magnitude (it is

now possible, using point spread function fitting techniques, to go fainter but our U plates are not sufficiently exposed).

In order to interpret the photometry, it is necessary to correct the observed UBV colours for interstellar extinction. Even a casual inspection of Fig. 1 or 2 shows that the reddening varies significantly from place to place in the nebula so that one must determine individual values for each star. In principle this is easily done in the UBV system if the wavelength dependence of the extinction is known. The parameters required are R = Av/E(B-V, (Av being the total visual extinction and E(B-V) the colour excess), and r = E(U-B)/E(B-V).

Since an extremely hot O star (say O3) has the same UBV colours as a much cooler one, and since it was necessary to verify the extinction properties of the dust, with the collaboration of Phillip Massey from the Dominion Astrophysical Observatory in Canady, I started a programme to obtain spectral types for a significant number of stars in the core of 30 Doradus using the image tube spectrograph at the 4 m telescope of the Cerro Tololo Interamerican Observatory. Combining the spectroscopy with the UBV photometry it is possible to check on the reddening problem, as well as to test the accuracy of the electronographic photometry and our ability to assign spectral types of very early type stars on the basis of UBV magnitudes and colours.

Preliminary (just out of the oven) results are presented in Figs. 3 and 4 which show colour-colour and colour-magnitude diagrams for stars within 2 arc-minutes from R136. The photometry is complete to V=15.0. The solid lines represent the ZAMS, the locus of hydrogen burning unevolved stars, and the effect of reddening on an O4 star assuming r = 0.79. Considering the photometric errors, the r = 0.79 line is seen to represent well the effect of reddening on the cluster stars. Combining the UBV photometry with spectral types for about 25 stars, and assuming a distance modulus of 18.6 to the nebula, I find that r = 0.79 and R = 3.1 (i.e. the galactic and Orion values) represent adequately the extinction law in 30 Doradus. As in the case of the Orion nebula, the detailed visual extinction law may be very different from the normal galactic curve.

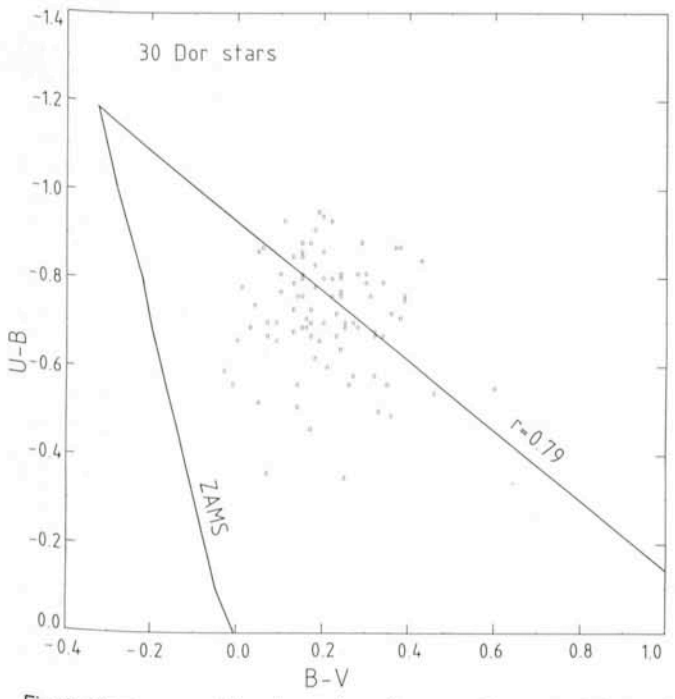

Fig. 3: *Electronographic colour-colour diagram of the central cluster of 30 Doradus.*

Fig. 4 shows the dereddened colour-magnitude plots. The line shows the ZAMS for early O-type stars taken from Schmidt-Kaler's review in Landolt-Bornstein. These plots show that most of the luminous stars in the nebula are early-type main-sequence stars. At first glance this may seem surprising, since the plot contains almost no ZAMS stars cooler than O3! In fact this is not so surprising. According to Schmidt-Kaler's review, an O4 ZAMS star has an absolute visual magnitude Mv = –5.2 which, for E(B-V)=0.6 corresponds to an apparent magnitude of 15.3, below the completeness limit of the photometry. I have marked in Fig. 1 a star of visual magnitude 14.3 (No. 4) which is classified as O3V from the slit spectrum and a star of V=15.0 (No. 66) classified as O3V(ZAMS) on the basis of its absolute magnitude and UBV colours. This illustrates the well-known (but apparently forgotten in 30 Doradus) fact that hot stars radiate very little at visual wavelengths.

Before returning to the discussion of the nature of R136a I would like to call your attention to the brightest stars in the core of 30 Dor. I have marked them A, B, . . ., F in Fig. 1 and I have listed in Table 1 their spectral types as determined from slit spectroscopy and their apparent magnitudes. Because these stars are too bright, giving saturation effects in the PDS scans, I have used published photoelectric observations.

TABLE 1

	Star	Sp. Type	V
A	R139	WN9 + O5	11.9
B	R145	WN6	11.9
C	R138	B0Ia	12.0
D	R137	B0.5Ia	12.1
E	R142	B0Ia	12.2
F	R140N	WC5	13.0

The important feature of the Table is that with the exception of R139 the brightest stars in the core of 30 Doradus are relatively cool OB or WR stars. I will return to these stars below. Now let us consider R136 once again.

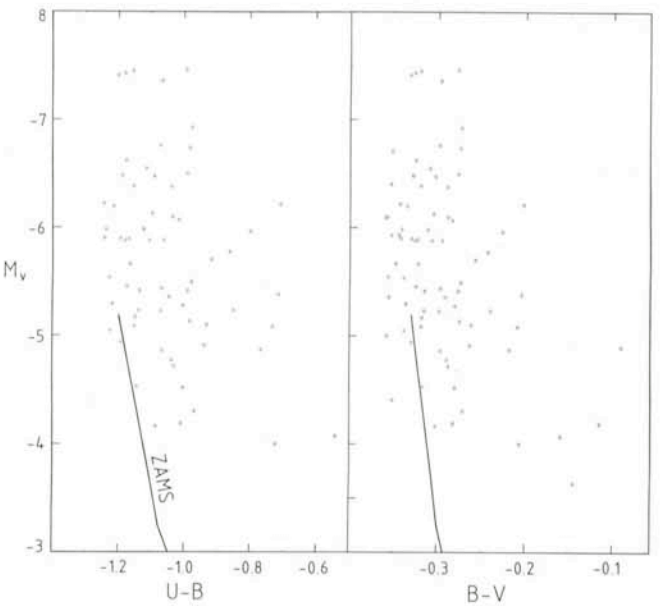

Fig. 4: *Colour-magnitude diagrams of the central cluster of 30 Doradus.*

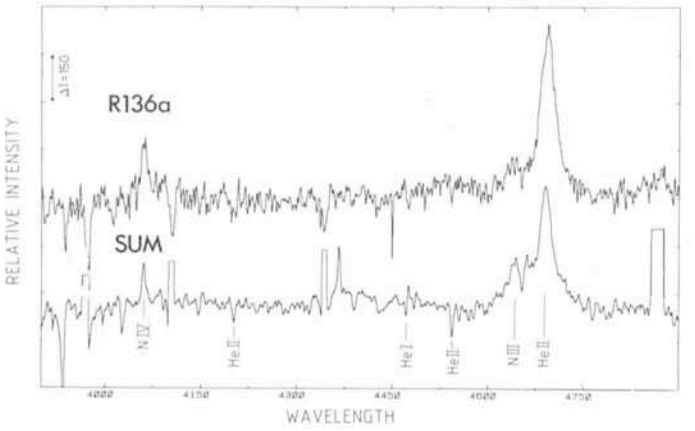

Fig. 5: *Comparison between the optical spectrum of R136a and the composite spectrum of the central arc-minute of the cluster.*

R136a: The Unresolved Core of the Ionizing Cluster of 30 Doradus

Most optical and all the ultraviolet observations of R136 have been obtained with apertures of 3 arc-seconds or larger. In fact most of the UV observations have been obtained through a 10 arc-second aperture. I have drawn in Fig. 1 a circle of 10 arc-seconds in diameter centered at R136a. Besides the components a, b and c, several other stars lie within this circle. Spectra of some of these stars obtained with the Intensified Reticon Scanner of the Du Pont telescope at Las Campanas on a night of magnificent seeing show that R136c and possibly R136b are WN7 stars while some of the others appear to be very early O stars. (Unfortunately, I have not yet received the data tapes, and these classifications are based on a quick look of spectra at the telescope.) It is, therefore, clear that, to be able to say something about R136a, we can only consider observations taken with a small diaphragm. This has been recognized by the Wisconsin workers who in a recent preprint have restricted their analysis to IUE observations taken with a 3 arc-second slit. Therefore in what follows, whenever I talk about R136a I will be explicitly referring to the central 3 arc-seconds of R136.

Because (as I mentioned above) the photometry is not complete down to ZAMS stars of types O4 and fainter, I will restrict the analysis to the central one arc-minute of the cluster. Also, since mass segregation may be important in 30 Doradus, it is more appropriate to compare R136 to the central part of the cluster.

Within one arc-minute from the centre, the mean colours of the cluster (excluding R136) are B-V = 0.16 and U-B = 0.72. The mean colour excess is E(B-V) = 0.46 identical to the value determined by the Bochum observers for R136. I am not aware of any photoelectric determination of the UBV colours of R136 with a diaphragm of 3 arc-seconds (or smaller); Using a 15 arc-second (diameter) aperture, Van den Bergh and Hagen give (U-B) = –0.75 and (B-V) = +0.14, slightly bluer than the mean colour of the rest of the cluster (although the difference is within the errors of the photoelectric observations). Thus if R136 is a composite object, it must contain a mixture of stars similar to that of the rest of the cluster. An independent check of this hypothesis may be obtained by comparing the spectrum of R136a with the sum of the spectra of the individual cluster stars. This is shown in Fig. 5. The spectrum of R136a is the sum of 24 Vidicon frames which I will discuss in detail below. The sum spectrum was obtained adding PDS tracings of the image tube spectrograms of each star, converted to intensity and weighted by the blue magnitude of the stars. The emission component of the composite spectrum is seen to be of slightly later spectral type than R136a while the converse is true for the absorption spectrum. The closest spectral type I can find for R136a is WN4.5+O6–7, in good agreement with the classification given by Conti and Ebbets from photographic spectra. The O6–7 type comes from the ratio of the He II λ 4542 to He I 4471 lines and is not affected by nebular emission since neither of these lines is present in our spectra of R136 out to a radius of 10 arc-seconds. The sum spectrum would have a type WN6+O5–6. Our classification for R136a differs from the type O3f given by Vreux and collaborators on the basis of their near infrared spectrum of R136a, and from the similar classification given by the Wisconsin observers from the UV spectrum. This indicates that R136a must be a composite object. The presence of the Si IV λ 4089 line in the optical spectrum of R136a is a further indication of its composite nature.

It is reasonable to assume, therefore, that R136a contains a mixture of stars similar to that found in the central arc-minute of the cluster. Using the UBV colours and the absolute visual magnitudes, I have estimated spectral types for all stars brighter than V_o=13.0 (visual magnitude corrected for extinction) in the central part of the cluster. From these, and the spectral types obtained from the image tube spectrograms, I find that there are about 30 O3–O5 stars and 10 WR stars in the core of 30 Doradus (this number is a lower limit since, as I mentioned above, the photometry is not complete for types O4V and O5V). The integrated apparent magnitude of the cluster is V=9.0; For R136a, the Bochum observers (also Moffat and Seggewiss) give V=10.8 corresponding to about 20 % of the cluster light since the extinction is similar in the two cases. Thus I conclude that R136a must contain more than 6 O3–O5 stars and more than 2 WR stars. The number of WR stars is uncertain because I cannot distinguish WR stars from late O and early B supergiants on the basis of the UBV photometry alone and I therefore have only counted WR stars observed spectroscopically.

The Wisconsin observers estimate that 10 to 15 of the most luminous known O or WN stars would be required to account for the observed UV luminosity of R136a. However, they have multiplied the observed fluxes " . . . by the standard factor of two to account for light losses in the (small) aperture". Since this correction is not appropriate for extended objects, only 5 to 8 stars are required, in excellent agreement with the number predicted above. But even 5 to 8 of these extreme stars would be quite extraordinary according to the Wisconsin workers

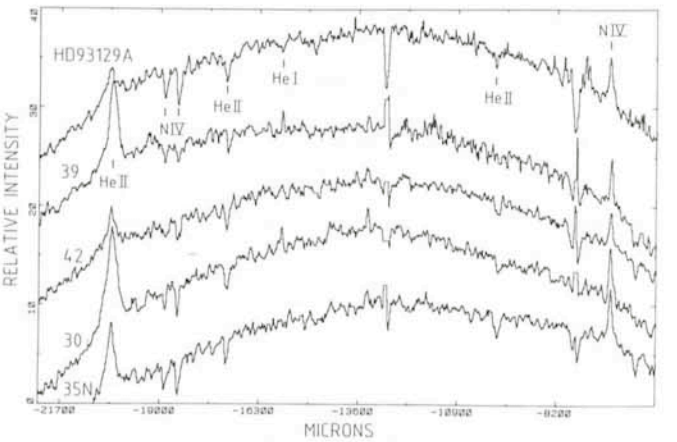

Fig. 6: *Optical spectra of very early supergiant O stars near R136. All stars shown have luminosities comparable to that of the most luminous star in the Galaxy, HD 93129A, also shown in the figure.*

since only two are known in the LMC. In Fig. 6 I show spectra of 4 very early O supergiant stars in the central part of the cluster very close to R136. I also show in the figure the spectrum of HD 93129A, which according to Conti and Burnichon is the most luminous star in our Galaxy. The 30 Doradus stars shown in the figure have bolometric luminosities similar to HD 9319A (some are even larger)! It is natural to expect more of these stars in R136a, especially if mass segregation effects are important.

At a distance of 53 kpc, 3 arc-seconds correspond to a diameter of about 0.8 pc, large enough to contain hundreds of stars. In fact galactic globular clusters have cores in this range of diameters. But, what about the speckle results?

The speckle interferometry results were obtained at optical wavelengths. As I have shown above, very hot O stars (which dominate the UV flux) are in fact very faint in the visible; as seen by the speckle, a compact group of these stars would not be resolved and may be what the speckle observers have called "complex background". In turn, later type O stars or late WN stars are much cooler and radiate much of their energy at optical wavelengths. This fact is illustrated in Table 1 where the most luminous stars in 30 Doradus in the visual band can be seen to be relatively cool compared to the hottest stars in the nebula. Thus, most likely, the speckle experiments have just detected one or two WN stars in the centre of R136a, probably the stars seen by Innes in 1927. After allowing for seeing effects, Moffat and Seggewiss find that within a diameter of 1.5 arc-second, R136a has a visual magnitude of V=12.1 even fainter than some of the stars listed in Table 1. Two of these stars (as seen by Weigelt and Innes) would then make up the optically (but not necessarily UV) brightest component. In order to test this hypothesis, in collaboration with Hernan Quintana from the Universidad Católica de Chile, I have obtained spatially resolved spectra of R136a with the 4 m telescope at CTIO. The slit was 0.5 × 3 arc-seconds centred in the brightest part (centre) one second of arc north (N) and one second south (S) of this position. Tracings of these spectra (each corresponding to an average of 8 Vidicon frames) are shown in Fig. 7. The spectrum is seen to vary significantly from north to south, particularily the emission line component (disregard the changes in the continuum which are due to atmospheric refraction. Also the zero point of the continuum has been shifted to separate out the components) changing from WN4.5 in the centre and N to WN7 in south. The asymmetry of the He II λ 4686 line may be due to absorption lines from early O-type stars (this is most prominent in S) which would imply that the O component of R136a is dominated by main-sequence stars.

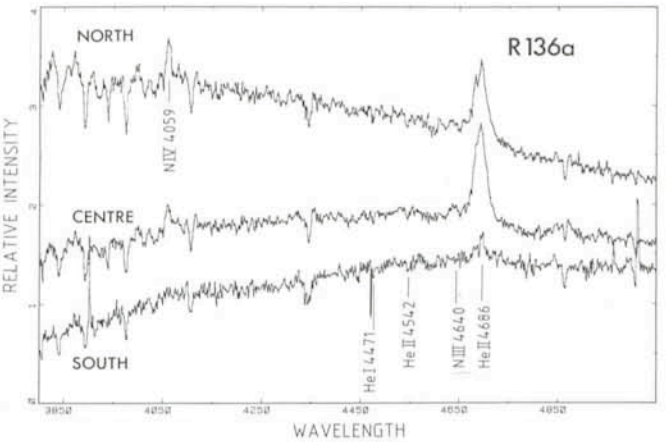

Fig. 7: *Spatially resolved spectrograms of R136a taken with a slit 0.5 arc-second wide and 3 arc-seconds long. The offset between centre and north or south is one arc-second.*

Epilogue

R136 is clearly the unresolved core of the ionizing cluster of the 30 Doradus nebula. It contains many very hot O stars which account for the observed UV luminosity and effective temperature. R136 also contains several late-type WR stars which account for the observed optical and infrared properties. The visually brightest of these WR stars, R136a, is the star (or 2 stars) found by the speckle interferometry. The luminosity, colour and infrared properties of this star are similar to that of other bright WR stars in the nebula. Most of the radiation required to ionize the nebula is emitted by stars outside R136. R136 itself contributes less than 30 % of the ionizing flux.

In their recent preprint, Moffat and Seggewiss, using data complementary to those I have presented here, reach the same conclusion regarding the nature of R136a.

References

To make the text easier to read, I have not included formal references. Complete references to most of the papers I have mentioned can be found in the article on R136a by Schmidt-Kaler and Feitzinger published in the proceedings of the ESO conference "The Most Massive Stars". All other articles I refer to are preprints kindly sent to me by the authors.

Stellar Granulation and the Structure of Stellar Surfaces

D. Dravins, Lund Observatory

Convection in Stars

Stellar convection is a central but poorly understood parameter in the construction of stellar models and the determination of stellar ages, influencing both the energy transport through the atmosphere and the replenishment of nuclear fuels in the core. The motions in stellar convection zones probably supply the energy for generating magnetic fields, heating stellar chromospheres and coronae, driving stellar winds, and for many other nonthermal phenomena. The inhomogeneous structure of velocity fields on stellar surfaces complicates the accurate determination of stellar radial velocities. Further, the temperature inhomogeneities on stellar surfaces induce molecular abundance inhomogeneities and entangle the accurate determination of chemical abundances.

New diagnostic tools are now making stellar atmospheric convection accessible to direct study. From solar physics has come the realization that effects from solar granulation (Fig. 1) are visible also in the spectrum of integrated sunlight, i.e. the Sun seen as a star (Dravins et al. 1981). Consequently, also the effects of stellar granulation should be visible in stellar spectra. Theoretical models of inhomogeneous atmospheres, incorporating three-dimensional, radiation-coupled, time-dependent hydrodynamics of stellar convection, have been

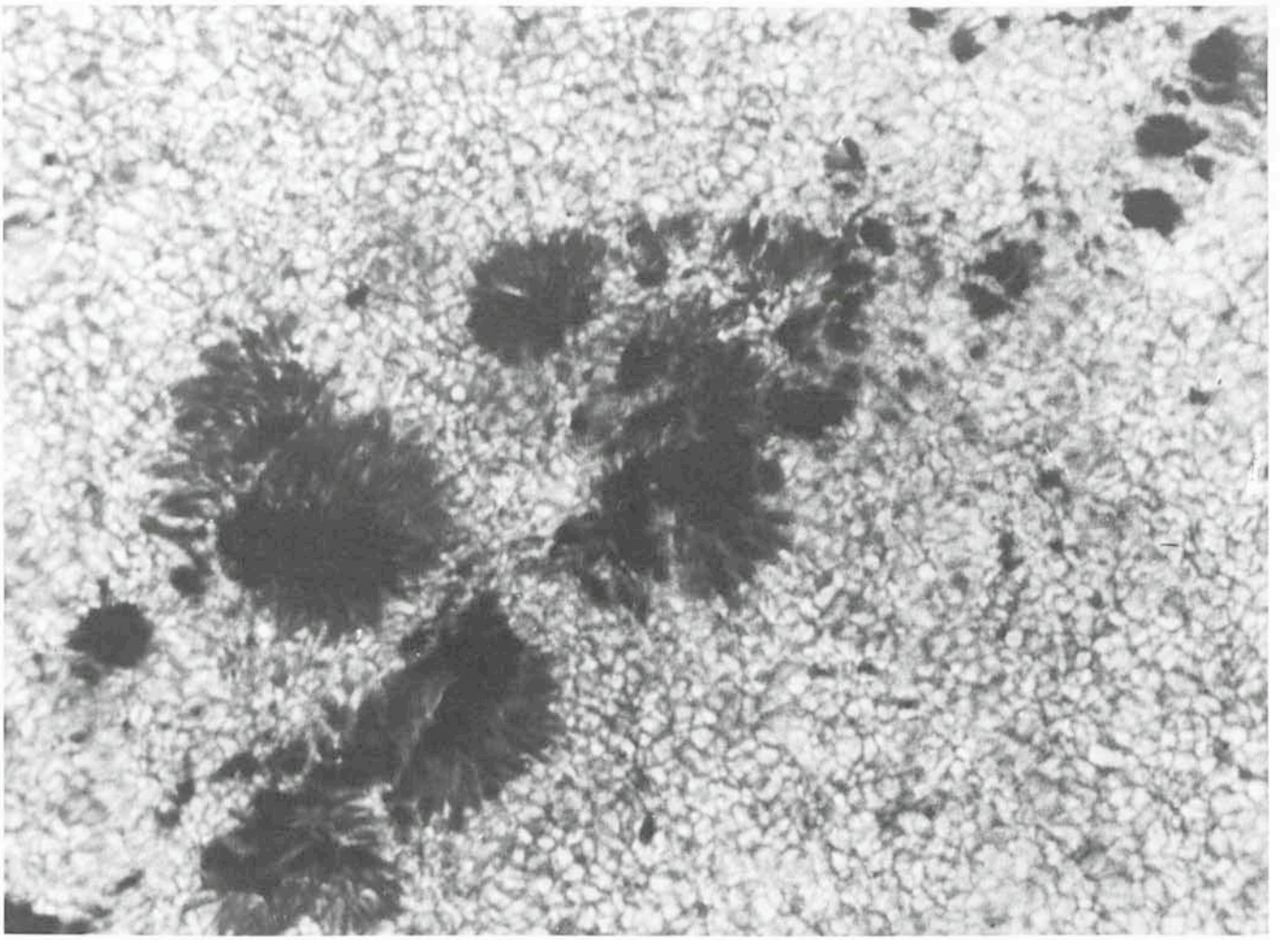

Fig. 1: *The solar surface gives a hint of what stellar surfaces may look like. In this white-light photograph, the convection cell pattern of solar granulation is prominent outside the dark sunspots. The effects of granulation are also manifest as subtle effects in the spectrum of the Sun seen as a star, and the corresponding phenomena in other stars are now being studied with the new coudé echelle spectrometer on La Silla. This photograph was recorded by G. Scharmer with the Swedish solar telescope on La Palma.*

developed and have successfully reproduced observed solar properties (Nordlund 1978, 1982). Work is now in progress to extend this to other stars. Taken together, these methods promise to open up stellar convection and stellar atmospheric inhomogeneities to detailed investigation (Dravins 1982a).

Such studies, however, are rather demanding, both on the observational and on the theoretical side. Granulation causes only rather subtle spectral line asymmetries, amounting to equivalent Doppler shifts of only some hundred m/s (Fig. 2). The measurement of such line asymmetries requires stellar spectra of much higher quality than has ordinarily been available. For each computation of a theoretical hydrodynamic model atmosphere, skilfully programmed codes require several hours for each run, even on very large and very fast computers such as CRAY or CYBER. However, the increased availability of powerful spectrometers and computers alike promise to make the study of stellar surfaces a fruitful one in the years ahead.

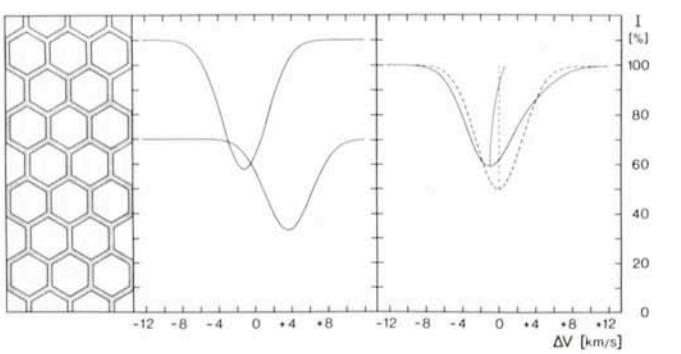

Fig. 2: *The correlation between temperature and velocity in stellar convection (hot elements are rising) causes slight asymmetries in photospheric absorption lines. In this model illustration, 75 % of the surface of a solar-like star is covered by bright areas of hot and rising gas, balanced by the downflow of cooler gas over the remaining 25 % of the surface (left). Spectrally blue-shifted profiles from hot, bright and rising elements contribute more photons than the darker, cool and sinking ones (centre). The resulting line profile, after averaging over the stellar surface, becomes asymmetric (solid curve at right) and its "C"-shaped bisector (median) demonstrates the asymmetry of the line. The dashed curve shows a classical symmetric profile, characteristic of classical stellar atmosphere concepts, dealing with homogeneous atmospheres containing turbulence only and without any organized velocity patterns.*

The ESO Coudé Echelle Spectrometer

At ESO on La Silla, an important new instrument has recently gone into operation, which permits one to obtain spectra of the required quality. This is the coudé echelle spectrometer (CES), primarily fed by the 1.5 m coudé auxiliary telescope, but also

accessible for the 3.6 m telescope via a fiber optics link. The progress of this instrument during its development has been reported in the *Messenger* by its main designer D. Enard (1977, 1979, 1981).

The CES is an instrument for the study of spectral line profiles. In its commonly used setup, it uses a multi-element detector, e.g. a Reticon diode array. This gives a very convenient way to obtain low-noise spectra of extended spectral regions, combined with high sensitivity. The spectral resolution ($\lambda/\Delta\lambda$) obtainable is about 100,000, corresponding to a Doppler shift of 3 km/s. Although this represents, by stellar standards, a very high resolution, it is still insufficient for serveral applications.

Actually, a lot of exciting phenomena in modern solar physics are studied from spectra featuring resolutions of up to one million. Further, such spectra are often recorded with Fourier transform or double-pass grating spectrometers with signal-to-noise ratios of the order of 1,000 : 1. Such low noise levels are not possible with any normal stellar spectrograph, irrespective of the detector used or the brightness of the star. Limitations arise because the optical construction of conventional stellar spectrographs, in the interest of light efficiency, does not sufficiently suppress stray light, which then contaminates the observed spectrum. Origins of such stray light may be e.g. diffuse scattering on optical surfaces or grating ghosts from a diffraction grating.

The Coudé Echelle Double-Pass Spectrometer

The CES incorporates a facility to allow observations of extremely high quality of selected spectral lines in very bright stars. It is possible to operate it as a double-pass scanner, a mode similar to that of several spectrometers used to record solar spectrum atlases. A double-pass spectrometer is characterized by the light passing the grating twice. After a first pass, a normal focused spectrum is formed inside the instrument. In a conventional system, the detector would have been placed at this point. However, in double-pass operation, the desired spectral element is transmitted through a narrow slit, while all other light is blocked off. The light is then sent back to the grating a second time to verify if really all of it is of the correct wavelength. Parasitic light of other wavelengths will not pass this test, and will not reach the exit slit to be detected by the photomultiplier. This forms a very efficient way of reducing stray light: the instrumental profile is, in effect, squared. If the straylight amplitude at some distance from the correct wavelength in conventional single-pass operation is 10^{-3}, say, in double-pass it will be down to 10^{-6}. Although the amplitude of stray light at any one point on the instrumental profile may appear small, the accumulated effects may cause a surprisingly large deterioration of spectral line parameters because stray light at any point in the spectrum is contributed from all other wavelengths. It was only after the introduction of double-pass spectrometers in the 1960s that the true shapes and depths of solar spectrum lines became known.

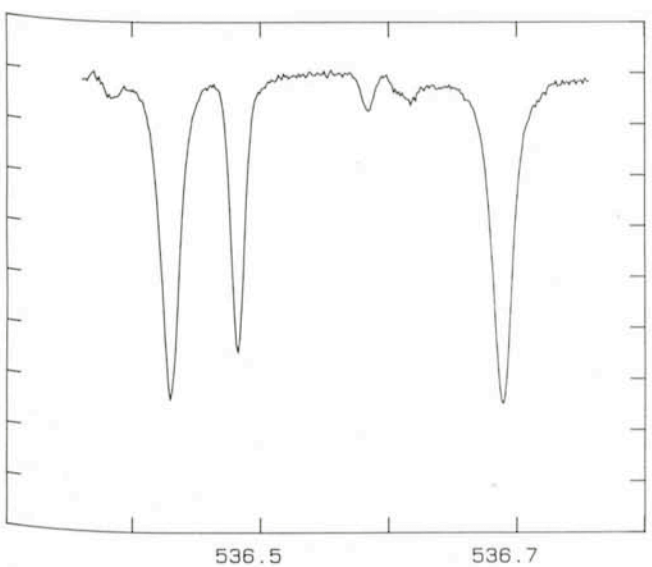

Fig. 3: *The coudé echelle spectrometer in its double-pass scanner mode can record stellar spectra with a fidelity that begins to be comparable to that in solar spectrum atlases. Here, a group of Fe I lines are seen in Alpha Centauri A, recorded with a nominal spectral resolution of more than 200,000. The numbers indicate approximate wavelengths in nanometres. The bisector for the leftmost line appears in Fig. 5.*

In addition, the CES double-pass mode doubles the dispersion and the spectral resolution since the set-up is equivalent to two identical echelle spectrometers in series. Consequently, recording of stellar spectra is possible with resolution $\lambda/\Delta\lambda$ of about 200,000. Further advantages include: uniformity of response and absence of pixel-to-pixel variations (since one and the same detector is measuring all spectral elements), and also constancy of focus and optical aberrations across the spectrum (assured by the placement of the fixed exit slit on the optical axis). The spectrum is scanned in wavelength by rotating the plane grating on its turntable. This scanning is done rapidly (typically 4 cycles per second) to reduce effects of atmospheric seeing variations.

Altogether, the CES double-pass system permits a superior recording of stellar spectra. Unfortunately, its high performance also carries a high price in photons and in observing time. Since only one spectral element is measured at any one time, the required observing times are much longer than for multi-element detectors. Nevertheless, it is an ideal instrument for the study of line shapes in the spectra of very bright stars (Fig. 3).

How to Detect Stellar Granulation

For several years, we have been working towards the goal to detect and study stellar granulation. Different high-resolution observations have been collected since 1975, and various feasibility studies carried out. For example, stellar observations have been simulated by convolving a solar spectrum atlas with instrumental profiles determined for actual stellar spectrographs, and the resulting spectrum analyzed. During the course of such studies, it was realized that the problem was more difficult than originally envisioned. The main obstacle is the presence of systematic (rather than random) errors in stellar data. Even a spectrograph resolution of 100,000 will perceptibly degrade the subtle asymmetries expected to be present in the spectra of solar-type stars. (Line broadening in even rather slowly rotating stars will cause a similar degradation.) Scattered light from distant wavelengths will induce fortuitous asymmetries, as will even symmetric instrumental profiles (because the stellar lines are asymmetric to begin with). In addition, the lines to be studied must be, as far as possible, free from blends. Merely to select candidate lines for detailed study requires an atlas-type high-resolution spectrum for each star in the programme.

To verify the ability to detect authentic line asymmetries, stellar spectrometers were used to perform observations of the Sun seen as a star. Such an observed spectrum can be checked against a standard spectrum of integrated sunlight, recorded with a more powerful spectrometer (Beckers et al. 1976). In the case of observations with the CES, integrated

sunlight can readily be obtained by pointing the coudé auxiliary telescope at the sunlight-illuminated dome of the 3.6 m telescope.

The analysis of such spectra gives a credible method to verify and optimize observing and reduction procedures, and to make the crucial solar-stellar connection. Fig. 4 shows these steps from solar to stellar photospheric line asymmetries. The bisector for the solar line, as measured by the CES, is reasonably similar to the "true" bisector from the Sacramento Peak atlas, and the sense of the small systematic deviation is consistent with the degradation expected from the lower resolution of the CES. The criticalness of the observations is illustrated by the noise bumps on the bisector that are well visible although, in the spectral continuum, more than 180,000 photons were accumulated in each 0.0013 nm (13 mÅ) wide channel. Similar observations have been made using different resolutions, different detectors and different spectrographs, confirming that the CES in double-pass with its highest spectral resolution yields the most truthful line bisectors. Although the CES is thus adequate to begin studies of stellar surface structure, it is not so by any wide margin.

Stellar Line Asymmetries

In our programme to search for photospheric line asymmetries, several brigth stars have been observed. In Fig. 5, samples of representative bisectors for lines in four stars are shown, illustrating the diversity of line asymmetries encountered. Lines in Canopus have a depressed blue flank close to the continuum, which accounts for that bisector's sharp turn towards shorter wavelengths. Possibly the line shape in this giant star may be influenced also by effects such as the atmospheric transition to stellar wind expansion. The asymmetry of lines in Arcturus is essentially opposite to that in the Sun, as noted already by Gray (1980, 1982).

The Structure of Stellar Surfaces

The shape of photospheric line bisectors is very sensitive to the detailed structure of stellar atmospheric inhomogeneities and convective motions, making bisectors a useful diagnostic tool to probe stellar surfaces. The most characteristic property of solar-type bisectors, their "C"-shape (Fig. 4) is caused by the vertical asymmetry of the granular velocity field (Fig. 2). An idealized way to see this is to consider the case of a very narrow line profile everywhere on the stellar surface. The spatially averaged profile then has the shape of the distribution function for the vertical velocities, e.g. a Gaussian in the case of Gaussian motions, etc. On the Sun, the relatively larger downward velocities in the intergranular lanes cause a distribution function with an extended "red" tail, which is the main cause of the upper redward bend of the bisectors. This characteristic solar property vanishes for a velocity field that is symmetric with respect to up and down. The line asymmetry becomes inverted if one instead has small granules with concentrated upward velocities, surrounded by larger areas of relatively gentle downflows. In such cases, the result is a ")"-shaped bisector, such as seen for Canopus (Fig. 5), and sometimes also observed over small areas on the Sun.

Spectral lines of different excitation potentials show different types of bisector, because different lines predominantly form in different surface inhomogeneities, e.g. the highest-excitation lines form mainly in the hottest elements. Lines in different wavelength regions will also show different bisectors because the relative brightness contrast in granulation (caused by a given temperature fluctuation in a blackbody radiator) decreases with wavelength, and thus changes the relative photon contributions from the hotter and the cooler elements.

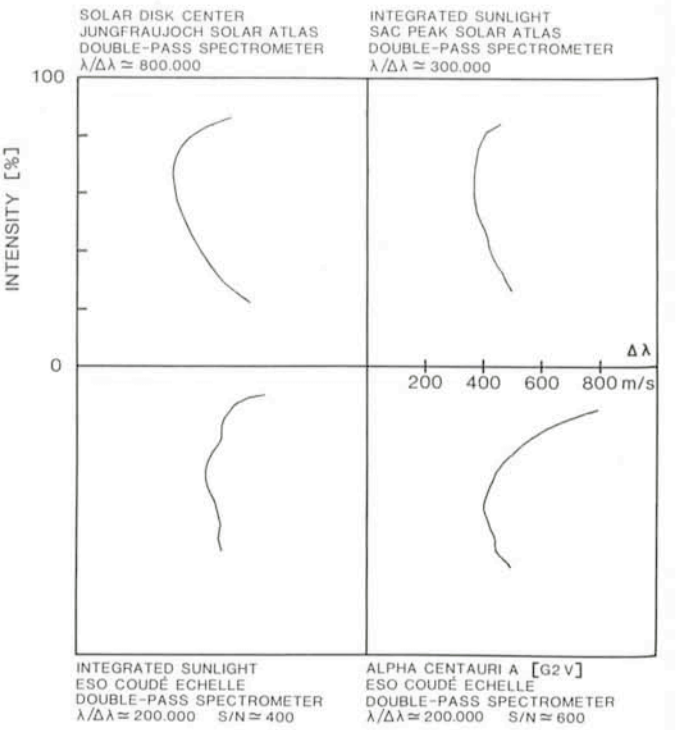

Fig. 4: *Observational steps towards stellar granulation. The asymmetry of an apparently unblended Fe I line is represented by its bisector (cf. Fig. 2), which shows the apparent radial velocity measured at different intensity levels in the line. For the Sun, the asymmetry is most pronounced at solar disk centre (top left), and somewhat less so in integrated sunlight (top right), because of e.g. line broadening due to solar rotation. At bottom left the same line of integrated sunlight is seen, as observed with the ESO coudé echelle spectrometer, confirming that instrument's ability to detect these subtle asymmetries. At bottom right is the same line in Alpha Centauri A. Although this star is of the same spectral type as the Sun (G2 V), it is actually somewhat more luminous and lies in the upper part of the main-sequence band in the HR diagram. The more pronounced asymmetry of this line in α Cen A might suggest more vigorous convection in this slightly evolved star that is clearly older than the Sun.*

For the Sun, such bisector behaviour has been studied, and it can be at least qualitatively understood from hydrodynamic model atmospheres (Dravins et al. 1981). For stars, such studies for different classes of lines are just beginning (Dravins and Lind 1983, Gray 1983).

Direct Observations of Stellar Surfaces

The probing of stellar surfaces through photospheric line asymmetries is, after all, only an indirect method that rests upon an extrapolation from solar conditions. In stars very different from the Sun, novel surface phenomena may well appear, e.g. in some stars the convection cells might be destroyed by "sonic boom" shock waves, generated when convective velocities reach the speed of sound. In cool stars, dust clouds might condense over the coldest surface formations. Quite possibly, our current understanding about stellar surfaces is even more naive than was our understanding about planets and moons before their exploration by spacecraft. To remedy this will ultimately require spatially resolved images of stellar disks and spatially resolved spectra for different parts of stellar surfaces.

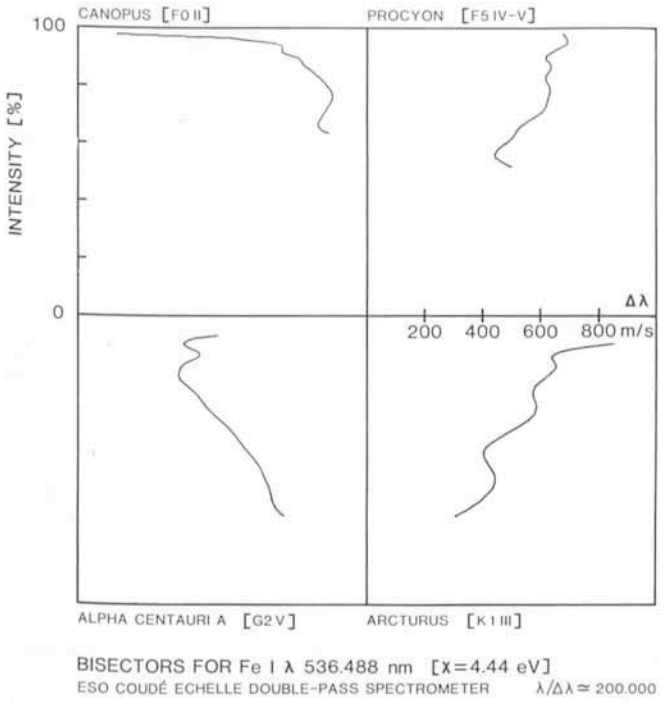

Fig. 5: *Considerable differences in surface convection patterns among different stars are here suggested by typical bisectors for four different spectral types. The small-scale undulations on the bisectors are due to noise, but their general slopes and curvatures are believed to be real. The bisector for the corresponding solar line is rather similar to that of α Cen A.*

Disks of a few stars with the largest angular diameters can be resolved already with current telescopes in the 4–6 meter range, while a fair number will become accessible to the planned very large telescopes. There are theoretical reasons to expect convection cells in giant stars to be much larger than those on the Sun: in fact, only a very small number of these might exist at any one time over the entire stellar surface. Optical phase interferometers currently under development promise to yield exciting data on such gross stellar structures.

Solar granules, however, have sizes around 1,000 km, only one thousandth of the solar diameter. Since a baseline of about 10 meters is required to resolve the disk of a nearby solar-type star, it will require a baseline a thousand times longer, i.e. 10 km, to resolve structures a thousand times smaller than a stellar diameter. The terrestrial operation of optical phase interferometers over such very long baselines would be coupled with formidable practical problems, caused by phase fluctuations in the Earth's atmosphere. However, an intensity interferometer (Hanbury Brown 1974), measuring not the interference between light waves, but rather the correlation between different telescopes of the quantum-mechanical intensity fluctuations in a source, is insensitive to phase, and can be operated regardless of a turbulent atmosphere. Intensity interferometry instead has various other limitations, including the circumstance that a faithful image of the source cannot be reconstructed in a simple manner. Rather the spatial power spectrum is obtained, i.e. information as to how contrasty the stellar surface is for different surface structure sizes.

As a spin-off from an ongoing development of a "quantum-optical spectrometer" at Lund Observatory, intended for studies of photon statistics with nanosecond resolution (Dravins 1982b), we are considering a possible modification of that instrument to be used for long-baseline intensity interferometry (Dravins 1981). In Fig. 6 potential baselines between telescopes around La Silla are marked. Of special interest is the 24 km baseline between the ESO 3.6 m telescope on La Silla and the 2.5 m Du Pont telescope of Carnegie Southern Observatory at Las Campanas. The line of sight goes across a valley at a considerable height above ground, promising small atmospheric extinction in horizontal optical paths.

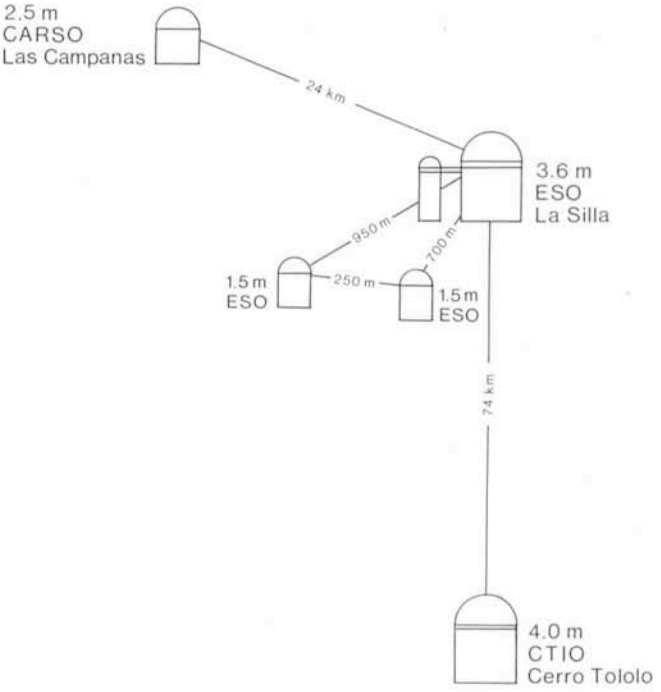

Fig. 6: *To directly observe the fine structure on stellar surfaces may ultimately require long-baseline optical interferometry. Inhomogeneities in the Earth's atmosphere in practice preclude phase interferometry over long baselines, but intensity interferometry does not suffer that limitation. In this sketch over telescopes on and around La Silla, potential baselines for future intensity interferometry are marked between telescopes that have free lines of sight between them. For example, the 24 km baseline between La Silla and Las Campanas offers an angular resolution of better than 10^{-5} arcseconds, adequate to detect structures the size of solar granulation on the surfaces of nearby stars.*

The concept would be to take light from one telescope (via a light fiber at the prime focus), collimate it and send it to a small receiving telescope at the other end, and then detect it there together with light from the other telescope. For the handling and processing of the signal, rather specialized units of digital electronics are required, and such are presently under construction. If these concepts ultimately prove workable, the resulting angular resolution would be measured in microarcseconds, and be equivalent to that of a 21 cm radio interferometer operating over a baseline of 10 million km! Such a spatial resolution, orders of magnitude superior to the highest so far achieved in astronomy, would be required to finally resolve structures of similar size as solar granulation on the surfaces of nearby stars.

References

Beckers, J. M., Bridges, C. A., Gilliam, L. B.: 1976, *A High Resolution Spectral Atlas of the Solar Irradiance from 380 to 700 Nanometers,* Sacramento Peak Observatory.

Dravins, D.: 1981, in M. H. Ulrich, K. Kjär (eds.) *ESO Conf. Scientific Importance of High Angular Resolution at Infrared and Optical Wavelengths,* p. 295.
Dravins, D.: 1982a, *Ann. Rev. Astron. Astrophys.* **20,** 61.
Dravins, D.: 1982b, in C. M. Humphries (ed.) *Instrumentation for Astronomy with Large Optical Telescopes,* p. 229.
Dravins, D., Lind, J.: 1983, to be published.
Dravins, D., Lindegren, L., Nordlund, Å.: 1981, *Astron. Astrophys.* **96,** 345.
Enard, D.: 1977, *The Messenger* No. 11, p. 22.
Enard, D.: 1979, *The Messenger* No. 17, p. 32.
Enard, D.: 1981, *The Messenger* No. 26, p. 22.
Gray, D. F.: 1980, *Astrophys. J.* **235,** 508.
Gray, D. F.: 1982, *Astrophys. J.* **255,** 200.
Gray, D. F.: 1983, *Publ. Astron. Soc. Pacific,* submitted.
Hanbury Brown, R.: 1974, *The Intensity Interferometer.*
Nordlund, Å.: 1978, in A. Reiz, T. Andersen (eds.) *Astronomical Papers Dedicated to Bengt Strömgren,* p. 95.
Nordlund, Å.: 1982, *Astron. Astrophys.* **107,** 1.

List of Preprints Published at ESO Scientific Group

February – May 1983

237. N. Panagia, E. G. Tanzi and M. Tarenghi: Infrared Observations of R 136, the Central Object of the 30 Doradus nebula. *Astrophysical Journal.* February 1983.
238. G. Chincarini: Redshifts and Large Scale Structures (Review). IAU Symposium No. 104, Crete 1982. February 1983.
239. I. Appenzeller, I. Jankovics and J. Krautter: Spectroscopy and Infrared Photometry of Southern T Tauri Stars. *Astronomy and Astrophysics Suppl.* February 1983.
240. P. A. Shaver et al.: PKS 0400–181: A Classical Radio Double from a Spiral Galaxy? *Monthly Notices of the Royal Astronomical Society.* April 1983.
241. B. E. Westerlund, M. Azzopardi, J. Breysacher and J. Lequeux: Discovery of a Wolf-Rayet Star in NGC 6822. *Astronomy and Astrophysics.* April 1983.
242. F. Pacini and M. Salvati: The Optical Luminosity of Very Fast Pulsars. *Astrophysical Journal.* April 1983.
243. S. D'Odorico, M. Rosa and E. J. Wampler: Search for Wolf-Rayet Features in the Spectra of Giant HII Regions: I. Observations in NGC 300, NGC 604, NGC 5457 and He2–10. *Astronomy and Astrophysics Suppl.* April 1983.
244. D. Gillet and J. P. J. Lafon: On Radiative Shocks in Atomic and Molecular Stellar Atmospheres. I. Dominant Physical Phenomena. *Astronomy and Astrophysics.* April 1983.
245. J. Danziger, R. D. Ekers, R. A. E. Fosbury, W. M. Goss and P. A. Shaver: PKS 0521–36, A BL Lac Object with an Optical and Radio Jet. (Talk given at the Turin Workshop on Astrophysical Jets, 7–8 Oct. 1982. D. Reidel Publ. Comp.) April 1983.
246. D. Baade: Can Shell Phases of Be Stars Be Predicted on the Basis of Rapid Spectroscopic Micro-Variability? *Astronomy and Astrophysics.* May 1983.
247. H. Pedersen, C. Motch, M. Tarenghi, J. Danziger, G. Pizzichini and W. H. G. Lewin: Optical Candidates for the 1978 November 19 Gamma-ray Burst Source. *Astrophysical Journal Letters.* May 1983.
248. C. G. Kotanyi and R. D. Ekers: A Westerbork Map of the Core of the Virgo Cluster. *Astronomy and Astrophysics.* May 1983.
249. L. Maraschi, E. G. Tanzi, M. Tarenghi and A. Treves: Quasi Simultaneous Ultraviolet and Optical Observations of PKS 2155–304 = H 2155–304. *Astronomy and Astrophysics.* May 1983.
250. W. K. Huchtmeier, O.-G. Richter, H.-D. Bohnenstengel and M. Hauschildt: A General Catalog of HI Observations of External Galaxies. May 1983.
251. D. Maccagni, L. Maraschi, E. G. Tanzi, M. Tarenghi and L. Chiappetti: X-ray and UV Observations of the BL Lacertae Object 3C 66A. *Astronomy and Astrophysics.* May 1983.
252. D. Gillet, E. Maurice and D. Baade: The Shock-Induced Variability of the Hα Emission Profile in Mira. *Astronomy and Astrophysics.* May 1983.

Distances to Planetary Nebulae

R. Gathier, Kapteyn Astronomical Institute, Groningen, The Netherlands

When astronomers want to determine the properties of an object in the universe, they need a reliable distance to that object. Consequently there always has been much effort to find methods for distance determination. In the case of planetary nebulae, distances are very difficult to determine. Several methods have been tried but individual distances in general are still uncertain by a factor of two to three, sometimes even more. We have used an in principle powerful method, the "extinction method" to derive accurate distances for about 10 planetary nebulae.

The Importance of Accurate Distances

Planetary nebulae are believed to represent a late stage in the evolution of the many stars in the Galaxy with intermediate masses. During the planetary nebula phase, the star loses mass that becomes visible as a gaseous nebula which surrounds the central star.
Without an accurate distance to a planetary nebula important parameters such as nebular radius, nebular mass, luminosity and radius of the central star remain unknown. It is important to know the nebular mass, for example, because it determines the amount of gas that is returned to the interstellar medium by the planetary nebula phenomenon. This mass return has a large influence on the evolution of the entire Galaxy.

We also need accurate distances to many planetaries in order to determine their distribution in the Galaxy. This distribution can then be compared with distributions of other kinds of stars in order to try to determine which stars pass through the planetary nebula phase and which do not. Especially a comparison with the galactic distribution of white dwarfs and red giants is very interesting since it is believed that the planetary nebula phase lies between the red giant phase and the white dwarfs. Once the distance to a planetary nebula is known, the luminosity of the central star can be determined. The effective temperature of the central star can usually be derived so that the star can then be placed in a luminosity–temperature diagram. Many positions of central stars in such a diagram define in fact how temperature and luminosity evolve with time. This enables astronomers to check theoretical calculations of the evolution of stars with different masses.

Reasons Why Standard Methods Cannot be Applied

The reason that most planetary nebulae have unknown distances is that standard methods for distance determination are usually not applicable. All nebulae are much too far for distance measurements by means of trigonometric methods. With our knowledge about normal stars it is usually possible to determine their intrinsic luminosities by means of spectroscopy

or photometry. The intrinsic luminosity, combined with the observed magnitude leads to the distance. This method cannot be used for the central stars of planetary nebulae. They differ strongly from normal stars; their intrinsic luminosities are as yet unknown, that is why we need accurate distances! Another problem is that planetary nebulae are usually not found in stellar groups for which distance determinations are possible. There are only a few nebulae for which one of the standard methods of distance determination is applicable. Some central stars have a normal companion star for which a distance can be determined. One planetary has been found in a globular cluster, M15, and also nebulae near the galactic centre and in extragalactic systems have known distances.

Specific Methods

For planetary nebulae one has to use specific methods that are only applicable to individual cases. One method makes use of the expansion of the nebulae. This method compares the observed angular expansion rate of the nebula with the radial expansion velocity of the gas as deduced from the splitting of emission lines. Another method is based on the fact that usually the total amount of extinction by interstellar dust to a planetary nebula can be derived. If it is also possible to determine the relation between interstellar extinction and distance along the line of sight to the planetary nebula, the distance to the nebula follows from this relation. We have applied this "extinction method" to 13 nebulae.

The "Extinction Method"

The total extinction to a planetary nebula can be derived in several ways. One method is to investigate the ultraviolet spectrum of the central star. Interstellar extinction causes a characteristic absorption near 2200 Å. From the strength of this absorption the extinction can be found. The extinction can also be measured from a comparison of the observed ratio of the strengths of certain nebular emission lines (such as HeII 1640 Å/4690 Å) with the theoretically expected ratio. Very often the extinction is derived from the *observed* ratio of radio to H_β flux density, compared with the *expected* ratio.

The relation between interstellar extinction and distance in the direction to the planetary nebula can be determined from spectroscopy or photometry of stars in that direction. Especially hot (early type) stars are used, since their theoretical energy distributions are well known and they are usually visible up to large distances. Spectroscopy or photometry gives the observed energy distribution of the star. This tells us how the stellar light is affected by absorption of interstellar dust particles. This absorption causes the colour of the star to become somewhat redder. From the amount of this "reddening", the total interstellar extinction to the star can be derived. A careful comparison of the theoretical and observed energy distribution gives the intrinsic luminosity of the star. Combined with the observed magnitude this leads to the distance of the star.

Thus, with spectroscopy or photometry of a "normal", preferably early-type star, it is possible to derive both its extinction and its distance. With extinctions and distances of many individual stars in a certain direction on the sky we can try to determine the relation between extinction and distance for that direction.

Our Approach

We selected a number of planetary nebulae for which extinctions could be determined with the methods described above. The ultraviolet spectra that we used to derive the extinction were obtained with the IUE satellite.

We have used photometry of stars along the line of sight to a planetary nebula to determine the extinction–distance relation. Because the interstellar material is distributed very irregularly throughout the Galaxy, extinction–distance relations can differ strongly for different directions. In order to determine a reliable relation it is therefore necessary to use stars that are as close as possible to the line of sight to a planetary nebula. This means that mainly planetaries near the galactic plane can be studied, where the density of stars is high enough so that many measurable stars are found within a small field around the nebula. Besides, extinction–distance relations for directions outside the galactic plane can only be determined for the first few hundred parsecs, since the interstellar dust is very concentrated to the galactic plane.

In total we selected 13 planetary nebulae near the galactic plane, with well-known extinctions. To determine the extinction–distance relations for the directions to these nebulae we used the Walraven VBLUW photometer with the Dutch 91 cm telescope at La Silla (J. Lub, *The Messenger* **19,** 1, 1979). The observations were done during January 1981 and February – April 1982. The VBLUW photometer is very well suited for our purposes. The light of a star is measured in 5 different wavelength bands, from the visual (V-band) to the near ultraviolet (W-band). This means that the energy distributions of early-type stars (temperatures > 9,000 K) can be observed over a wide wavelength range. As mentioned earlier the intrinsic energy distributions are well known for these early-type stars and are therefore very suitable for determining extinction–distance relations. Moreover, these stars can be seen over large distances in the galaxy. Another advantage of the photometer is that light is measured simultaneously in the five different wavelength bands. With this instrument it is therefore possible to measure many stars in a short time.

Construction of Extinction–Distance Diagrams

I will try to explain now in more detail how we can derive from the photometry of an individual star its distance and extinction. With the five wavelength bands, four independent so-called colour indices can be constructed (e.g. [V-B], [B-U], [B-L] and [U-W]). The observed VBLUW colours of an early-type star, compared with the intrinsic colours, give the amount of reddening of the star, usually expressed as the colour-excess E_{B-V}.

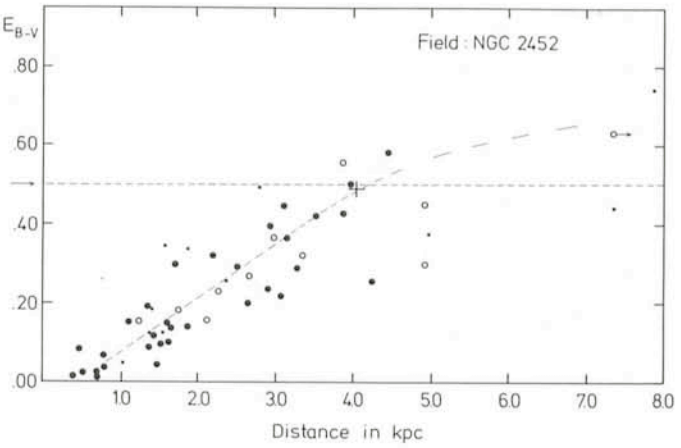

Fig. 1: *Diagram of reddening E_{B-V} as a function of distance for stars within a field of 0.5 degree around the planetary nebula NGC 2452. The different symbols indicate the accuracy of individual points. Small dots have large uncertainties, open circles are better determined and filled circles are the most accurate measurements. The cross at 4 kpc represents the young open cluster NGC 2453. The reddening to NGC 2452 is indicated by the horizontal dotted line.*

This quantity leads to the total amount of extinction. The observed brightness of the star can then be corrected for the extinction. Now we have to find the intrinsic luminosity of the star. The energy distribution of an early-type star is mainly determined by its temperature T and pressure p at the surface of the star. It is possible to make certain combinations of VBLUW colour indices that are insensitive to reddening. These are called reddening-free indices. The observed reddening-free indices can be compared with indices, calculated with theoretical spectra, as a function of T and p, of early-type stars (we used models by Kurucz). From this comparison we then find T and p of the star (for an application of this method to cool stars, see J. W. Pel, *The Messenger* **29,** 1, 1982). Now we use calculations of stellar evolution (for example by P. M. Hejlesen, *Astron. Astrophys. Suppl. Ser.* **39,** 347, 1980). These calculations give for a star with given mass its T, p and luminosity L as a function of time. We have determined T and p, so L follows. Since we now have the intrinsic luminosity of the star together with the observed brightness, corrected for extinction, the distance can be calculated.

Fig. 1 shows the results for stars along the line of sight to the planetary nebula NGC 2452. Only stars within 0.5 degree from the nebula are included. Many late-type foreground stars are not shown in the figure. The symbols used indicate the accuracy: thick dots are the better determined points (in terms of T and p). Individual distances have on average estimated accuracies of ~ 30 %, while individual reddenings are accurate to ~ $0^{m}.03$ in E_{B-V}. Most of the scatter in this diagram is believed to be caused by multiple stars and an irregular reddening distribution across the field. The cross at 4.0 kpc with E_{B-V} = 0.49 represents the young open cluster NGC 2453, only 8'.5 away from NGC 2452. The circle with arrow at 7.3 kpc represents a lower limit to the distance of a very distant B2 supergiant. NGC 2452 has a reddening of $E_{B-V} = 0^{m}.50 \pm 0^{m}.05$. It is determined from the observed HeII 1640 Å/4690 Å ratio and from the ratio of the radio to H_{β} flux density. From the relation in Fig. 1 we find a distance to NGC 2452 of ~ 4.1 kpc with an estimated accuracy of 25–30 %. Previous distance estimates by several authors range from ~ 1.5 to ~ 3.0 kpc, but with larger uncertainties.

This example shows that the "extinction method" is very powerful in deriving distances to planetary nebulae. Similar diagrams as Fig. 1 will be available soon for 12 other nebulae.

Large Scale Structure of the Universe, Cosmology and Fundamental Physics

As announced in the *Messenger* No. 30, this first ESO/CERN symposium will be held from 21 to 25 November 1983 at CERN in Geneva.

PROGRAMME

Introductory Lecture (D. W. SCIAMA, Oxford University and ISAS, Trieste).
Electroweak Unification and its Experimental Status (P. Darriulat, CERN, Geneva).
Unified Field Theories (P. FAYET, Ecole Normale Supérieure, Paris).
Experimental Tests of Unified Field Theories: Proton Decay and n-$\bar{n}$ Oscillations (E. FIORINI, University of Milan); **Monopoles** (G. GIACOMELLI, University of Bologna).
Dynamical Parameters of the Universe (A. SANDAGE, Mount Wilson and Las Campanas Observatories, Pasadena, CA).
Radiation in the Universe (D. T. WILKINSON, Princeton University, NJ).
Galaxies (S. M. FABER, University of California, Santa Cruz).
Clusters, Superclusters and their Distribution (J. H. OORT, University of Leiden).
Formation of Galaxies and Structures (Ya. B. ZELDOVICH*, Institute of Applied Mathematics, Moscow).
Neutrinos (R. L. MÖSSBAUER, Technical University, Munich).
Early Nucleosynthesis (J. AUDOUZE, Institute of Astrophysics – CNRS, Paris).
Observational Evidence for the Evolution of the Universe (L. WOLTJER, ESO, Garching bei München).
Unified Field Theories and the Early Universe (A. D. LINDE*, Lebedev Physical Institute, Moscow).
Quantum Gravity (S. W. HAWKING, University of Cambridge).
Closing Lectures (J. ELLIS, Stanford University, CA, and CERN, Geneva); M. J. REES, University of Cambridge).

The following scientists will act as chairmen and discussion leaders of the various sessions: N. CABIBBO (University of Rome), G. COCCONI (CERN), A. D. DOLGOV* (Institute of Theoretical and Experimental Physics, Moscow), M. S. LONGAIR (Royal Observatory Edinburgh), A. SALAM (Imperial College and ICTP), E. E. SALPETER (Cornell University), D. N. SCHRAMM (Chicago University), J. SILK (IAP, Paris, and University of California, Berkeley), N. STRAUMANN (University of Zurich), H. VAN DER LAAN (University of Leiden).

* Participation has not yet been confirmed.

The aim of the symposium is to establish the status of our knowledge on the subject and to provide a forum for discussions among people from different disciplines. To this end about equal time will be dedicated to the formal lectures and to the general discussions on each topic. The audience will be mainly composed of about equal numbers of astrophysicists and particle physicists and will be limited to approximately 150 participants.
The participation in the symposium is by invitation only. People who are definitely interested in participating in the symposium should write to the chairmen of the Organizing Committee at the addresses below prior to 31st July 1983.

Prof. G. Setti
ESO
Karl-Schwarzschild-Str. 2
D-8046 Garching b. München
F. R. G.

Prof. L. van Hove
CERN
TH Division
CH-1211 Genève 23
Switzerland

Hα Observations of the Rosette Nebula and the Distribution of Interstellar Dust

W. E. Celnik, Astronomisches Institut, Ruhr-Universität Bochum

Introduction

The Rosette nebula is a well-known HII region in the constellation of Monoceros with a diameter of more than 2°. The nebula has a nearly circular shape forming a ring around a deep local intensity minimum (Fig. 1). The open star cluster NGC 2244 is visible within the HII region, containing early-type stars which emit enough hard UV radiation to ionize the nebula. Adjacent to the north-eastern border of the Rosette nebula there is the large supernova remnant of the Monoceros Loop.

Looking at the prints of the Palomar Sky Survey it is obvious that many dust clouds are directly related to the Rosette nebula. In order to state this more quantitatively it is useful to compare optical and radio frequency measurements of the nebula. Observations in the radio domain are not affected by interstellar dust grains along the line of sight. But optical Hα emission line radiation emitted from the HII gas will be partially absorbed by interstellar dust. Now both the intensities of the optically thin radio continuum and that of the Hα recombination line emitted from the HII region depend on the same physical parameters of the nebula, the electron temperature and the emission measure $E = \int n_e^2 \cdot ds$ of the electron density n_e and the effective path length s in the nebular gas. Therefore it is possible to calculate theoretical values for the Hα emission line intensity from the radio continuum intensity and the electron temperature. Oster (1961, *Ap. J.* **134,** 1010) gives the theoretical continuum emission coefficient needed for this.Comparing the theoretical values of the intensities in the Hα line with the measured ones the distribution of interstellar dust across the Rosette nebula can be determined.

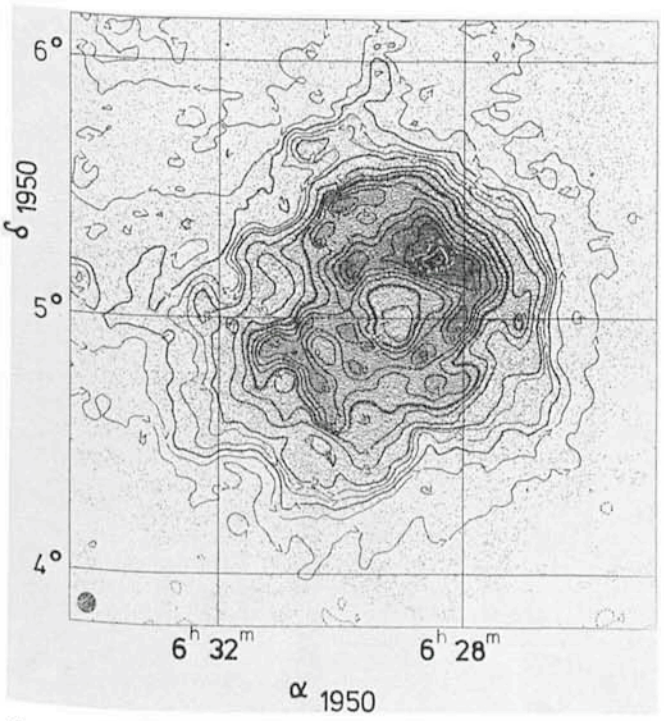

Fig. 1: *Distribution of the intensity in the Hα line across the Rosette nebula. Lowest contour line at O, thick (numbered) isophotes at $3 \cdot 10^{12}$, thin isophotes at 1, 2, 4 and $5 \cdot 10^{12}$, line with tick-marks at $15 \cdot 10^{12}$ i.f.u./beam; the angular resolution is 4'.75.*

The Hα Emission Line Intensity Distribution

The Rosette nebula was observed in the Hα emission line with the Bochum 61 cm Cassegrain telescope at La Silla during December 1979 and January 1981 using a photoelectric photometer with a cooled multiplier (EMI 9558 A) and interference filter (ESO 28) which has a full width at half transmission $\Delta\lambda = 10.2$ Å around $\lambda_o = 6564.8$ Å. Such a small bandwidth was necessary because only then both the emission lines of [NII] at λλ 6548, 6584 on both sides of the Hα line could be excluded. The angular resolution was set to 4'.75 by a diaphragm. Scanning the nebula with resting telescope using earth rotation permitted an integration time of 4 sec per point, while the length of each scan reached 30 minutes. Subtracting background radiation and correcting for atmospheric extinction, a complete map of the Hα line intensity distribution could be constructed from 76 scans with an extension of 2°.4 × 2°.4 (Fig. 1). But the intensity scale was arbitrary, it still had to be tied into sources with absolutely known flux.

The Calibration of Hα Line Intensity

The calibration of the Hα line intensities in absolute units follows a rather complicated way. Two stars (α Car, β Cen) whose spectral continua had been calibrated absolutely by Tüg (1978, thesis, Ruhr-Universität Bochum) were measured before and after scanning the nebula. Thus the count rates from the nebula scaled to 100% filter transmission could be calibrated by the count rates I_o obtained from the stellar continuum spectrum $I(\lambda$ multiplied with the transmission curve $T(\lambda)$ of the interference filter. A special problem in this calibration resulted from the fact that Tüg's absolute values referred to such wavelengths where the stellar continuum is reasonably unperturbed by stellar lines, but the Hα measurements are strongly affected by the stellar Hα line. In order to determine how much the stellar continuum is depressed in the line, coudé spectra of the Hα region with a dispersion of 12.5 Å/mm for α Car and β Cen were taken by D. Reimers in January 1981. These plates were evaluated with the Grant machine and the IHAP system at ESO Garching, the linearity of the resulting intensity scale was checked by photoelectric low-resolution scanner spectra of the same stars obtained by D. Kaiser with the Bochum 61 cm telescope at La Silla in December 1981. In this way the shape of the stellar Hα line could be determined and the Hα nebular intensities could be calibrated in units of $W \cdot m^{-2} \cdot beam^{-1}$.

The nebula is ring-shaped, surrounding a deep central intensity minimum. But the map contains the contribution of many stars besides the line radiation of the gas, so stars with $m_v \leq 9.1$ had to be identified and subtracted from the map by Gaussian fitting. After this the maximum value of Hα flux densities is $S_{max} = 39.9 \cdot 10^{12}$ i.f.u./beam (1 i.f.u. = 1 integrated flux unit = 10^{-26} W · m^{-2}). In Fig. 1 some weak filaments of the Monoceros Loop are visible near the northern and eastern border of the map, but their intensities are not higher than 8% of the maximum intensity of the Rosette nebula. The mean error of the intensity at a single point is 1.1%, including the errors of the calibration in i.f.u./beam this increases to 5.0%. The rms noise in the map is $0.12 \cdot 10^{12}$ i.f.u./beam.

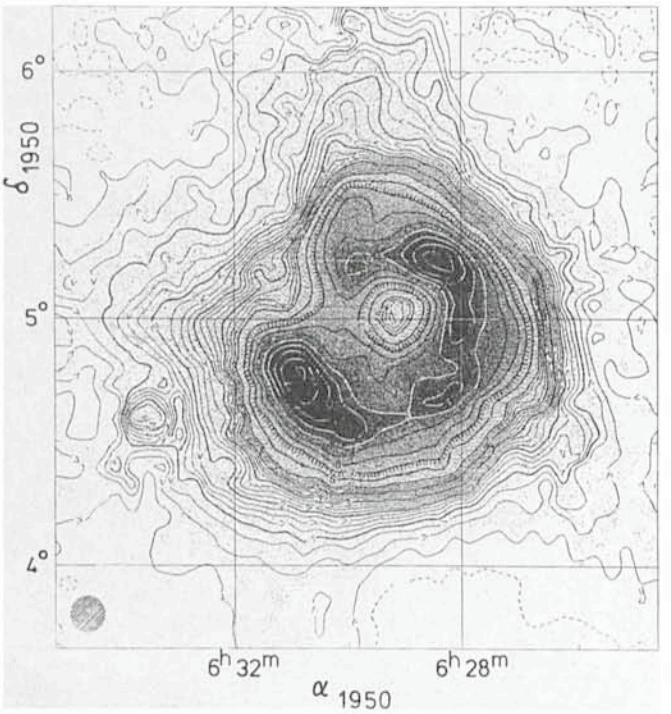

Fig. 2: *Distribution of the brightness temperature at 1410 MHz across the Rosette nebula. Lowest contour line at 0, thick (numbered) isophotes give brightness temperature in units of K, thin isophotes at 0.25, 0.5, 0.75 . . . 4.75 K, line with tick-marks at 7 K; the resolution is 9'.24.*

The Radio Continuum Observations

Two radio continuum maps of the Rosette nebula were obtained at 1410 MHz and 4750 MHz respectively. The intensity distribution at 1410 MHz (21.3 cm) was mapped with the 100 m telescope at Effelsberg in August 1980. 40 scans in right ascension and declination fully sampled with 4' point separation were connected to a map of 2°.7 × 2°.7 (Fig. 2). The angular resolution is 9'.24 and the intensity calibration was made using the point source 3C147. The maximum brightness of the nebula is T_b=14.1 K, the rms noise in the map is less than 0.1 K.

A map of the continuum intensity at 4750 MHz (6.3 cm) was obtained with the same telescope in June 1981. 180 scans in right ascension and declination with a sampling distance of 1' resulted in a map of 3° × 3° extension. The angular resolution is 2'.43 and the intensity scale was determined by observing the sources 3C48, 3C138, 3C147 and 3C249.1. The maximum brightness of the nebula at 4750 MHz is 1.7 K, the rms noise in the map is nearly 0.03 K. The map represented here (Fig. 3) is only a 1°.65 × 1°.65 section from the complete map. The radio data also show the Rosette nebula to be ring-shaped.

The Radio Recombination Line Observations

As discussed above, the electron temperature in the HII region is needed in order to compute the theoretical Hα line intensity from radio continuum measurements. The electron temperature can be estimated from measurements of radio recombination lines. Mezger and Henderson (1967, *Ap. J.* **147,** 471) gave a formula for this under conditions of local thermodynamic equilibrium (LTE), but effects of deviations from LTE can be taken into account using correction factors given by Brocklehurst (1970, *MNRAS* **148,** 417). The helium abundance was obtained from the ratio of the total line intensities of the He 112α and the H112α lines resulting in $<N_{He}+/N_H+>=0.116\pm0.032$, the mean electron temperature derived was $T_e=(5790\pm1070)$K. Due to the low brightness temperature of the radio recombination lines (T_b(He112α)= 0.01 K) integration times of more than 4.5 hours were needed for a single position in these investigations.

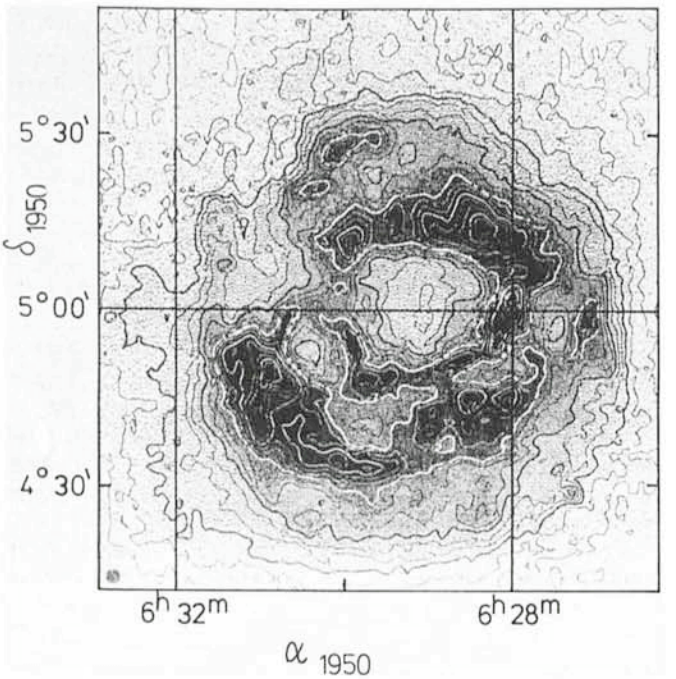

Fig. 3: *Distribution of the brightness temperature at 4750 MHz across the Rosette nebula. Lowest contour line at 0, thick isophotes at 0.3, 0.6, 0.9 . . . K, thin isophotes at 0.1, 0.2, 0.4, 0.5, 0.7 . . . K; the resolution is 2'.43.*

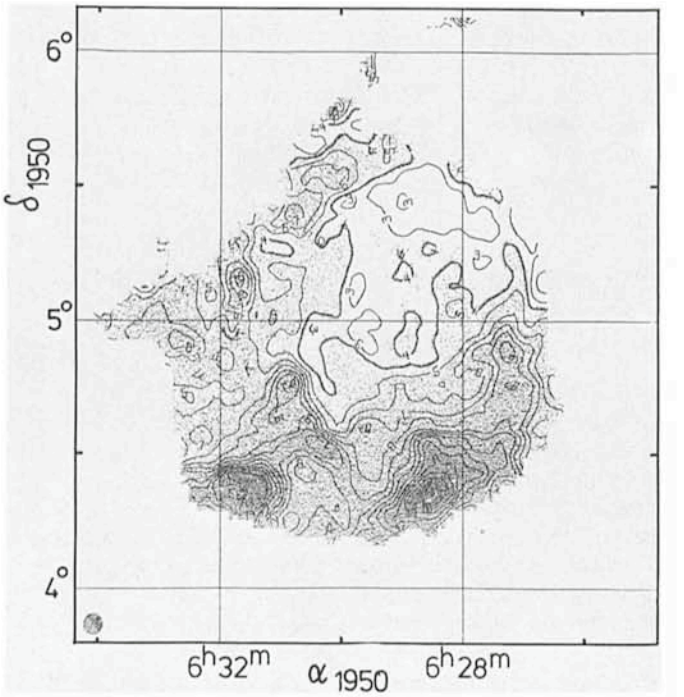

Fig. 4: *Distribution of the local absorption at Hα across the Rosette nebula from the comparison of the intensities in Hα and in the continuum at 4750 MHz, contour line 3 at 1.27 mag, contour line 4 at 1.47 mag and contour line 5 at 1.67 mag absorption; the resolution is 4'.75.*

The Distribution of Interstellar Dust

Comparing the distribution of the observed Hα line intensity in Fig. 1 with the distribution of continuum emission across the Rosette nebula (Fig. 2, 3) it turns out that the features in the north-western region are very similar on both maps, but that strong differences are visible in the southern region. Fig. 4 shows the comparison of the observed and the expected Hα emission estimated from the 4750 MHz continuum emission quantitatively. Only points at which both the Hα and radio continuum intensities are greater than 2.5 times the rms noise were used. The mean value of interstellar extinction between the nebula and earth at 6563 Å is $A(H\alpha)=(1.21\pm0.04)$mag. This value results from UBV photometry data of NGC 2244 by Ogura and Ishida (1981, *Publ. Astron. Soc. Japan* **33,** 149) who obtained a reddening of $E(B-V)=0.47$ mag, and from the mean interstellar extinction law $A(1/\lambda)$ reviewed by Schmidt-Kaler (1982, in: Landolt-Börnstein, Gr. VI, Bd. 2b, 449). After subtracting this value of the "interstellar" A(Hα) from the absorption map the remaining absorption must be "local", that is must occur in the direct neighbourhood of the HII gas in front of the Rosette nebula. Its mean value in Fig. 4 is (1.9 ± 0.5) mag. In the north-western region $A(H\alpha)=(1.3\pm0.1)$ mag is nearly constant down to the noise limit at the nebula edge. In southern condensations it increases up to (4.3 ± 0.1) mag, but varies around a mean value of (2.5 ± 0.2) mag. The mean error of a single value is 0.3 mag.

A Model of the Rosette Nebula and Its Neighbourhood

The measured radio continuum intensities of Fig. 2 and Fig. 3 integrated in rings of 1 and 4 arcmin width around the nebula centre could be reproduced by a spherical symmetrical radial distribution of electron density with a central cavity and a hole in the shell pointing approximately to the direction of the line of sight. The mean value of the electron density in the shell is $N_e=(15.0\pm1.5)$ cm^{-3}. This model results in a total mass of ionized material in the nebula of $M_{ion}=(29{,}700\pm3{,}800)\ M_\odot$.

Interstellar dust clouds and molecular cloud complexes are frequently correlated. Blitz and Thaddeus (1980, *Ap. J.* **241,** 676) have observed CO molecules in the Mon OB2 molecular cloud complex in the Rosette nebula region with angular resolutions very similar to that of the A(Hα) map. Both the shape of CO cloud structures and their distribution correspond quite well to that of the absorption by interstellar dust. Using the assumption that all CO molecular clouds within the considered region contain dust grains, it is possible to distinguish between CO clouds lying in front of and those lying behind the HII region, because dust absorption is only visible from dust clouds in front of the nebula.

Indeed the CO clouds are distributed behind as well as in front of the nebula. This suggests that the HII region is embedded in the molecular cloud complex. The centre and the greatest part of the nebula are visible within a region of relative small dust absorption (Fig. 4). Thus we suppose that the HII region is lying at the border of the complex. A more detailed model of the complex (Celnik, 1982, thesis, Ruhr-Universität Bochum) could be established using the velocity field within the complex. Radial velocity information had been given by Fountain, Gary and O'Dell (1979, *Ap. J.* **229,** 971) and by Blitz and Thaddeus. Assuming a spherical shape of the complex we find for the total mass of the dust $M_d = 5{,}400\ M_\odot$. The total mass of the whole cloud complex consists of the masses of neutral hydrogen, molecules, stars, ionized matter and dust grains. Different authors have previously estimated the masses of neutral hydrogen ($1.5\cdot10^5\ M_\odot$, Raimond, 1964, thesis, Leiden), molecules ($1.3\cdot10^5\ M_\odot$, Blitz and Thaddeus) and stars ($5{,}000\ M_\odot$ for NGC 2244, Ogura and Ishida). For the total mass we derive $M_{tot} = 3.2\cdot10^5\ M_\odot$, which corresponds to a density of about $0.5\ M_\odot/pc^3$. 82% of the total mass is in the form of neutral hydrogen and molecules.

Conclusions

From the comparison of the photoelectrically measured distribution of the Hα emission line intensity across the Rosette nebula with the distribution of the radio continuum intensity it was possible to construct the distribution of interstellar dust in front of the nebula. The comparison of this dust distribution with measurements of molecular spectral lines from other authors resulted in a model of the molecular cloud complex Mon OB2 in three dimensions. The Rosette nebula is embedded in this complex near the border, on the side turned to the direction of the Sun. No evidence could be found that the Monoceros Loop has any connection to the Rosette nebula or the molecular cloud complex.

The Copenhagen Binary Project

J. V. Clausen, Copenhagen University Observatory

While this short contribution is written and the rain has been pouring down in Denmark, surely setting up new records, we strongly hope for an unbroken long series of clear, stable photometric nights at La Silla. The last long-term (40 nights) photometric observing run for our eclipsing binary project at the Danish 50 cm telescope began a few nights ago. Last – at least with the characteristically shaped, well-known *uvby* photometer mounted at the manually operated telescope, a combination which through the years has demonstrated its accuracy and reliability in a large number of projects in different fields of galactic research.

Besides these important features, we have benefitted from a remarkably stable photometric instrumental system (E. H. Olsen, 1977, *Astron. Astrophys.* **58,** 217). A discontinuity will now be introduced. A most welcome one, since much faster Strömgren photometers of the type known from the Danish 1.5 m telescope are now available. A year from now – according to the schedule – the observer will find a renovated microcomputer-controlled, fast-moving 50 cm telescope, equipped with a new efficient 6-channel *uvby-beta* photometer in the dome.

So it might be opportune to give a brief status report at this stage of the project even though more spectroscopic observations are still needed.

More Than 500 Nights

The first observations for the Copenhagen binary project were made at the Danish 50 cm telescope at La Silla in 1971. Since then more than 500 nights have been allocated, and well-

covered and accurate *uvby* lightcurves have been obtained for about 40 relatively bright (approximately 4.5–9.5 mag) southern eclipsing binaries. Many astronomers contribute or have contributed to the project which was started by the late B. Grønbech, K. Gyldenkerne and H. E. Jørgensen. During the following years B. Nordström, Bo Reipurth, J. Andersen, B. E. Helt and I have been collaborating on the photometric observations and analyses and lately A. Giménez and L. P. Vaz have joined the group.

For many of the systems, high-quality radial velocity curves have also been established from high-dispersion coudé spectra observed with the ESO 1.5 m telescope. This indispensable part of the binary project is carried out by J. Andersen. In one case the radial velocities have been observed with the CORAVEL and the Danish 1.5 m telescope.

The majority of the candidates selected for the project are well *detached double-lined systems with main sequence components,* between which the interactions are rather week and the lightcurves thereby relatively uncomplicated. This selection is closely guided by the main scientific purpose – to contribute with a significant increase to the available information on *absolute stellar dimensions* and to use the precise binary data for *empirical tests of stellar evolution calculations.*

Until now about 40 papers on individual eclipsing binaries have been published and some 25 more lightcurves are finished. Those for which sufficient spectroscopic material is also available are presently under analysis. However, some of the important candidates are still lacking spectroscopy, and more observing time is needed.

But Why?

Well, more than 500 generally perfect La Silla nights is a considerable amount of observing time – why at all was such a large observing project started?

Undoubtedly the main source of inspiration was the IAU Colloquium No. 6 held in Denmark back in 1969 (eds. K. Gyldenkerne and R. M. West, published by Copenhagen University Observatory 1970). At this meeting D. M. Popper presented a review on the knowledge of masses and radii of eclipsing binaries and their accuracy. It clearly demonstrated first of all that only very few reliable dimensions were available, but also especially that more lightcurves were at that time strongly needed. Several systems had good spectroscopy but no photometry.

Furthermore, the review gave inspiration to an investigation which very nicely illustrated the potential of combining absolute dimensions from analyses of eclipsing binaries with theoretical stellar model calculations (D. M. Popper, H. E. Jørgensen, D. C. Morton and D. S. Leckrone, 1970, *Astrophys. J.,* **161,** L57). It presented a determination of the helium to hydrogen ratio for Population I stars on the basis of masses and luminosities for the presumably unevolved components of *seven* eclipsing binaries. Together with *six* more systems, which from their mass-radius relationship were found to be evolved, they made out the total and thus very insufficient empirical material available for B9–G2 main-sequence systems (approximately 1–3 solar masses) at that time.

Having ⅔ of the observing time at the Danish 50 cm telescope, newly installed at La Silla and equipped with a new *uvby* photometer for simultaneous observations in the four bands, it was therefore quite natural to include also lightcurve observations in the list of projects for that instrument. The more so because new extensive programmes on stellar model calculations were at that time carried out at the institute.

Besides the eclipsing binaries without lightcurves, mentioned above, several favourable southern systems were known (mainly listed by D. M. Popper) but lacked both accurate photometry and good spectroscopy. Since about 1973, when the spectroscopic part was started at the ESO 1.5 m telescope, most of these systems have been observed in the Copenhagen binary project together with new candidates, discovered mainly in the radial velocity programmes and in the extensive *uvby* field programmes carried out at La Silla by Danish astronomers.

Altogether I think it is fair to say that we have had the facilities and possibilities for a contribution of a size which only few other European groups could have made. The need for so many systems and so much observing time as mentioned above is probably best illustrated by shortly looking at the present situation with respect to reliable binary data.

Absolute Stellar Dimensions

That the situation has improved significantly since 1969 is clearly seen from the recent critical review on stellar masses by D. M. Popper (1980, *Ann. Rev. Astron. Astrophys.* **18,** 115) and from a glance to the empirical stellar mass – luminosity relation based on the data included there (see R. C. Smith, 1983, *Observatory* **103,** 29). Our project has contributed with accurate dimensions for 13 of the 48 eclipsing binaries, including – if the reader will please not accuse me for priding myself (I am doing photometry, not spectroscopy) – 3 of the only 4 real confident masses for stars earlier than B6 (approximately 4 solar masses).

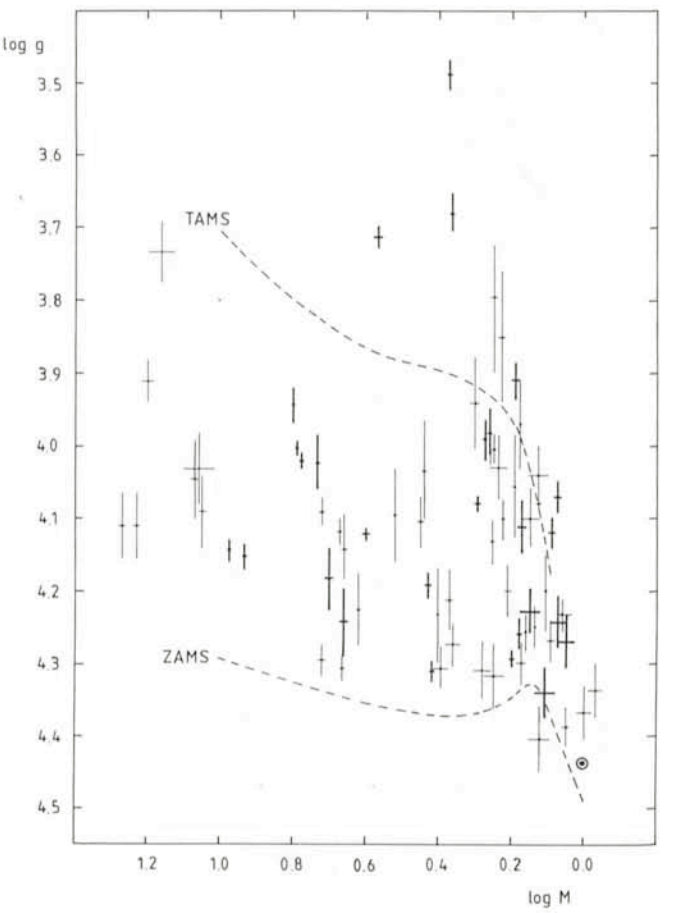

Fig. 1: *Log g – log M diagram based on masses and radii and their mean errors from Tables 2 and 4 in the review by D. M. Popper (a few systems given comments are left out). Heavy symbols indicate results from the Copenhagen binary project (a few unpublished systems added).*

Already this small number for the early type region indicates a need for still more data. And what if we want to trace evolutionary effects within the main-sequence band and want to make a critical empirical test of the available theory? Here the answer is not easily obtained from the mass-luminosity diagram which almost hides the dimension of evolution.

Let me give a short illustration of the present possibilities and limitations in a simplified frame where only the two most fundamental parameters – *mass and radius* – obtained from combined photometric and spectroscopic analyses of double-lined eclipsing binaries are used.

Fig. 1 presents a mass-surface gravity diagram where the data have again been taken from the review by D. M. Popper. Results from the Copenhagen binary project are indicated by heavy symbols. The two curves also shown represent the theoretical zero-age main-sequence (ZAMS) and the top of the main-sequence band (TAMS) for theoretical models where a chemical composition of (X, Z) = (0.70, 0.02) has been assumed (P. M. Hejlesen, 1980, *Astron. Astrophys. Suppl. Ser.* **39,** 347). For the most favourable systems and the most complete analyses the stellar dimensions are determined with an accuracy of 1–2 per cent, and as seen, this gives very good resolution and pinpoints a star (fixed mass) within about 1/20 of the main-sequence band. However, it also speaks for itself that this nice possibility of recognizing evolutionary effects within the core hydrogen burning phase of evolution is lost if the accuracy is not of this level. Even some of the data shown in Fig. 1 cannot be considered quite useful in this connection. The reader will also notice that a reliable empirical ZAMS is not defined by the too few systems at hand.

Here it should of course be mentioned that the position of the theoretical ZAMS depends on the chemical composition of the models. A change in the metal content parameter Z of ± 0.01 will e.g. shift the theoretical ZAMS by approximately ± 0.05 in log g, whereas the dependence on the hydrogen/helium content is much lower. Therefore, a detailed empirical test of theoretical model calculations cannot be based on radii and masses alone; less directly determined parameters for the binary components are also needed.

The theoretical frame can instead be effective temperature-surface gravity diagrams for a network of different chemical compositions, giving theoretical mass tracks and isochrones (see e.g. the paper by P. M. Hejlesen mentioned above). The *effective temperatures* for the components are derived from the colour indices and the calibration of the photometric system, and in some cases information on the metallicity can also be obtained in this way, e.g. for F-type systems through the m_1-index of the *uvby* system. Sufficient accuracy in the temperature determination is of course only obtained if accurate photometry in a well-calibrated multicolour system is available.

It is then interesting to investigate if, for a given chemical composition, the two components are located at the same isochrone (i.e. are of the same age) and simultaneously both lie at the theoretical evolutionary tracks for their mass. This determines, in principle and if correct theoretical models are assumed, the age and chemical composition of the binary. And more important, from a large number of carefully selected, well observed and critically analysed detached systems a detailed check of the *slope of the isochrones* is thereby obtained.

Such comparisons with theory have been published together with the absolute stellar dimensions for many of the individual systems in the Copenhagen binary project, and the reader is referred to our series of papers in *Astronomy and Astrophysics* for more details. Analyses for about 15 individual systems have been published until now. A brief presentation of the fundamental parameters for some of the systems and of the helium content derived from these data has been given by H. E. Jørgensen (1978, IAU Symp. No. 80, 433).

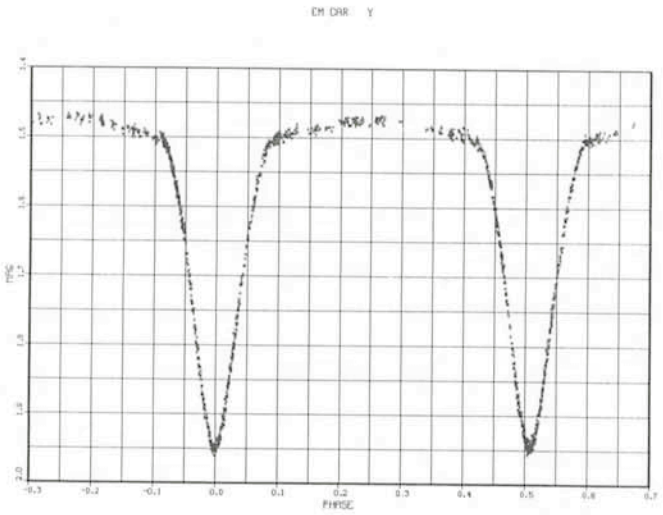

Fig. 2: *y lightcurve of the O-type system EM Car observed with the Danish 50 cm telescope at La Silla. Observations from February 1983 are not included, only the 1,175 points obtained before, mainly in 1982, are shown.*

The articles referred to above also describe in detail the methods of observation, reduction and analysis. Critical remarks on the determination of absolute dimensions can be found in J. Andersen, J. V. Clausen and B. Nordström, 1980 (IAU Symp. No. 88, 81), and I will not repeat all what can just as well be read there. On the other hand I would like to stress that routine work is not the route which leads to accurate stellar dimensions, and that reliable observations (accurate light-curves in several bands of a well calibrated intermediate band system, good high-dispersion spectra), use of a physically realistic binary model (we have widely used a modified version of that developed by D. B. Wood [WINK]), and *simultaneous analysis of photometry and spectroscopy* are essential. This, I think, is very clearly illustrated by our analysis of the interesting B2V system QX Car (in press).

More Data Still Needed

From the mass-luminosity diagram mentioned above and from Fig. 1 it is seen that the 1–3 solar mass range of the main sequence (i.e. A and F stars) is now reasonably well covered, but as already mentioned precise data for more massive early-type systems are still lacking. A large fraction of the yet unanalysed systems in the Copenhagen binary project belongs to this group, and especially interesting is the O-type binary EM Car for which the *y* lightcurve is shown in Fig. 2. Detached systems with such a nice uncomplicated lightcurve and well separated components are rare in this mass range (about 20 solar masses), and we expect EM Car to yield the most accurate absolute dimensions available for O-stars.

In the late-type end of the main sequence, below 1 solar mass, the situation also needs to be improved. Here new double-lined candidates can hopefully be discovered and also observed spectroscopically with the CORAVEL or similar instruments.

Without going into the situation for the more advanced evolutionary stages I will draw attention to one more candidate, namely TZ For. It is (to my knowledge) the only known double-lined eclipsing binary containing two normal giants. The period of TZ For is long – about 75 days – and the *uvby* lightcurves have been obtained at the Danish 50 cm telescope in a campaign

including many observers. The highly accurate radial velocities have been observed with the CORAVEL.

With the photometric as well as spectroscopic observations of all the selected southern systems hopefully completed in the first half of 1984, the data base for accurate absolute dimensions will be significantly increased – although still quite incomplete in some mass regions – and we look forward to carrying through a comprehensive and detailed discussion based on all results obtained from this long-term observing programme at La Silla.

Some News About the Coudé Spectrograph of the ESO 1.52 m Telescope

P. Giordano and E. Maurice, ESO

The coudé spectrograph was installed at La Silla early in 1969; the first reference spectra were obtained in May 1969. Since the beginning of the routine observations, several thousands of spectra have been taken, 8,127 with camera 1 at 20.1 or 31.3 Å/mm^{-1}, 12,913 with camera 2 at 12.3 or 19.4 Å/mm^{-1} and 2,058 with camera 3 at 2.6, 3.3 or 5.1 Å/mm^{-1}. After 14 years of often heavy duty, it appeared necessary to do a careful overhaul of the spectrograph. Some significant improvements were done during this 14-year period, but some important components had not been touched during a very long time, for instance the two closed cameras 1 and 2. The overhaul was done between August 1982 and February 1983 under the supervision of P. Giordano and with the help of B. Buzzoni. A. Torrejón, E. Araya and J. Pérez actively participated in the focussing phase and P. Alvarez and J. Torres, from the workshop, in the mechanical phase.

Most of the work done will only be noticed by the observer from the improved quality of his spectra (mainly with camera 1). Other changes have been made in order to simplify the normal observation procedure and to allow some special operations such as, for instance, exposing several spectra on a single plate.

Among the more important optical adjustments done on the spectrograph we mention the following: the coudé has been realigned with the telescope polar axis. The spectrograph itself has undergone a thorough optical alignment with particular attention paid to cameras 1 and 2. The mirrors of these cameras have been realuminized. The slit assembly has been repolished and thereafter protected by a special coating.

Some mechanical improvements have also been done. The movable plate-holder supports have been renewed to insure a more exact positioning in the focal plane. A revision of the plate-holders themselves is also foreseen in order to improve the fit of the plates to the curved focal surface. Presently 3 plate-holders may be used for both cameras 1 and 3 (in both cases plate-holders Nos. 1, 2 and 3). In the case of camera 2 (Fig. 1) only plate-holder No. 3 is presently usable but other plate-holders are currently beeing modified.

Finally a complete electric re-cabling of the spectrograph was done.

A number of modifications and improvements which affect the use of the spectrograph have also been made. Following the light path, first, the comparison lamps device has been changed: instead of using only an integrating sphere as effective light-source, a plane diffuser and a flat mirror have been added. Changing from one of these systems to the other is instantaneous. This permits the use of the new iron hollow-cathode source with reasonable exposure times. Remember that the flat-mirror system is 3.3 times faster than the plane-diffuser which in turn is 3.3 times faster than the integrating sphere. Exact exposure times will be available at the spectrograph.

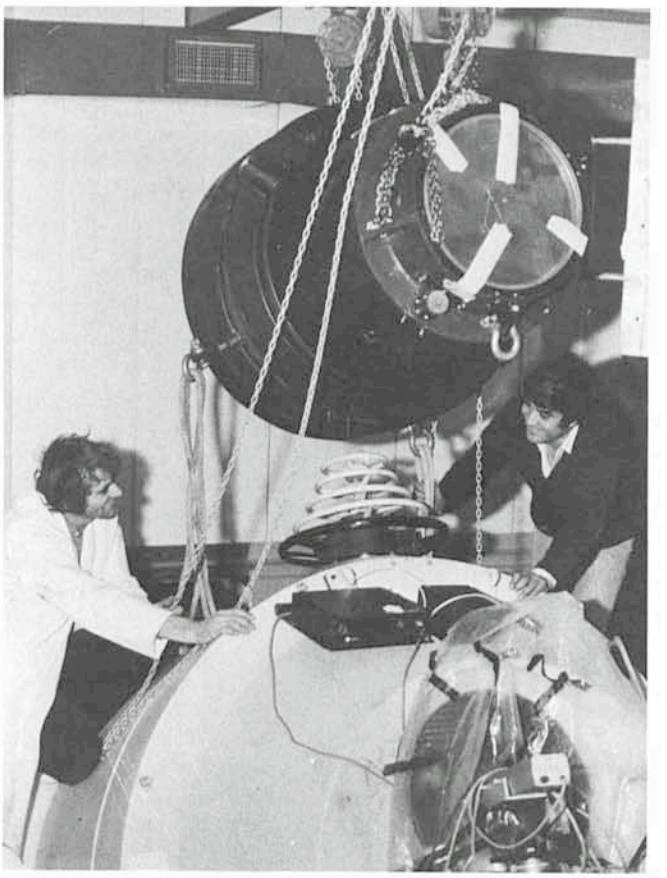

Fig. 1: *B. Buzzoni and P. Alvarez disassembling camera 2.*

Together with the new iron hollow-cathode lamp, the comparison lamps now in use are the following: the iron-arc, a mercury lamp, a neon lamp and a tungstene lamp for photometric calibration of plates in the coudé spectrograph itself. A colour filter to isolate the currently used grating order is now installed in the diaphragm of the source. Thus, it is no longer necessary to change these diaphragms if the comparison lamp is changed.

Following the light path, we now arrive at the decker immediately in front of the slit: the old prism-system is unchanged but new deckers (Fig. 2) will soon be installed. These will permit a better definition of the edges of the spectrogram and an easier guiding; some special deckers will also permit several (two at present) exposures on the same plate. Each of these deckers will also make it possible to insert a step-wedge, containing 8 neutral density levels, in front of the slit, for photometric calibration purposes. This will enable calibration plates to be

taken in exactly the same way as the stellar plates. Of course, the ETA spectrograph will remain in use if one prefers to expose calibration plates during observations. The movements of these new deckers will be controlled by accurate encoders.

We then arrive at the spectrograph shutter. The old mechanical shutter has been replaced by a motorized one which permits it to be linked to the exposure meter; if the shutter is closed, the exposure meter will be turned off. This avoids the accumulation of dark counts on top of the measured stellar signal. On cloudy nights (very rare) this is very useful if one is forced to make interruptions in the stellar exposure. The old exposure meter is still in use but will soon be replaced by a new one, identical to the one at the CES spectrograph which permits dark current subtraction. The photomultiplier tube will remain the same.

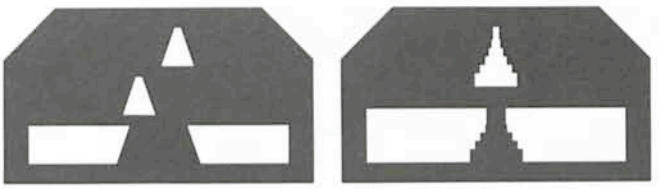

Fig. 2: *The two new deckers of the coudé spectrograph.*

The last modification planned for the spectrograph will be the motorization of the movements of cameras 1 and 2. This will be of help to night assistants when short exposures are done. Since the motors will in general move the cameras more gently than human hands, the danger of misalignments of the cameras' optics (mainly the mirror) will be reduced.

Fine Structure Lightcurve of (51) Nemausa

P. Gammelgaard, Institute of Astronomy, University of Aarhus, and
L. K. Kristensen, Institute of Physics, University of Aarhus.

From the beginning of the discoveries of minor planets in the last century their brightness has been a subject for study. For astronomers mainly interested in variable stars and stellar magnitudes, the minor planets could be a useful tool for transferring the magnitude scale uniformly over the sky. From the observational point of view, minor planets were like variable stars with light variations which could be computed from the distances to the Sun and the Earth. However, at that time the stellar magnitude scale was arbitrary and based only on subjective estimates. It was therefore necessary to determine the ratio of light corresponding to a difference of one unit of stellar magnitude. We owe the magnitude scale of our time to N. Pogson, who in his ephemerides of the brightness of 36 minor planets for the year 1857 (1) adopted a light ratio of 2.512 for the difference of one magnitude.

When F. Argelander in 1854 discussed the brightness of minor planets (2) he recommended minor planet magnitudes to be thoroughly investigated. He gave a list of diameters which are surprisingly accurate for the 18 S-type objects it contains. One of the reasons given by Argelander for studying the brightness of minor planets was that *all* information about the circumstances of an observation may possibly be used for increasing the accuracy of the position! It is exactly an improvement of the positions we have in mind by the lightcurve observations of (51) Nemausa.

(51) Nemausa was selected by B. Strömgren at the Copenhagen observatory in 1939 for the purpose of improving the fundamental star catalogues. Resulting from the requests for observations many series of precise photographic observations are now available and their residuals seem to indicate a systematic displacement of the observed photocentre towards the illuminated side of the body. This means that precision has reached a level where the diameter, of order 0".15, and the flattening of the body can no longer be ignored.

At present we do not even know which side of the body is facing the observer at a given moment, so a first step must be to determine the sidereal period of rotation and the axis of rotation with an accuracy which allows us to compute ephemerides for physical observations.

It is planned to secure very precise positions in the future by having (51) Nemausa observed by the astrometric satellite "Hipparcos", and by observations of occultations of stars which will have their positions observed by the satellite. The mission length of the satellite is expected to be less than the orbital period of minor planets but by the use of occultations this interval will effectively be extended. If size and shape of the planet are known, the occultation observations can be reduced to the centre of mass of the body and an occultation will provide a more accurate position than a direct observation. For this purpose all occultations of catalogued stars by (51) Nemausa until the year 2017 have been found by Gordon E. Taylor, Herstmonceux.

Although occultations are rare events, an occultation of SAO 144417 has already been successfully observed in the U.S.S.R. on August 17, 1979. Due to the accuracy of the orbit and of the star, which happened to be a Southern Reference Star, the error of the prediction was only 90 km and the ground track was predicted long in advance of the event. The derived diameter was D = 153 $\pm$ 7 km (3). The determination of size and shape of the body by the powerful tool of occultations is greatly facilitated by a good orbit and vice versa, – if size and shape are known, an occultation gives a position with an accuracy equal to that of the star, so the orbit can be much improved if the position of the star has the high accuracy of "Hipparcos".

One of the occultations found by G. E. Taylor is especially favourable and will occur on 1983 September 11. It is the occultation of the bright star 14 Psc of visual magnitude $5^{m}.9$ which will be visible in the densely populated eastern part of the United States. Hopefully, many observations at this rare occasion will be secured, so that a detailed profile can be determined, it may even happen that the silhouette could explain why the lightcurve has *three* maxima.

A campaign of photometric observations of (51) Nemausa has been initiated in 1980/81 and coordinated by H. J. Schober, Graz, with the ultimate aim to determine the pole, flattening and sidereal period (4). The observations now to be described continue this programme.

The observations were made with the ESO 1 m telescope and single-channel photometer during the two periods March 19–25 and April 2–5, 1982. The time was chosen well in advance of the date of opposition, May 3, 1982, in order to

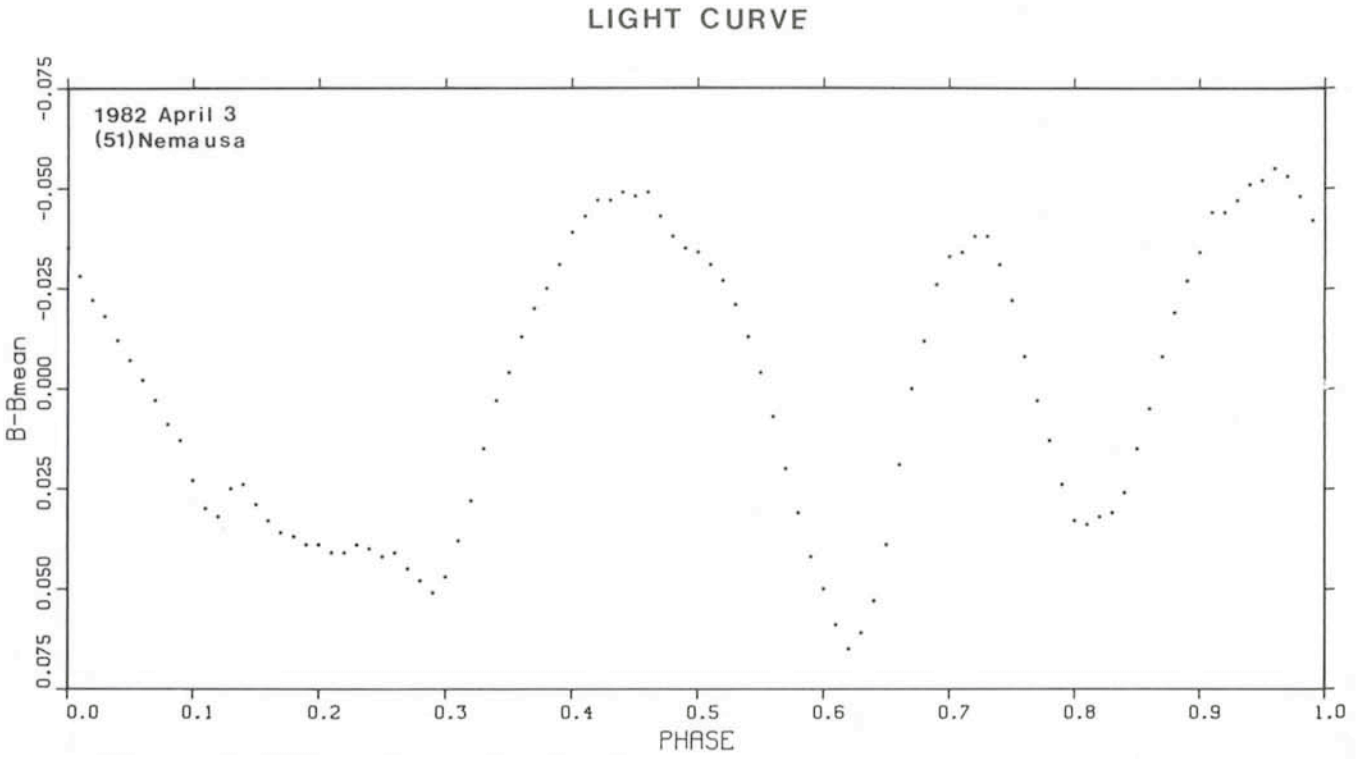

Fig. 1: *Lightcurve of minor planet (51) Nemausa. The B magnitude is given relative to the mean over a period of rotation. The phase is zero at the arbitrary date 1982 April 3 3^h30^m U. T.*

facilitate a continuous count of cycles since the previous opposition by making the time interval to be bridged as short as possible. The planet was stationary on March 22, so the daily motion was small at the time of observation; this makes the observed synodic period an approximation to the sidereal period. However, a disadvantage of observing far from opposition was that only a part of a revolution could be covered during a night.

The quick off-set facility of the telescope controle system was used to make differential photometry between (51) Nemausa and two nearby comparison stars, HD 133352 and HD 134088. The observations, generally in B, of the planet, star and sky background were stored on magnetic tape. The total number of observing hours was $22^h.2$ and the number of Nemausa observations was 4,123 of which 48 were rejected. The integration time was generally 10 sec giving the possibility to detect rapid variations. The comparison stars were chosen sufficiently close in position and colour that errors due to different airmass will not exceed $^m.001$. The mean error of a single differential observation is $\pm\ ^m.005$.

Also a number of observations were made in order to obtain UBV magnitudes of the comparison stars and of (51) Nemausa, using E-region standard stars.

The 4075 differential observations were analysed by a rigorous least squares adjustment solving for: (1) the synodic period of rotation, (2) one hundred equidistant points defining the lightcurve by interpolation, (3) the linear phase coefficient, (4) the colour index B–V, and finally, (5) the difference between the magnitudes of the comparison stars.

The main results of the 4,075 differential observations are the period $7^h.7845 \pm 0^h.0011$ and the lightcurve shown on Fig. 1. The lightcurve gives the B magnitude relative to its mean value over a period as a function of phase. The phase is arbitrarily chosen as zero at the epoch 1982 April 3 3^h30^m U. T. which is near the mean epoch of all observations. The curve clearly displays the strange three maxima already found by Chang and Chang (5); the period found in that work was $7^h.785$ the accuracy of which is confirmed by the present results. Three points on the lightcurve, viz. phases $0^P.98$ to $1^P.00$, were unfortunately not covered by the observations and are here the results of an interpolation. Except for the neighbourhood of these points the statistical error of the points on the lightcurve is of the order of $\pm\ ^m.001$ so the fine structure features at for instance the phases $0^P.29$ and $0^P.48$ are real. There are, however, systematic effects in the residuals at the $^m.005$ level which may probably be due to the changing phase and aspect.

The differential observations determine the linear phase coefficient (in B) with a high formal accuracy $^m.0358 \pm ^m.0002$ mag/deg. This result may, however, be affected by unknown systematic effects due to the changing aspect angles.

The UBV magnitudes of Nemausa were obtained in two different ways. First the direct standard photometry of Nemausa was reduced for the phase angle and lightcurve variations. Secondly the UBV magnitudes of the comparison stars were combined with the results of the 4075 differential observations. The two methods gave consistent results. For the mean of B over a rotation period we obtain $\overline{B}\ (1,0) = 8^m.556 \pm ^m.007$. The colour index seems to be constant during the half period over which V magnitudes were obtained, $B-V = ^m.788 \pm ^m.005$. No differential photometry was made in U, but standard photometry of Nemausa gave $U-B = ^m.494 \pm ^m.007$. The mean value of the phase angles of all the observations is $14^\circ.6$ and the mean of the times of observations is April 2.71 corresponding to the position: $\alpha = 15^h02^m$, $\delta = -7^\circ$ (1950.0), by which the aspect is determined. The mean errors given for the magnitudes are based on the internal scatter of the measures.

References

(1) Argelander, F., *Astron. Nachr.* **41,** (1855) 337.
(2) Pogson, N., *Monthly Notices R.A.S.* **17** (1856) 12.
(3) Kristensen, L. K., *Astron. Astrophys. Suppl. Ser.* **44,** (1981) 375.
(4) Schober, H. J., and Kristensen, L. K., in *Sun and Planetary System.* Proc. of the 6th European Regional Meeting, W. Fricke and G. Teleki (editors) (1982).
(5) Chang, Y. C. and Chang, C. S., *Acta Astron. Sinica.* **11** (1963) 139.

The Variable Central Star of Planetary Nebula NGC 2346

L. Kohoutek, Hamburger Sternwarte

NGC 2346, known already to Sir William Herschel, has been classified as a planetary nebula by R. Minkowski (1946) on the basis of its appearance on direct photographs. Morphologically it possesses a distinct axial symmetry and belongs to the class of bipolar nebulae (Fig. 1).

The bright central star is of spectral type A (Aller, 1968) and cannot be responsible for the radiation of the nebula: the observed HeII λ 4686 nebular emission line requires a source of ionizing radiation of at least 45,000°K. The binary hypothesis for the central star (A + sdO), based on photometry (Kohoutek, Senkbeil, 1973) was supported by Méndez et al. (1978) who found the stellar radial velocity to be variable. Later Méndez and Niemela (1981) derived an orbital period of $15^d.995 \pm 0^d.025$ for this single-lined spectroscopic binary.

In 1974 we included NGC 2346 in our list of bright central stars which were searched for variability using the ESO 50 cm telescope at La Silla. Between 1974 and 1980 we measured this star in 7 observing runs and found no substantial changes of its brightness ($V \simeq 11^m.2$). At present very careful reduction of these observations is being made which would detect even small light variations.

The observing period January–February 1982 at La Silla brought a rather surprising result: we recorded light variations over 2 mag obviously containing parts of two consecutive minima (Kohoutek, 1982). The minimum of February 1982 was broad with a depth of 2.2 mag in V and 2.6 mag in B. We interpreted it as a partial eclipse of the main A-type component and we tentatively classified the system as a semidetached close binary. However, further observations of Gathier using the Dutch 90 cm telescope at La Silla ruled out an eclipse by stars. Méndez, Gathier and Niemela (1982) reported further spectrograms taken in March–April 1982 which did not show any changes of the spectrum of the A-type star, even at light minimum. In addition, the radial velocity at minimum light was significantly larger than expected from the orbital motion. The rotation of the star was proposed to be the cause for this excess. Méndez, Gathier and Niemela suggested that a dust cloud is passing in front of the binary central star of NGC 2346. They derived the parameters of a single model and made the following predictions: the eclipse of the binary system (assuming an isolated spherical cloud) must have started in May or June 1981 and must finish in March or April 1983.

Fig. 1: *ESO 3.6 m photograph of NGC 2346, March 12, 1977, 127-04 + RG 630, exp. 90 min, seeing 2.0 arcsec. (Photo: S. Laustsen.)*

In January 1983 we obtained new UBV photometric data on NGC 2346 using the Bochum 61 cm telescope (Kohoutek, 1983). The lightcurve of the central star differed substantially from that of 1982: now we observed a narrow maximum reaching $V \simeq 12.5$ mag, $B \simeq 13.0$ mag only, and part of two very broad and deep minima with brightness ranging from 14.8 to 15.3 mag (V), and from 15.3 to 16.0 mag (B), respectively. Unfortunately, the Bochum telescope was too small for accurate photometry of such a faint star at minimum.

The main uncertainty of the photometry of the central star was evidently caused by the nebula (Fig. 2). At maximum the contribution of the nebular radiation, measured through a diaphragm of 18.2 arcsec, was small and the internal errors of the stellar V, B. U magnitudes could be estimated to be ± 0.01 mag, ± 0.02 mag and ± 0.06 mag, respectively. Near minimum light these errors increased to ± 0.10 mag (V) and ± 0.25 mag (B); the stellar U magnitudes were not reliable. In order to eliminate the contribution of the nebular radiation we measured through different diaphragms.

The V brightness of this variable observed in 1982 and in January 1983 are compared in Fig. 3 where the evolution of the lightcurve is clearly visible. Comparing the ascending branch of the minimum of January 1982 with that of February 1982 we can see a shift of 1.63 day: we assume that the total width of the January minimum was 3.26 days smaller than that of February, i.e. 11.6 days. If we extrapolate this evolution back we can estimate November 29 (± 5) 1981 to be the beginning of the present eclipsing behaviour. A similar result – November 1981 – was achieved by Schaefer (1983) according to the archival photographic plates at Harvard College Observatory. The first minimum probably occurred on December 8, 1981 with a total width of only 1.9 day. We suppose that the minimum of February 26, 1982 had already spread over the whole cycle and that the maximum started to diminish. We expect that by the beginning of October 1983 the maximum brightness will drop to 13.5 mag (V) and 14.0 mag (B). The brightness at minimum seems to decline quicker than that at maximum and not linearly with time. At present it is not clear how long the decrease of the minimum will last.

We have combined the time of two observed minima of 1982 (February and March/April) with the maximum in 1983 and obtained the following photometric elements:

Min.hel. = JD 244501 $0.60 + 15^d.957 \times E$

$\pm .17 \quad \pm .014$ m.e.

We have assumed that the minimum observed in January 1983 occurred at phase 0.50. Nevertheless, this assumption is

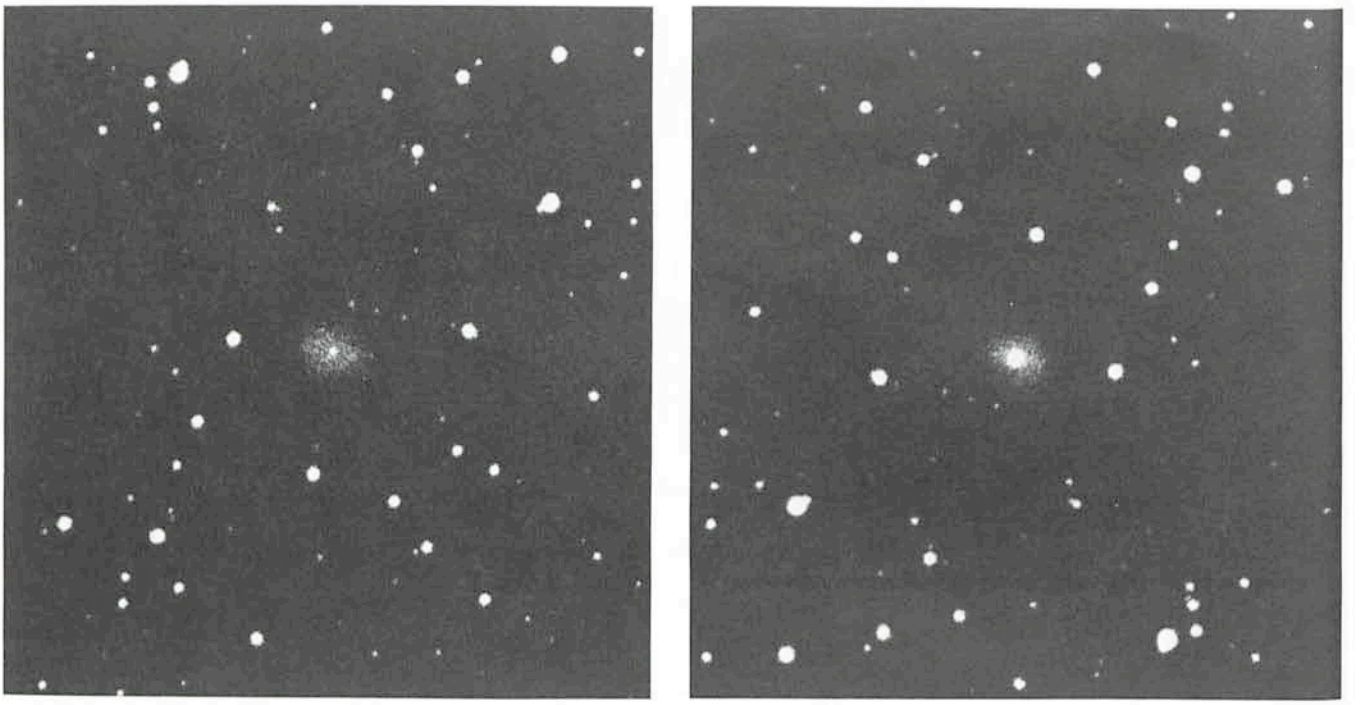

Fig. 2: *Photographs of NGC 2346 with the 80/120 cm Schmidt camera (moved from Hamburg-Bergedorf), DSAZ Calar Alto; 103a-D + GG 11 (V system), exp. 4 min. (a) Dec. 18/19, 1982 – near light maximum; (b) Dec. 11/12, 1982 – near light minimum. (Photo: L. Kohoutek.)*

rather uncertain and the effect of the phase on the derived period is large.

The photometric period is somewhat shorter than the period of the binary system based on the RV curve. At present we do not intend to discuss this small difference of about $0^d.04$ because it exceeds only slightly the errors of the period determination. However, a change of period could reflect evolutionary changes of the binary system, so that attention should be paid to this matter in the future.

The observed changes of the lightcurve and the duration of the present eclipse behaviour are not compatible with the simple model of Méndez et al. (1982). On the other hand, the existence of a dust cloud near the centre of NGC 2346 seems to be very likely. We have plotted the colour B-V versus V and found a linear relation with a slope of 6.6. If we interpret the brigthness drop of the central star as a result of an extinction in the dust cloud, the observed slope is then the ratio R of the total to selective extinction. Deviations up to R ~ 6 are well documented for some regions of star formation, but they would be unusual with planetary nebulae. Nevertheless, Greenstein (1981) found an anomalous reddening inside A 30 due to the dust, too.

The slope 0.86 of the relation U-B versus B-V, being greater than the standard value, is also evidence for high internal extinction. In addition, the older infrared observation (Cohen, Barlow, 1975) as well as recent measurements made by W. Wargau exhibit an appreciable near-infrared excess indicating a large amount of dust in NGC 2346.

Generally the internal extinction due to dust is not considered to be high in planetary nebulae. However, there are exceptions which reveal that the role of dust in planetary nebulae may be greater than expected. Let us mention A 30 and A 78, extended planetaries of very low surface brightness, which show a central concentration of IR emission. Cohen and Barlow (1974) suggested that the dust condensed in the outflowing stellar wind from the emission-line nuclei of these nebulae. A dust cloud (or shell) moving from the nucleus and causing the observed light changes can in principle also be imagined for NGC 2346.

The observations of binary and variable central stars can provide us with data which are very valuable for investigating the physical parameters and the evolution of planetary nebulae and their nuclei. NGC 2346 doubtless belongs to the most interesting objects of this class. The stellar lightcurve is rapidly changing, which obviously reflects varying geometrical or physical conditions. More and systematic observations would be necessary in order to understand the nature of the present eclipse phenomenon and the evolution of this puzzling system.

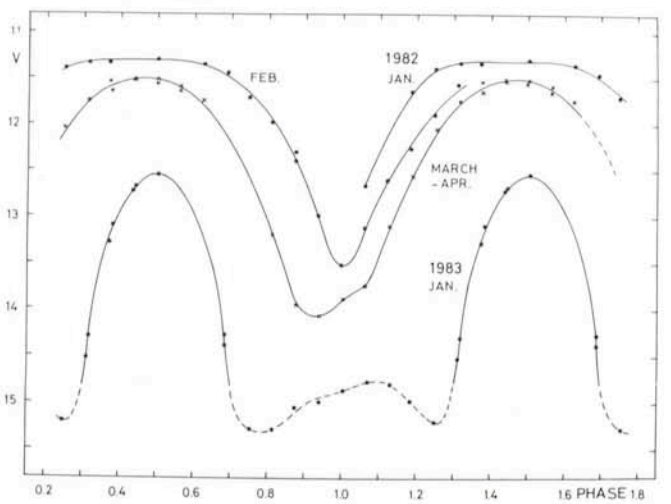

Fig. 3: *V lightcurves of the central star of NGC 2346 from 1982–83 as a function of phase ($P = 15^d.957$). Observations of March-April 1982 are from Méndez et al. (1982). Values below $V \sim 14^m.5$ are uncertain.*

Acknowledgements

I would like to thank J. C. Duflot, R. Kiehling, T. J. van der Linden and H. M. Maitzen for their valuable additional observa-

tions of NGC 2346, and the staff of La Silla Observatory for assistance.

References

Aller, L. H.: 1968, IAU Symp. No. 34 – *Planetary Nebulae* (eds. D. E. Osterbrock and C. R. O'Dell), p. 339.
Cohen, M., Barlow, M. J.: 1974, *Astrophys. J.* **193,** 401.
Cohen, M., Barlow, M. J.: 1975, *Astrophys. Letters* **16,** 165.
Greenstein, J. L.: 1981, *Astrophys. J.* **245,** 124.
Kohoutek, L.: 1982, IBVS Budapest No. 2113 (see also IAU Circ. No. 3667).
Kohoutek, L.: 1983, *Monthly Notices* (submitted).
Kohoutek, L., Senkbeil, R.: 1973, *Mém. Soc. Roy. Sci. Liège,* 6° sér., t.V, 485.
Méndez, R. H., Niemela, V. S.: 1981, *Astrophys. J.* **250,** 240.
Méndez, R. H., Gathier, R., Niemela, V. S.: 1982, *Astron. Astrophys.* **116,** L5.
Méndez, R. H., Niemela, V. S., Lee, P.: 1978, *Monthly Notices Roy. Astron. Soc.* **184,** 351.
Minkowski, R.: 1946, *Publ. Astron. Soc. Pacific* **58,** 305.
Schaefer, B. E.: 1983, IBVS Budapest No. 2281.

CCD Pictures of Peculiar Galaxies with Jets or Extensions

H. Sol, Observatoire de Paris-Meudon

Astrophysical Jets

The phenomenon of "jets" seems to be rather universal in astrophysics. The astrophysical jets are seen in different wavelengths, from radio to X-rays. Their more general definition is "some emitting material well collimated along a straight or curved line". Such features appear on very different scales. Jets having a length of the order of a megaparsec and of a kiloparsec have been detected in different extragalactic systems, respectively QSO (e.g. 4C18.68; Gower, Hutchings, *Ap. J.* **253,** L1, 1982) and radio galaxies (e.g. PKS 0521-36; Danziger et al. *MNRAS,* **188,** 415, 1979). Jets of a few parsecs have also been suspected in galactic objects as the exotic SS 433, Sco X-1 and R Aquarii. Königl (*Ap. J.,* **261,** 115, 1982) even proposed to call jets the asymmetrical outflows which appear in the models of bipolar nebulae, bipolar CO emission lobes and aligned Herbig-Haro objects. Part of the galactic jets could be miniature models of some of the extragalactic ones.

Jets in Galaxies

The presence of jet asymmetry is relatively frequent in the nuclei of galaxies. 50% of the high-luminosity radio sources and 10% of the low-luminosity ones show a jet of a few kiloparsecs; all strong X-ray radio galaxies could have a jet; and the asymmetry of the VLBI structures is usually the rule (Fomalont, Workshop on Astrophysical Jets, Turin, 1982). Precessing radio jets in the centre of our own galaxy have also been reported.

Difficulties arise if one tries to precise the first mentioned general definition and to classify the different cases of observed jets, because they do not seem to form a very homogeneous class of objects. In particular, their spectral properties are not well defined. A great number of jets is seen only in radio, but radio-quiet jets exist too, as the optical jets of NGC 1097 (Wolstencroft, ESO/ESA Workshop on Optical Jets, 1981). Other jets emit in both energy ranges, as the well-known jet of M87. Strong optical emission lines can be present without any continuum counterpart (NGC 7385), although cases with an optical continuum and no lines (M87) are also found, as well as intermediate cases with both optical continuum and line emission (3C277.3; Nieto, Workshop on Astrophysical Jets, Turin, 1982). That diversity implies that the materials and the radiation processes are not the same in all jets. The jet of M87 is probably made of a plasma which emits synchrotron radiation, while some other jets could be a mixture of stars and gas.

The first duty of a theoretical model of jets is to propose a way to break the usual spherical symmetry of many astrophysical phenomena. Astronomers found different possibilities: rotation of a compact object, anisotropy of the ambient medium, two-body interaction, magnetic field, etc. Two main families of jets have been suggested in the literature (i) matter ejected from an active nucleus, as the M87 jet, or relics of such an ejection, (ii) tidal extension or bridge due to gravitational interaction or collision of galaxies, as in the case of IC1182 (Bothun et al., 1981, *Ap. J.,* **247,** 42). Cases concerning both of those families could also exist, since for example the activities of galactic nuclei are expected to be enhanced during a collision event.

CCD Observations

Only a small number (< 20) of optical jets in galaxies have been studied in some detail until now. But a greater number of galaxies have been suspected by visual inspection of Schmidt plates to have a jet and are classified in different catalogues as "jet-galaxy" or "galaxy with extension". Last year I made a CCD survey of 50 of those suspected cases in order to search for and to study optical jets in a statistical way. Some jet galaxies already described in the literature have also been observed to be used as references: M87, 3C273, 3C120, IC1182, PKS0521-36. At the same time, new information has been obtained about them. The jet of 3C273 appears to be composed of 3 regions which coincide with the radio wiggles. The westward 4 arcsec optical elongation of 3C120 as well as the jet nature of the feature seen in PKS0521-36 are confirmed (Sol, Workshop on Astrophysical Jets, Turin, 1982.

The observations were made at the 1.5 m Danish telescope equipped with ESO's CCD during three different runs in January, July and November 1982. The CCD was still in its testing phase for the first two runs. Pictures of the galaxies have been obtained in different colours, using a set of broad-band filters which covers the wavelength range of the CCD response, from 4000 Å to 1 micron (B and V Johnson's filters and g, r, i and z filters described in Wade et al., *PASP,* **91,** 35, 1979).

As mentioned by Pedersen and Cullum in the *Messenger* of December 1982, the CCD data reduction is not completely without problems if one wants to optimize the CCD capabilities. The first difficulty to face is the correction of several effects as the discrepancy in sensitivity of the different pixels, the non-linearity of the cold columns and the interference rings due to the night sky emission lines. A good and easy way to clean the pictures from those three effects is simply to divide the frame of scientific interest by a correction frame, the offset and dark current being first subtracted from both frames respectively. The correction frame is a picture of the night sky obtained by

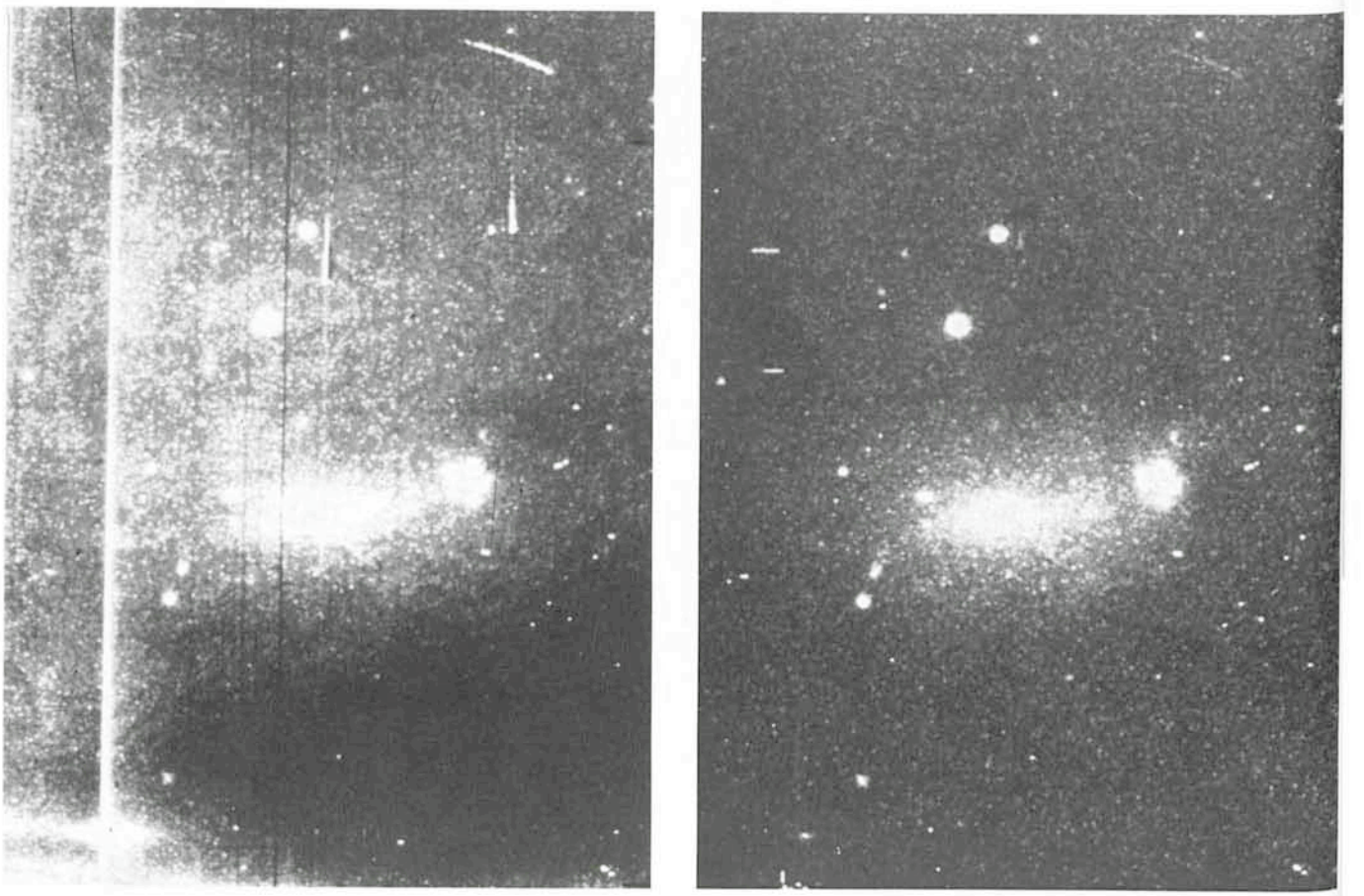

Fig. 1: *(a) First image of the galaxy NGC 1602 in the near IR (January 1982; 15-min exposure; z filter); (b) Image obtained after a pixel-to-pixel division of the image (a) by the night sky correction frame. Note the peculiarity of the galaxy which presents a bright region with multiple condensations at the edge of a large diffuse component. A knotty jet hardly visible here is seen in bluer colour bands.*

erasing all the objects contained in the scientific frames in one given filter during one observing night, and by adding the empty frames obtained that way. The creation of that correction frame does not consume any observing time, except if all the objects of the scientific programme are very extended. (As long as we do not know if standard correction frames can be made once and for all and used by every astronomer, it might be a good idea to incorporate in the programme of every observing night some rather empty fields, for example for detection of faint objects, which can be used to build the correction frames.) The photographs 1 a and b show the result obtained after such a correction. The large-scale background variations were initially (photo 1 a) of 10 % in the central zone of the picture, and the fluctuations due to the interference rings of 2 % of the sky value through the z filter. On the corrected image (photo 1 b) the interference pattern as well as the cold lines are no more visible and the background variations are reduced to less than 1 %.

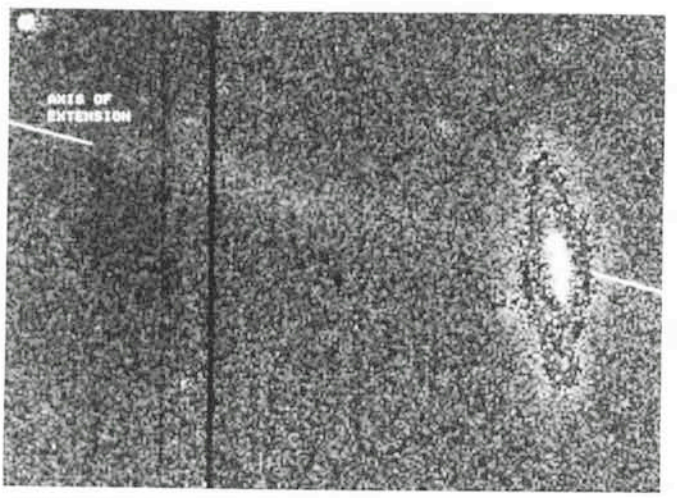

Fig. 2: *This 15-min exposure (January 1982; g filter) of the galaxy ESO 347 G22 shows several nuclear condensations. A large jet feature aligned with the central condensation is clearly visible (1 pixel = 0.471 arcsec).*

Of course the cleaning procedure outlined above cannot reduce the interference rings when they are due to emission lines of the studied objects themselves. Other problems also remain, as the dead and hot pixels and the cosmic ray events, which can be cleaned by the use of software routines now available in the MIDAS image-processing system (Banse et al., *The Messenger*, March 1983). The charge transfer which occurs in the CCD during the picture read-out was not perfect during the testing phase of the CCD. A few per cent of the electrons corresponding to a stellar image were not well transferred and produce faint nebulosities around the stars. Although that effect does not seem to affect directly the photometric results in a very strong way, it makes difficult the precise determination of the sky background in the vicinity of stars (Sol et al., submitted to *A.A.*, 1983). The charge transfer is expected to be substantially improved by an adequate preflash of the CCD chip before each exposure. The outflow of charges from the strongly exposed to the underexposed zones which occurs in regions of high luminosity gradient would also be reduced by a preflashing procedure.

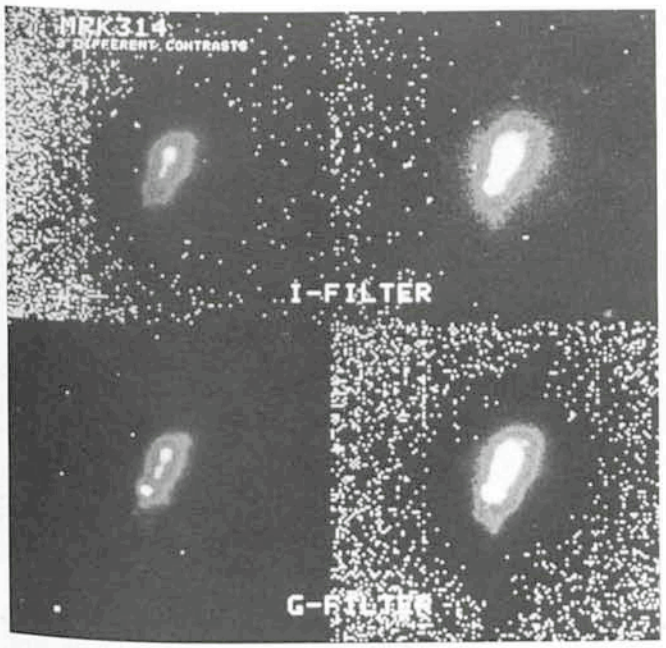

Fig. 3: *The two upper (respectively lower) pictures have been obtained from one exposure of the central part of the galaxy Mrk 314 (July 1982; 15-min exposure) in the i (respectively g) colour band, seen with 2 different contrasts. There is a bridge of matter between 2 main condensations, the southern one is very blue. Mrk 314 is likely to be an interactive case. The inner parts of 2 curved extensions are slightly visible at the upper and lower parts of the g exposures.*

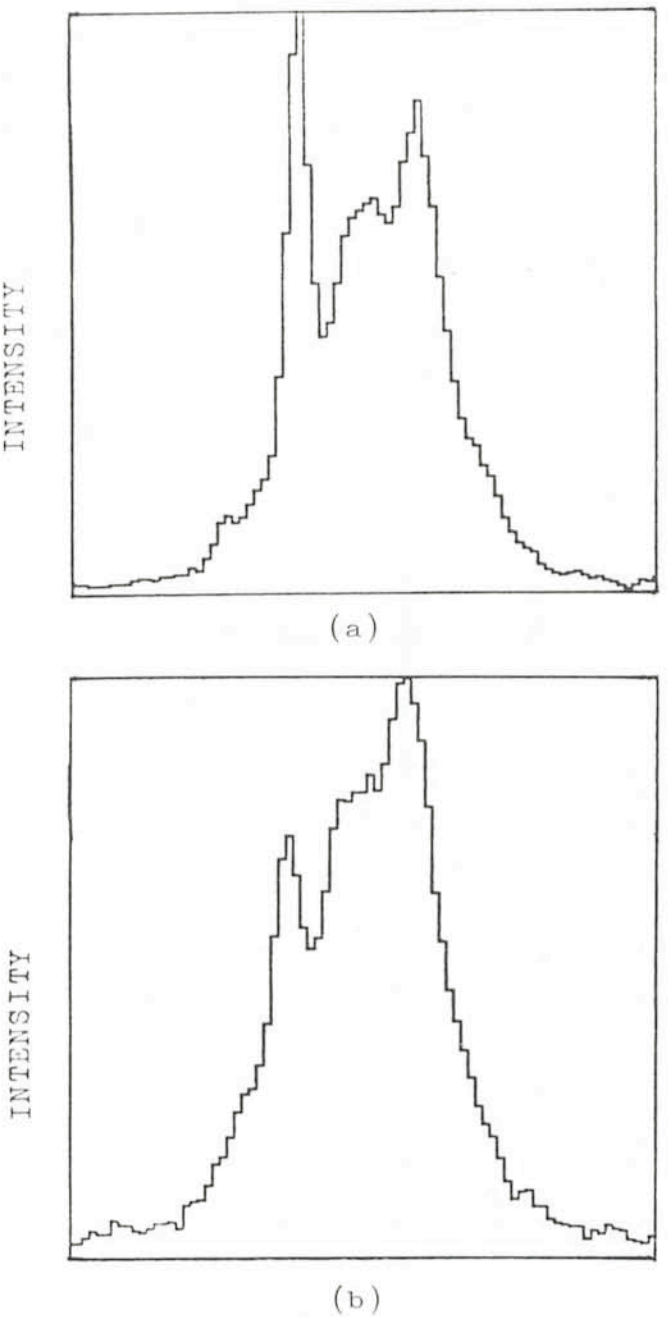

Fig. 4: *Intensity profiles along the line of the central condensations of Mrk 314. (a) for the g colour band (bluer); (b) for the i colour band (redder).*

From a qualitative point of view, the main superiority of a CCD image of one galaxy as compared to what is seen on a Schmidt plate concerns the resolution of the brightest central regions of the galaxy. The sensitivity of the CCD permits a statistical approach while its dynamical range allows a simultaneous investigation of the faint extensions themselves and of the parent galaxies. It is therefore possible to roughly classify all the objects of the sample into different groups by using (i) morphological criteria on the extensions and on the parent galaxies and their nuclei, (ii) photometric properties as the jet-to-galaxy or jet-to-nucleus luminosity ratio in different colours. Among the objects of the sample, 10 % appeared, on the CCD images, to be possibly a superposition of classical astronomical objects, as faint stars or edge-on galaxies. The majority of the objects, however, remain very peculiar. 20 % are likely interactive cases with tidal extensions. 20 % show, besides their jet-like features, multiple nuclear condensations, illustrated by the photographs 2 and 3 and the Fig. 1. No jet strikingly similar to the case of M87 seems to have been found, but further information as spectroscopic and radio data on the jet features are necessary to draw more precise conclusions.

Thanks should go to Massimo Tarenghi for initiating this work and to Preben Grosbøl and Andrezj Kruszewski who helped me to use the ESO data reduction system. I am also grateful to the image processing group and photographers of ESO-Munich, as well as to the staff members of La Silla.

New Optical and X-ray Observations Yield Progress in Understanding of an Old Nova

H. Drechsel, J. Rahe, W. Wargau, Remeis Observatory Bamberg, Astronomical Institute University Erlangen-Fürth

Nova Aquilae 1918 was the brightest new star that was discovered since Tycho's and Kepler's supernovae in 1572 and 1604, which reached a peak brightness of -4^m and -3^m, respectively. On June 10, 1918, Nova V603 Aquilae went through a sharp maximum of visual brightness $-1\overset{m}{.}1$, followed by a subsequent steep decrease, making it an outstanding

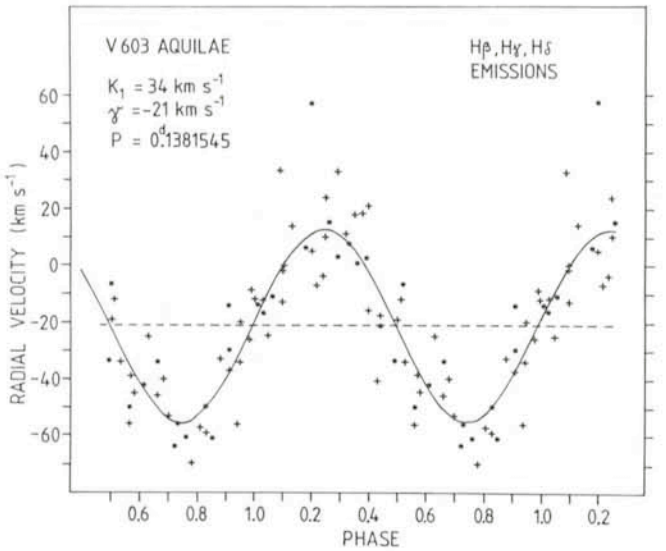

Fig. 1: *Radial velocity curve of the primary component of V603 Aql. The crosses represent our measurements of the Hβ and Hγ emission lines, while the dots give earlier measurements of Hγ and Hδ by Kraft for comparison. The data have also been used for an exact determination of the period.*

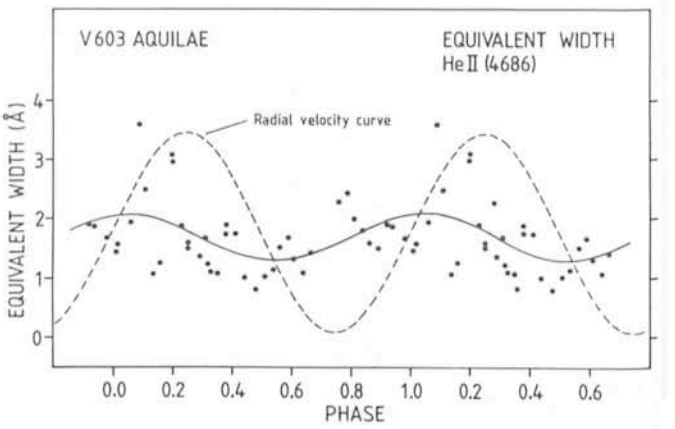

Fig. 2: *Equivalent width of the He II (4686) emission line in the spectra of V603 Aql as a function of orbital phase. The solid line gives the best fit to the data, and suggests mean light intensity changes of about 30 %, which are correlated with the orbital period; superimposed are larger short-term fluctuations. The dashed line is the radial velocity curve of the primary component and illustrates the phase relation of the emission line flux variations.*

example of a classical fast nova. Consequently, it has been the subject of many investigations.

In 1964, Kraft was the first who showed it to be a close binary system with an orbital period of 0.138 days. First evidence for periodic visible light variations correlated with the orbital phase came from photometric observations obtained by the authors during more than two contiguous cycles with the FES instrument aboard the IUE satellite, while UV spectroscopy was carried out simultaneously. At that time, the system was quiet, and at a relatively low mean brightness of about $11^{m}.9$. Subsequent photoelectric measurements and high speed photometry did not reveal any evidence for regular eclipses, because strong non-coherent flickering and photometric disturbances were present at those epochs, when the system was at the higher mean light level of about $11^{m}.4$.

Optical Spectroscopy

Optical spectroscopic observations were obtained with the ESO 3.6 m and 1.5 m telescopes in 1980 and 1981. A total of 65 IDS spectra cover several orbital cycles continuously.

These measurements, together with 23 spectra taken by Kraft during two consecutive nights in 1962, were used to determine the spectroscopic period more precisely. If period changes can be neglected, the power spectrum analysis yields an accurate value for the orbital period of 0.1381545 days, in agreement with the early determination of Kraft. Fig. 1 shows the radial velocity curve of V603 Aql. The crosses represent our data of 1980 and 1981; they are mean values of the Hβ and Hγ emission lines, which are attributed to the more luminous primary component consisting of a white dwarf surrounded by an accretion disk. The dots give Kraft's data of 1962, corresponding to the mean values of the Hγ and Hδ emissions. The relatively small amplitude of the order of 35 km s^{-1} confirms the previously assumed small inclination of about 15°–20°, which makes it difficult to explain the periodic dips in the continuum light curve as regular eclipses.

The optical spectra reveal pronounced time variations of the profiles and intensities of prominent emission lines. As an example, the equivalent width of the He II line at 4686 Å is depicted in Fig. 2 as a function of orbital phase. The amplitude of the mean curve (solid line) corresponds to 30 % changes, while many larger short-term fluctuations are superimposed. The dashed line is the primary radial velocity curve and illustrates the relationship of the line intensity variations with the orbital phase. It is apparent that the maximum intensity of the emission line flux is observed during the phase of conjunction. At that time, the observer on Earth most directly views those surface areas of the late main sequence star which are differentially heated by the radiation of hot regions in the accretion disk or by the central white dwarf. If only a few per cent of the X-ray flux emitted by the primary component is intercepted by the secondary star and partly reprocessed into optical radiation, the variable line-of-sight aspect of the heated surface layers would give rise to the observed modulation of

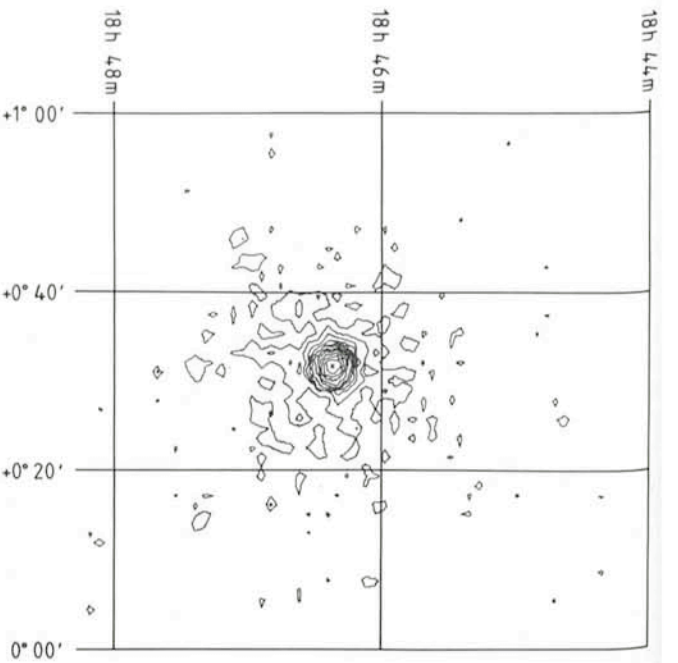

Fig. 3: *The field of V603 Aql as seen by the Image Proportional Counter (IPC) onboard the Einstein satellite. The lines are contours of constant X-ray surface brightness. The old nova shows as a point source, with no obvious emission from an extended shell.*

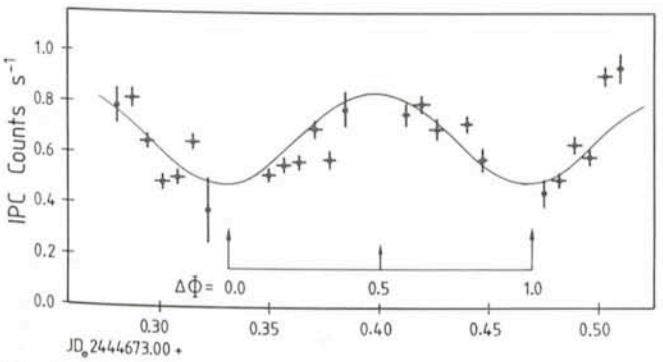

Fig. 4: *The X-ray lightcurve of V603 Aql, measured in the 0.15–4.5 keV range. The dots represent count rates which have been binned in 10-minute intervals. The abscissa is scaled in Julian days, and relative phase units $\Delta\Phi$ are indicated, which have been computed with the optical spectroscopic period. Orbital phase-dependent flux variations are obvious.*

the optical continuum and emission line flux with the orbital period.

X-ray Satellite Observations

More insight into these problems was expected from phase-dependent X-ray measurements which were carried out in 1981 with the Einstein satellite.

Nova Aquilae 1918 was found to be one of the brightest X-ray emitters among cataclysmic variables, with a luminosity of up to 3×10^{33} erg s^{-1} in the 0.2–20 keV energy band. Fig. 3 shows a contour map with lines of constant X-ray surface brightness for a one square degree field centered on the old nova. V603 Aql shows as a point source, which means that the observed X-rays are emitted somewhere within the close binary system, and not from an extended shell. The X-ray position coincides with the astrometric position of the optical counterpart.

The source was monitored over a time interval of about 20,000 seconds, corresponding to approximately 1.7 orbital cycles. X-ray lightcurves were measured in the Image Proportional Counter (0.15–4.5 keV) and Monitor Proportional Counter (2–6 keV) ranges. Fig. 4 displays the X-ray flux variations in the 0.15–4.5 keV energy band. The smooth solid line illustrates the best representation of the data. Obviously, the general trend of the flux variations follows the orbital revolution. The count rates have been binned in 10-minute intervals.

Integration in shorter time steps of 100 second length shows the presence of rapid X-ray flickering with an amplitude of about $0^m.8$. These variations exceed the optical fluctuations by a factor of 2 to 3, but occur on a comparable time scale of a few hundred seconds. This suggests that the optical and X-ray flickering are an outcome of the same mechanism for the generation of the radiation, and that the optical emission may at least partly emerge from reprocessing of the X-rays.

The X-ray source is almost certainly connected with the transfer of matter which is lost by the Roche lobe filling secondary star and accreted by the white dwarf, either directly along magnetic field lines, or from the inner edge of the accretion disk. The observed high X-ray temperature (20–30 keV) and luminosity (3×10^{33} erg s^{-1}) can be explained by applying models for the emission of a hot transition region between the disk and the surface of the star. Such a hot region can persist due to the more or less continuous release of the kinetic energy and momentum of matter rotating in the disk. An accretion rate of only a few 10^{-10} solar masses per year is sufficient to produce the observed X-ray flux with the radiating power of the Sun.

Optical and X-ray data show that the orbital inclination of the binary is small. Why is the X-ray flux then modulated with the orbital period, if we can rule out a partial eclipse of the X-ray source by the secondary star or by material contained in the accretion disk? The variation must be due to the source geometry or to a variable mass accretion rate correlated with the binary orbit. It still remains open, whether the white dwarf is corotating, and a weak magnetic field channels material to particular surface areas, or wheter the orbit is eccentric, leading to variable mass accretion.

We need more observations before a definite model can be developed for this system, which might serve as a representative example for a whole class of by now extensively discussed objects. Especially phase-dependent observations carried out simultaneously in the optical, X-ray, and possibly other spectral ranges would be most useful.

The Optical Jet of R Aquarii

H. Sol, Observatoire de Paris-Meudon

R Aquarii is a stellar system containing a long-period (386 days) Mira variable of spectral type M7e. The presence of an irregularly variable blue continuum and possibly of a several years modulation in the lightcurve suggests that the Mira has a companion, namely a white dwarf with an accretion disk. The most spectacular feature of this symbiotic system is a brigth circumstellar nebula (photographs of which are shown in *Sky and Telescope,* **64,** 141, 1982 by Kaler). This nebula is very likely due to a nova outburst undergone by R Aquarii centuries ago and described in Japanese astronomical records of AD 930 (Kafatos, Michalitsianos, *Nature,* **298,** 540, 1982).

For several years R Aquarii has been known to eject some material as it presents P Cygni type profiles. Besides, an optical protuberance appeared sometime between 1970 and 1977. Photographic plates of 1980 show that it extends to 10 arcsec from the star with two brightness peaks at about 6 and 8 arcsec and that there is a gap between the inner end of the jet and the star (Sopka et al. *Ap. J. Lett,* **258,** L35, 1982). This jet probably corresponds to a collimated ejection of matter from the stellar system. If the observed expansion is due to a real transfer of matter, the jet velocity appears to be $\geq$ 300 km/s, which is a rather large value. It is therefore possible that we observe in fact the speed of displacement of a zone of gas ionization, the gas itself moving outwards more slowly. Sopka and his collaborators detected this jet in radio wavelengths also.

The Mira variable has been kind enough to be almost at its minimum during my observing run of last November in La Silla. Thus I obtained CCD exposures of different exposure time (30 sec, 1, 2, 5, 10, 20 min) of its system in the B and V Johnson colour bands, in order to study the inner part of the jet, close to the star. Fig. 1 shows a 2-min exposure. The 10 arcsec nodule extended towards a position angle $\sim 30°$ and already seen in

1980 is clearly visible as well as a new feature which extends about 4 arcsec from the star towards a position angle ~ 40°. The 30 sec exposures show that the brightness peak of this second nodule is at about 2 arcsec from the star. It coincides with a new radio spot signaled by Kafatos et al. (*Ap. J.*, **267,** L 103, 1983). The integrated luminosities of the 10 and 4 arcsec nodules are roughly 7 % and 6 % of the luminosity of the star in the V colour band (namely $m_{(10)} = 13.9$ and $m_{(4)} = 14.1$ for $m_{Mira} = 11$, assuming a linear response of the CCD even at very low and very high fluxes). The simplest interpretation of the 4 arcsec nodule is that it is due to a new ejection of matter which occurred between 1980 and 1982, unless it was not detected on the 1980 plates because of an overexposition of the star. The difference in the position angles of the two nodules expresses that those nodules have been ejected in two independent events or rather that they belong to the same beam curved by some effect as precession of the emitting system.

Due to its relative vicinity (200 parsec), R Aquarii is one of the few objects which could be used to confront directly with the observations the models of ejection of matter along the axis of an accretion disk, since its accretion disk is supposed to have an angular size of the order of 0.1 arcsec and could be resolved by interferometric techniques or by the space telescope. As it seems to be now in an active phase (are we observing a slow nova outburst?) it would be of interest to obtain a few times every year photographic (possibly with a stellar coronograph) and spectroscopic data of the object. The material difficulty to organize such a surveillance of a single object is expressed in the general question of M. Gerbaldi (*Messenger* of December 1982): how to obtain (officially) occasional observations without applying for several telescope nights?

Thanks are due to Nicolas Mauron for pointing out to me the existence of R Aquarii.

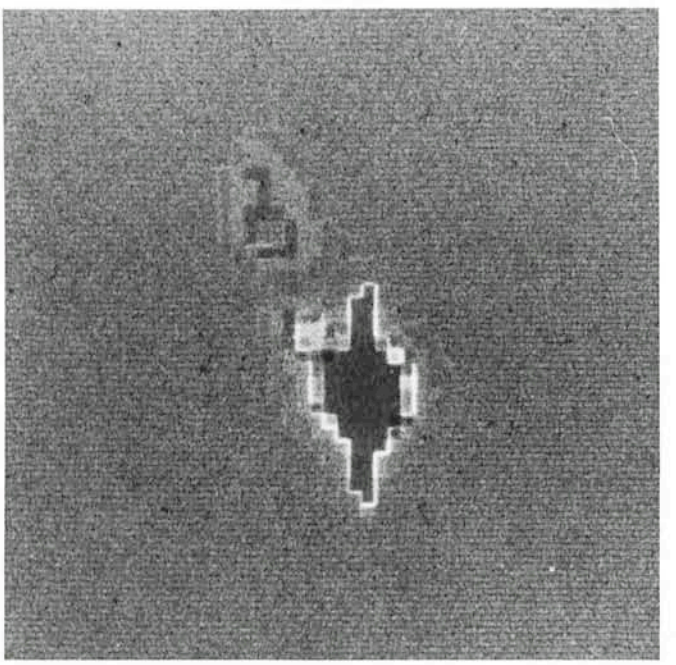

Fig. 1: *This photograph of the central region of the R Aquarii complex has been obtained on November 25 1982. The minimum of the Mira was expected for December 3. A curved jet constituted by 2 nodules described in the text extends to 10 arcsec from the star, northeastwards (north is at top, east to the left). At the distance of the star (200 pc) these 10 arcsec correspond to a linear size of 1,000 astronomical units. The vertical line in the middle of the picture is due to a saturation of the CCD in the zone of the bright star: the excess of charges is transferred above and below the overexposed region. (V filter; 2 min exposure; 1 pixel = 0.471 arcsec.)*

The Proceedings of the ESO Workshop on

PRIMORDIAL HELIUM

which took place on 2–3 February 1983 in Garching, are now in print and will be available at the beginning of July. (Eds. P. A. Shaver, D. Kunth and K. Kjär.) The price for this 420-p. volume is DM 50.— and has to be prepaid.

Payments have to be made to the ESO bank account 2102002 with Commerzbank München or by cheque, addressed to the attention of:

ESO, Financial Services
Karl-Schwarzschild-Str. 2
D-8046 Garching bei München

Please do not forget to indicate your full address and the title of the volume.

List of Available ESO Publications

Some copies of the following ESO publications are still available and may be ordered at ESO-Garching:

Conference on "The Role of Schmidt Telescopes in Astronomy", Hamburg, March 21–23, 1972. Proceedings. Ed. by U. Haug, 160 p. (DM 16.—).

ESO/SRC/CERN Conference on "Research Programmes for the New Large Telescopes", Geneva, 27–31 May 1974. Proceedings. Ed. by A. Reiz, 398 p. (DM 25.—).

ESO Conference on "Optical Telescopes of the Future", Geneva, 12–15 December 1977. Proceedings. Ed. by F. Pacini, W. Richter and R. N. Wilson, 554 p. (DM 40.—).

"Modern Techniques in Astronomical Photography", May 1978. Proceedings. Ed. by R. M. West and J. H. Heudier, 304 p. (DM 16.—).

ESA/ESO Workshop on "Astronomical Uses of the Space Telescope", Geneva, 12–14 February 1979. Proceedings. Ed. by F. Macchetto, F. Pacini and M. Tarenghi, 408 p. (DM 40.—).

"Dwarf Galaxies", Proceedings of the First ESO/ESA Workshop on the Need for Coordinated Space and Ground-based Observations. Geneva, 12–13 May 1980. Ed. by M. Tarenghi and K. Kjär (free).

ESO Workshop on "Two Dimensional Photometry", Noordwijkerhout, 21–23 November 1979. Proceedings. Ed. by P. Crane and K. Kjär, March 1980, 412 p. (DM 40.—).

"Scientific Importance of High Angular Resolution at Infrared and Optical Wavelengths". ESO Conference. Garching, 24–27 March 1981. Proceedings. Ed. by M. H. Ulrich and K. Kjär, 444 p. (DM 50.—).

ESO Workshop on "The Most Massive Stars". Garching, 23–25 November 1981. Proceedings. Ed. by S. D'Odorico, D. Baade and K. Kjär, 366 p. (DM 50.—).

"The ESO/Uppsala Survey of the ESO (B) Atlas". Ed. by Andris Lauberts. 1982. 504 p. (DM 40.—).

"Evolution in the Universe". Symposium held on the occasion of the inauguration of the ESO Headquarters building in Garching on 5 May 1981 (DM 20.—).

ESO Workshop on "The Need for Coordinated Ground-based Observations of Halley's Comet". Paris, 29–30 April 1982. Proceedings. Ed. by P. Véron, M. Festou and K. Kjär. 310 p. (DM 35.—).

"Second ESO Infrared Workshop". Garching, 20–23 April 1982. Proceedings. Ed. by A. F. M. Moorwood and K. Kjär, 446 p. (DM 50.—).

Aluminization of Mirrors

The Optical Laboratory, in charge of aluminizing, informs us that as a general practice, astronomical main mirrors are aluminized every 18 months (Fig. 1). In the case of small main mirrors (upper limit 1 m), it is intended to intercalate a washing between two aluminizations, with the main purpose of reducing the chemical effects on the mirror blank. Secondary mirrors, less exposed to dust, are not included in this scheme.

For national telescopes, the agreement of the person responsible for the telescope is requested before any action is taken; so they are previously informed when a new aluminization is deemed necessary.

Laboratory tests performed with the fiber optic reflectometer have shown the following evolution (Fig. 2):

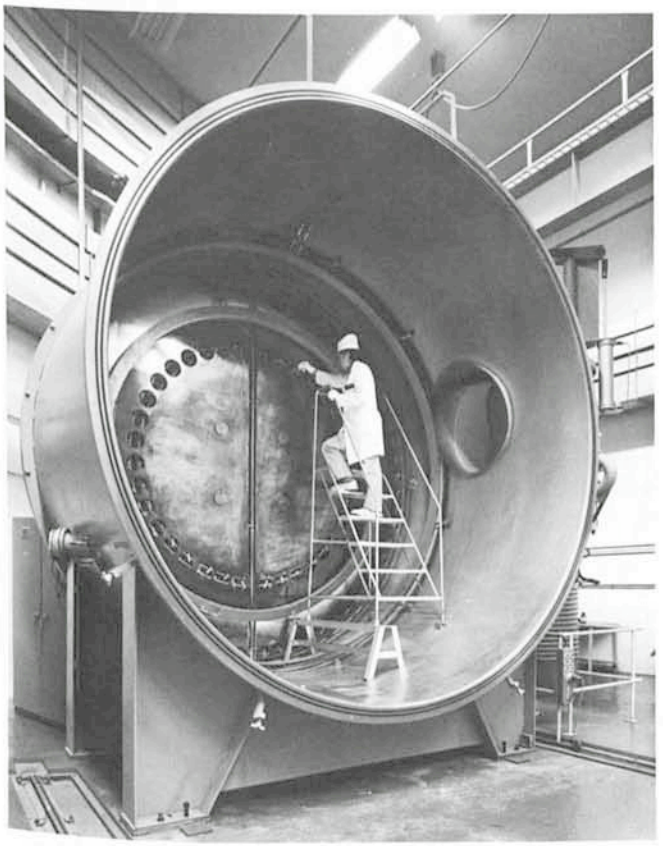

Fig. 1: *The aluminizing plant on the first floor of the 3.6 m telescope building (photo C. Madsen).*

10 days after fresh coating	average loss between 4034 Å and 5300 Å	= 1 %
	average loss at 3500 Å	= 4 %
after 14 months	average loss between 4034 Å and 5300 Å	= 8.4 %
	average loss at 3500 Å	= 15.6 %

The last mirrors aluminized are the ones of the 1.5 m Danish telescope, on 23 March, and of the Schmidt telescope, on 27 April. Aluminization of the 2.2 m telescope mirror is scheduled for May and of the 3.6 m telescope main mirror for the end of August 1983.

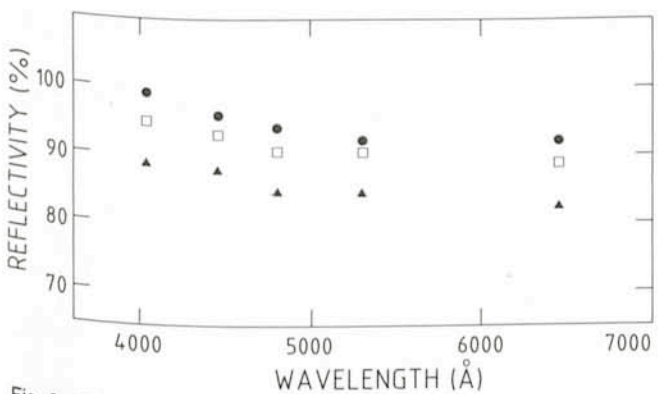

Fig. 2: *Changes of reflectivity with time at various wavelengths at the Danish 1.5 m telescope.*
(●) *reflectivity as measured immediately after aluminization of both primary and secondary mirrors.*
(□) *reflectivity of the secondary mirror 30 months after realuminization (status in March 1983).*
(▲) *reflectivity of the main mirror as measured 30 months after realuminization (status in March 1983).*

PERSONNEL MOVEMENTS

STAFF

Arrivals

Chile

BOHL, Thomas (D), Infrared Instrumentation Engineer, 1.7.1983 (in Europe 6 months to 1 year).
RAFFI, Gianni (I), Software Engineer, 25.5.1983 (change of duty station from Garching to La Silla for 6 months).

Departures

Europe

WOUTERS, Jacobus (NL), Designer/Draughtsman, 10.6.1983.

Chile

GIORDANO, Paul (F), Senior Technician in Optics, 15.6.1983.

FELLOWS

Arrivals

Europe

CRISTIANI, Stefano (I), 1.4.1983.

ASSOCIATES

Arrivals

Europe

CHINCARINI, Guido (I), 11.6.1983.

COOPERANTS

Arrivals

Chile

FOING, Bernard (F) 1.3.1983.
BOUVIER, Jerome (F), 22.4.1983.

Cometas – distantes y cercanos

Cometa Halley observado con el telescopio danés de 1,5 m

Cuando en 1977 fue publicada la pronosticada órbita del cometa Halley para su reaparecimiento, varios astrónomos comenzaron una búsqueda sistemática para recuperar el objeto. Fuera del honor de ser el primero en ver el cometa, se presenta igualmente un aspecto meramente práctico. Se han planeado no menos de cuatro naves espaciales para captar el cometa en 1986, y por eso es muy importante conocer lo antes posible la órbita exacta del cometa.

Las primeras observaciones acertadas se hicieron con el telescopio de 5 m del Monte Palomar, seguidas en corto plazo por los telescopios de 4 m de Kitt Peak y de 3,5 m de Canada-Francia-Hawai. En 1980 ya se hicieron en ESO los primeros intentos (desafortunados) con placas fotográficas tomadas por el telescopio de 3,6 m y con el telescopio danés de 1,5 m por medio de la cámara electronográfica McMullan. Sin embargo estos intentos estaban condenados al fracaso, pues, y como sabido hoy en día, en aquel entonces la magnitud del cometa correspondía a menos de 25.

ESO, the European Southern Observatory, was created in 1962 to . . . establish and operate an astronomical observatory in the southern hemisphere, equipped with powerful instruments, with the aim of furthering and organizing collaboration in astronomy . . . It is supported by eight countries: Belgium, Denmark, France, the Federal Republic of Germany, Italy, the Netherlands, Sweden and Switzerland. It operates the La Silla observatory in the Atacama desert, 600 km north of Santiago de Chile, at 2,400 m altitude, where twelve telescopes with apertures up to 3.6 m are presently in operation. The astronomical observations on La Silla are carried out by visiting astronomers – mainly from the member countries – and, to some extent, by ESO staff astronomers, often in collaboration with the former. The ESO Headquarters in Europe are located in Garching, near Munich.
ESO has about 120 international staff members in Europe and Chile and about 120 local staff members in Santiago and on La Silla. In addition, there are a number of fellows and scientific associates.

The ESO MESSENGER is published four times a year: in March, June, September and December. It is distributed free to ESO personnel and others interested in astronomy.
The text of any article may be reprinted if credit is given to ESO. Copies of most illustrations are available to editors without charge.

Editor: Philippe Véron
Technical editor: Kurt Kjär

EUROPEAN
SOUTHERN OBSERVATORY
Karl-Schwarzschild-Str. 2
D-8046 Garching b. München
Fed. Rep. of Germany
Tel. (089) 32006-0
Telex 5-28282-0 eo d

Printed by Universitätsdruckerei
Dr. C. Wolf & Sohn
Heidemannstraße 166
8000 München 45
Fed. Rep. of Germany

ISSN 0722-6691

Con la instalación de la cámara CCD en el telescopio danés de 1,5 m fue posible observar objetos extremadamente débiles durante el año pasado. Pero sin embargo, aun existían dudas sobre la posibilidad de observar el cometa, pues de acuerdo a observaciones americanas y francesas tendría una magnitud de aproximadamente 24,5.

Combinando una óptima visibilidad, observaciones extremadamente precisas, y admitido, algo de buena suerte, el Dr. Pedersen pudo finalmente obtener la primera fotografía del cometa Halley el dia 10 de diciembre de 1982. El 14 de enero de 1983 fue tomada otra fotografía que confirmó la existencia del débil objeto. En ambas fotografías el cometa fue encontrado exactamente en las posiciones anticipadas, por lo que las observaciones hechas por ESO contribuyeron en gran parte a la exacta determinación de la órbita.

En la primera fotografía se midió una magnitud de 24,5; es impresionante que un objeto tan débil puede ahora ser observado con un telescopio de 1,5 m.

Cometa 1983 d pasa cercano a la tierra

Cuando el cometa Halley fue observado por primera vez en ESO, éste se encontraba aun a una distancia de 1600 millones de kilómetros de la tierra. El día 11 de mayo de 1983 el recientemente descubierto cometa IRAS-ARAKI-ALCOCK (1983 d) pasaba a tan solo 4,5 millones de km de la tierra. ESO también participó en las observaciones, sin embargo, de una manera poco usual.

El cometa había sido descubierto en forma independiente por el satélite IRAS y los astrónomos aficionados Araki (Japon) y Alcock (Reino Unido). Combinando las posiciones entregadas por IRAS, Araki y Alcock, el Dr. Marsden de la Oficina Central de Telegramas de la IAU pudo calcular la órbita preliminar del objeto, y era evidente que el cometa pasaría muy cercano a la tierra. La Oficina Central despachó un telegrama anunciando la importancia de obtener posiciones exactas para precisar mejor la órbita con el fin de poder realizar observaciones con grandes radio telescopios y telescopios ópticos durante su mayor acercamiento.

Cuando el Dr. West leyó dicho telegrama en la biblioteca de la ESO en Garching se preguntó si no sería posible obtener observaciones desde Munich, y contactó al Sr. Stättmayer, un astrónomo aficionado del Observatorio Público de Munich que posee un pequeño observatorio en las cercanías de Munich. El Sr. Stättmayer estuvo de acuerdo y logró obtener algunas fotografías del objeto (una de las cuales se puede ver en la página 2). Estas fotografías fueron medidas en la máquina Optronics en Garching y el Dr. West pudo así transmitir posiciones exactas al Dr. Marsden. Estas posiciones contribuyeron significativamente a la determinacion de la órbita y con ello directamente al éxito de los experimentos de radar con las antenas de Arecibo y Goldstone.

Contents

R. M. West: Comets – Distant and Nearby 1
Prof. Otto Heckmann, 1901 – 1983 1
J. Caplan and L. Deharveng: Absolute Photometry of HII Regions 3
R. Schoembs: CN Orionis, Cooperative Observations for 24 Hours per Day Monitoring 6
J. Melnick: R136: The Core of the Ionizing Cluster of 30 Doradus 11
D. Dravins: Stellar Granulation and the Structure of Stellar Surfaces 15
List of Preprints Published at ESO Scientific Group 20
R. Gathier: Distances to Planetary Nebulae 20
Programme of First ESO/CERN Symposium "Large Scale Structure of the Universe, Cosmology and Fundamental Physics 22
W. E. Celnik: Hα Observations of the Rosette Nebula and the Distribution of Interstellar Dust 23
J. V. Clausen: The Copenhagen Binary Project 25
P. Giordano and E. Maurice: Some News About the Coudé Spectrograph of the ESO 1.52 m Telescope 28
P. Gammelgaard and L. K. Kristensen: Fine Structure Lightcurve of (51) Nemausa 29
L. Kohoutek: The Variable Central Star of Planetary Nebula NGC 2346 31
H. Sol: CCD Pictures of Peculiar Galaxies with Jets or Extensions 33
H. Drechsel, J. Rahe, W. Wargau: New Optical and X-ray Observations Yield Progress in Understanding of an Old Nova 35
H. Sol: The Optical Jet of R. Aquarii 37
List of Available ESO Publications 38
Aluminization of Mirrors 38
Personnel Movements 39
Cometas – distantes y cercanos 39